https://doi.org/10.15388/vu.thesis.997
https://orcid.org/0000-0003-0919-7826

VILNIUS UNIVERSITY

Vaida Paketurytė-Latvė

Structural Recognition in Carbonic Anhydrase–Sulfonamide Complexes: Isozyme and Ligand Effects on Binding Thermodynamics

DOCTORAL DISSERTATION

Natural Sciences,
Biochemistry (N 004)

VILNIUS 2026

This dissertation was written between 2019 and 2025 at Vilnius University.

Academic supervisor:
Prof. Dr. Daumantas Matulis (Vilnius University, Natural Sciences, Biochemistry – N 004).

Dissertation Defence Panel:
Chair – **Dr. Gintautas Tamulaitis** (Vilnius University, Natural Sciences, Biochemistry – N 004).
Members:
Prof. Dr. Dalia Barsyte-Lovejoy (University of Toronto, Canada, Natural Sciences, Biochemistry – N 004).
Dr. Laurynas Dagys (Vilnius University, Natural Sciences, Physics – N 002).
Dr. Kliment Olechnovič (Vilnius University, Natural Sciences, Biochemistry – N 004).
Dr. Miglė Tomkuvienė (Vilnius University, Natural Sciences, Biochemistry – N 004).

The dissertation shall be defended at a public meeting of the Dissertation Defence Panel at 2 p.m. on 29 October 2026 in room No. R401 of the Life Sciences Center, Vilnius University. Address: Saulėtekio av. 7, Vilnius, Lithuania; e-mail: vaida.paketuryte@gmc.vu.lt

https://doi.org/10.15388/vu.thesis.997
https://orcid.org/0000-0003-0919-7826

VILNIAUS UNIVERSITETAS

Vaida Paketurytė-Latvė

Struktūrinis atpažinimas karboanhidrazių–sulfonamidų kompleksuose: izofermentų ir ligandų efektai jungimosi termodinamikoje

DAKTARO DISERTACIJA

Gamtos mokslai,
biochemija (N 004)

VILNIUS 2026

Disertacija rengta 2019 – 2025 metais Vilniaus universitete.

Mokslinis vadovas –
prof. dr. Daumantas Matulis (Vilniaus universitetas, gamtos mokslai, biochemija – N 004).

Gynimo taryba:
Pirmininkas – **dr. Gintautas Tamulaitis** (Vilniaus universitetas, gamtos mokslai, biochemija – N 004).
Nariai:
prof. dr. Dalia Barsytė-Lovejoy (Toronto universitetas, Kanada, gamtos mokslai, biochemija – N 004).
dr. Laurynas Dagys (Vilniaus universitetas, gamtos mokslai, fizika – N 002).
dr. Kliment Olechnovič (Vilniaus universitetas, gamtos mokslai, biochemija – N 004).
dr. Miglė Tomkuvienė (Vilniaus universitetas, gamtos mokslai, biochemija – N 004).

Disertacija ginama viešame Gynimo tarybos posėdyje 2026 m. spalio 29 d. 14 val. Vilniaus universiteto Gyvybės mokslų centro R401 auditorijoje.
Adresas: Saulėtekio al. 7, Vilnius, Lietuva; el. paštas: vaida.paketuryte@gmc.vu.lt

Contents

Abbreviations and Variables **vii**

Introduction **1**
Scientific novelty 4
Defending statements 5

1 Literature Overview **6**
1.1 Structure-Based Drug Design: Potential and Challenges . 6
1.2 Protein–Ligand Binding: Physical Basis and Thermodynamic Description 10
1.2.1 Interactions Governing Protein–Ligand Binding . 10
Interactions Governing Protein–Ligand Binding 10
1.2.2 Thermodynamic Description of Protein–Ligand Binding 16
Thermodynamic Description of Protein–Ligand Binding 16
1.3 Carbonic Anhydrases as a Model System 20
1.3.1 Structural Features of Carbonic Anhydrases . . . 20
1.3.2 Sulfonamides as Carbonic Anhydrase Inhibitors . 32

2 Methods **38**
2.1 Materials 39
2.1.1 Carbonic Anhydrase Isozymes 39
2.1.2 Sulfonamide Inhibitors 40
2.2 Experimental Determination of Protein–Ligand Interactions 40
2.2.1 Fluorescent Thermal Shift Assay 41
2.2.2 Isothermal Titration Calorimetry 42
2.3 Determination of Protonation Parameters 42
2.3.1 Sulfonamide $\mathrm{p}K_{\mathrm{a}}$ Measurements 42
2.3.2 Sulfonamide Protonation Enthalpy Measurements 43
2.4 Calculation of Intrinsic Thermodynamic Parameters . . . 43
2.4.1 Correction of Binding Constants 44
2.4.2 Correction of Binding Enthalpies and Entropies . 44
2.5 Structural Studies 45

3 Summary of Results **47**
3.1 Determinants of Protein–Ligand Recognition 47
3.1.1 Enthalpy-Entropy Compensation 48
3.1.2 Affinity and Selectivity 50
3.1.3 Structure-Thermodynamics Relationships 53
3.2 Reliability of Thermodynamic Measurements 55
3.2.1 FTSA Standardization 55
3.2.2 Uncertainty Quantification 56

Discussion **59**

Conclusions **63**

Bibliography **64**

Santrauka (Summary in Lithuanian) **81**
Įvadas 82
Mokslinis naujumas 85
Ginamieji teiginiai 86
Literatūros apžvalga 86
Metodai 92
Rezultatai 100
Diskusija 111
Išvados 115

Acknowledgements **116**

PUBLICATIONS INCLUDED IN THE DISSERTATION **118**

Copies of Publications (Full Texts Excluded from This Version) **119**
Enthalpy–Entropy Compensation (Publication 1) 120
Affinity and Selectivity (Publication 2) 121
Structure–Thermodynamics Relationships (Publication 3) . . 122
FTSA Standardization (Publication 4) 123
Uncertainty Quantification (Publication 5) 124

Publications not included in the dissertation **124**

List of scientific events **129**

Curriculum Vitae **132**

Abbreviations and Variables

Abbreviations

AZM — acetazolamide, a classical sulfonamide carbonic anhydrase inhibitor;
CA — carbonic anhydrase. CA followed by a Roman numeral denotes a specific isozyme;
DMSO — dimethyl sulfoxide;
FTSA — fluorescence-based thermal shift assay (also called thermal shift assay, TSA), alternatively termed ThermoFluor® or differential scanning fluorimetry (DSF);
GPI — glycosylphosphatidylinositol;
IC — intracellular domain/tail;
ITC — isothermal titration calorimetry;
PDB ID — Protein Data Bank identifier;
PG — proteoglycan-like domain;
PLBD — Protein–Ligand Binding Database (plbd.org);
TM — transmembrane region;
TRIS — tris(hydroxymethyl)aminomethane;
Zn^{II} — zinc ion;

Terminology

Intrinsic — refers to binding between the protein and ligand in their binding-competent protonation states, with contributions from linked protonation equilibria accounted for. Intrinsic thermodynamic quantities and equilibrium constants are denoted by the subscript "int". See Figure 1.12 for an illustration of its meaning and practical application;
Observed — refers to binding as measured experimentally under the specified solution conditions and therefore includes contributions from linked protonation equilibria. Observed thermodynamic quantities and equilibrium constants are denoted by the subscript "obs".

Thermodynamic quantities

ΔG — standard Gibbs energy change of binding (equivalent to ΔG°);
ΔG_{int} — intrinsic standard Gibbs energy change of binding;
ΔG_{obs} — observed standard Gibbs energy change of binding;
ΔH — standard enthalpy change of binding (equivalent to ΔH°);
ΔH_{int} — intrinsic standard enthalpy change of binding;
ΔH_{obs} — observed standard enthalpy change of binding;
ΔS — standard entropy change of binding (equivalent to ΔS°);
ΔS_{int} — intrinsic standard entropy change of binding;
ΔS_{obs} — observed standard entropy change of binding;
$\Delta H_{\mathrm{pr,buf}}$ — standard enthalpy change of buffer protonation;
$\Delta H_{\mathrm{pr,CA}}$ — standard enthalpy change of CA–$\mathrm{Zn^{II}}$ bound hydroxide protonation;
$\Delta H_{\mathrm{pr,SA}}$ — standard enthalpy change of protonation of deprotonated sulfonamide amino group;

Equilibrium constants

K_{b} — equilibrium binding constant;
$K_{\mathrm{b,int}}$ — intrinsic equilibrium binding constant;
$K_{\mathrm{b,obs}}$ — observed equilibrium binding constant;
K_{d} — equilibrium dissociation constant;
$K_{\mathrm{d,int}}$ — intrinsic equilibrium dissociation constant;
$K_{\mathrm{d,obs}}$ — observed equilibrium dissociation constant;
$\mathrm{p}K_{\mathrm{a}}$ — negative decimal logarithm of the acid dissociation constant;
$\mathrm{p}K_{\mathrm{a,CA}}$ — negative decimal logarithm of the acid dissociation constant of the $\mathrm{Zn^{II}}$-bound water molecule in carbonic anhydrase;
$\mathrm{p}K_{\mathrm{a,SA}}$ — negative decimal logarithm of the acid dissociation constant of the protonated sulfonamide group;

Other variables and constants

R — gas constant ($8.314\,\mathrm{J\,mol^{-1}\,K^{-1}}$);
T — absolute temperature (K);

Introduction

Drug discovery relies on identifying molecules that bind selectively and strongly to their biological targets. Advances in structural biology, biophysics, and computational chemistry have greatly expanded our ability to characterize protein–ligand interactions and have become essential components of modern drug design [1, 2]. High-resolution structures, molecular simulations, and structure-based drug design approaches provide valuable insights into binding modes and guide the optimization of lead compounds [3]. Nevertheless, accurately predicting how structural modifications influence binding affinity and selectivity remains a major challenge [4].

Protein–ligand recognition arises from a complex interplay of intermolecular interactions, hydration, protonation equilibria, and conformational dynamics. Although these factors collectively determine binding thermodynamics, their individual contributions are often difficult to isolate and quantify. As a result, molecules with similar structures may exhibit unexpectedly different binding properties, whereas comparable affinities can arise through fundamentally different energetic mechanisms. Understanding these relationships remains an important objective for both experimental and computational studies of molecular recognition.

Several factors are particularly important for the interpretation and prediction of protein–ligand binding:

- **Enthalpy–Entropy Compensation and Hydration Networks:** Binding affinity is determined by the balance between enthalpic and entropic contributions, which frequently compensate each other [5]. Similar binding affinities can therefore arise from markedly different thermodynamic signatures. Such differences are often associated with changes in hydration networks, which remain challenging to characterize and predict quantitatively [6–9].

- **Conformational Effects:** Small chemical modifications can alter ligand geometry, flexibility, and intramolecular interactions, thereby influencing the energetic cost of adopting a binding-competent conformation. These effects may substantially influence protein–ligand interactions [6, 10].
- **Observed versus Intrinsic Thermodynamics:** Experimentally measured binding parameters often include contributions from linked protonation reactions and buffer-dependent processes [11, 12]. Consequently, observed thermodynamic quantities do not always directly reflect the intrinsic energetics of molecular recognition, complicating mechanistic interpretation and comparison between systems.

Together, these factors illustrate that molecular recognition cannot be fully understood from affinity measurements or static structures alone. A suitable model system is therefore required to systematically investigate how structural, thermodynamic, and environmental factors contribute to binding. Carbonic anhydrases (CA) provide an excellent model system for investigating these challenges [13]. Although their catalytic architecture is highly conserved, subtle differences in active-site composition and hydration-network organization can produce substantial differences in ligand recognition. Sulfonamide inhibitors are particularly useful probes because they share a common zinc-binding group while allowing systematic modification of substituents that interact with distinct regions of the active site. This combination enables detailed investigation of how structural changes influence binding thermodynamics, affinity, and selectivity.

Reliable interpretation of structure–thermodynamics relationships requires not only mechanistic understanding but also robust treatment of experimental uncertainty, particularly when comparing parameters derived from non-linear binding models. The central hypothesis of this dissertation is that meaningful relationships between protein–ligand structure and thermodynamics require the systematic separation and characterization of the underlying processes that contribute to molecular recognition.

Goal:

To identify and quantify the structural, thermodynamic, and environmental factors that govern protein–ligand recognition using carbonic anhydrases and primary sulfonamide inhibitors as a model system.

Objectives:

1. To determine how subtle differences in active-site residues, ligand structure, and hydration networks, modulate the balance between enthalpic and entropic contributions to binding. (Publication 1)

2. To investigate the impact of minor ligand modifications on conformational effects, including intramolecular hydrogen bonding and conformational energetics, and their role in determining binding affinity and selectivity. (Publication 2)

3. To systematically separate protonation-linked contributions from experimentally observed thermodynamic parameters to derive intrinsic thermodynamic parameters. (Publication 3)

4. To standardize FTSA experimental protocols for robust affinity determination and to implement asymmetric profile-likelihood confidence intervals for the accurate quantification and interpretation of uncertainty in non-linear binding models. (Publication 4 and Publication 5)

Scientific novelty

The scientific novelty of this dissertation lies in its integrated approach to investigating protein–ligand recognition by combining high-resolution structural analysis, intrinsic binding thermodynamics, and rigorous uncertainty evaluation. This work goes beyond conventional affinity measurements to demonstrate how ligand structure, protein environment, hydration networks, and proton-linked equilibria collectively shape the energetic landscape of molecular recognition.

Key novel contributions:

- **Identification of the structural basis for divergent energetics:** demonstrated that closely related CAs (CA II, CA XII, and CA XIII) achieve comparable binding affinities through fundamentally opposing enthalpic–entropic mechanisms. These distinct thermodynamic fingerprints are modulated by subtle differences in active-site residues and the reorganization of conserved hydration networks. (Publication 1)
- **Insight into the energetic cost of ligand conformation:** identified that a single-atom oxidation change (from sulfanyl to sulfinyl and sulfonyl) altered binding affinity by up to a million-fold. This drop in affinity is linked to the formation of unfavorable intramolecular hydrogen bonds that distort ligand conformation and create steric hindrance. (Publication 2)
- **Revealing the limitations of observed thermodynamic parameters:** demonstrated that binding-linked protonation equilibria substantially alter experimentally observed thermodynamic parameters. Dissection of these contributions enabled meaningful correlations between atomic-resolution structures and the underlying energies of molecular recognition. (Publication 3)
- **Consistent representation of uncertainty across thermodynamic quantities:** emphasized that conventional symmetric error estimates lead to misleading interpretations when binding affinities are transformed between dissociation constants and Gibbs energies. In contrast, asymmetric profile-likelihood confidence intervals preserved the underlying uncertainty structure and ensured consistent interpretation across different representations of binding affinity. (Publication 4 and Publication 5)

Defending statements

- Subtle structural differences in proteins and ligands can produce disproportionately large changes in protein–ligand recognition and selectivity because binding is governed by the entire molecular environment, including protonation equilibria, hydration, conformational effects, and intermolecular interactions. (Publication 1, Publication 2, and Publication 3)
- Protein–ligand recognition cannot be fully understood from structural information and observed thermodynamic parameters alone; reliable interpretation requires the integration of atomic-level structural features with intrinsic thermodynamic parameters. (Publication 1, Publication 2, and Publication 3)
- The representation of uncertainty influences the interpretation of protein–ligand binding measurements; asymmetric profile-likelihood confidence intervals provide a consistent description of uncertainty, while conventional symmetric standard errors are inappropriate. (Publication 4 and Publication 5)

Chapter 1

Literature Overview

1.1 Structure-Based Drug Design: Potential and Challenges

The discovery and development of new medicines remains a costly and high-risk process. Although estimates vary considerably, the median capitalized research and development investment per new therapeutic agent has been estimated at approximately US $1 billion, including costs associated with failed development programs [14]. A major challenge at the discovery stage is the identification and optimization of compounds with sufficient potency, selectivity, and other properties required for further development. Large numbers of initially considered compounds are progressively reduced to only a few candidates that enter clinical development (Figure 1.1). Improving the efficiency of early compound identification and optimization is therefore an important objective of modern drug discovery.

Drug discovery encompasses both biological products and small molecules, with small molecules accounting for approximately $65\,\%$ of new drug approvals in 2025 [17]. Small molecules are amenable to systematic chemical modification and optimization against diverse molecular targets. Their discovery may proceed through several complementary strategies (Table 1.1), ranging from phenotypic and target-based screening to approaches exploiting prior knowledge of active ligands or three-dimensional target structures [18, 19]. The research presented in this dissertation is centered on structure-based drug design, utilizing high-resolution structures of carbonic anhydrases integrated with

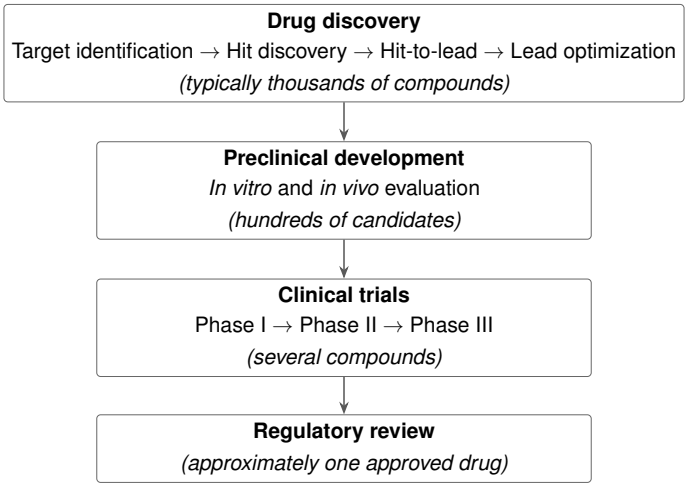

Figure 1.1: Simplified representation of the small-molecule drug discovery and development process, illustrating the substantial reduction in candidate numbers from thousands of compounds during discovery to approximately one approved drug over a typical period of 10–15 years [15]. Even after entry into clinical development, attrition remains substantial: an analysis of 3,999 drug candidates reported an overall probability of marketing approval of $12.8\,\%$ [16]. The research presented in this dissertation focuses on the first stage of this process (Drug discovery), specifically on hit-to-lead and lead optimization phases.

binding thermodynamics to guide the systematic optimization of ligand affinity and selectivity.

Structure-based drug design (SBDD) represents one such approach and exploits three-dimensional information about a biological target to guide ligand discovery and optimization. The importance of structural information in modern drug discovery is illustrated by an analysis of 34 low-molecular-weight, protein-targeted anticancer drugs approved by the US FDA between 2019 and 2023. Structural information contributed to the discovery or development of all 34 drugs, while structure-guided drug discovery contributed to more than $80\,\%$ of cases, either confirmed or probable [21]. Experimentally determined structures can reveal the architecture of binding sites, ligand binding modes, and specific protein–ligand interactions. Protein–ligand structures can therefore guide chemical modification by identifying interactions and binding-site regions that may be exploited during optimization. These experimental data can also be combined with computational approaches to screen compound libraries, generate or evaluate ligand poses, investigate molecular

Table 1.1: Major approaches to small-molecule discovery and design [20].

Approach	Starting point	Typical methods
Phenotypic screening	Desired biological phenotype	Cell- or organism-based screening
Target-based screening	Defined molecular target	High-throughput biochemical or biophysical screening
Ligand-based drug design	Known active ligands	Similarity searching, pharmacophore modeling, quantitative structure–activity relationships
Fragment-based drug discovery	Small, low-complexity fragments	Biophysical or structural screening followed by fragment growing, linking, or merging
Structure-based drug design	Three-dimensional target structure	Molecular docking, structure-based virtual screening, structure-guided ligand optimization

dynamics, and estimate the energetic consequences of chemical modifications [20, 22].

The particular value of SBDD lies in its ability to relate chemical modifications of a ligand to specific features of the target binding site, providing a structural basis for iterative ligand optimization. However, the presence of a favorable interaction in a protein–ligand structure does not directly establish its contribution to binding affinity. A chemical modification intended to introduce or strengthen a particular interaction may simultaneously alter ligand and protein conformation, desolvation, solvent organization, protonation equilibria, and the entropic cost of binding. The energetic consequences of structural modifications are therefore determined by multiple coupled processes and cannot generally be inferred from individual structural interactions alone.

Computational methods complement experimental structures by addressing different aspects of molecular recognition, ranging from ligand-pose prediction and virtual screening to molecular dynamics and binding-energy calculations (Table 1.2). However, these approaches differ substantially in physical detail, computational cost, and their

ability to predict binding affinity quantitatively [20].

Table 1.2: Major computational approaches used in protein–ligand modeling and binding-affinity prediction [20]. The diverse methods summarized here illustrate the various strategies employed to model molecular recognition, while their inherent limitations underscore the physical and computational challenges that complicate the accurate prediction of binding affinity in drug design.

Method	**Main application**	**Major limitation**
Molecular docking	Generation of plausible protein–ligand binding poses and scoring of protein–ligand interactions	Binding-affinity prediction depends strongly on the scoring function and treatment of the molecular system
Molecular dynamics	Sampling of protein–ligand conformations, solvent, and ion dynamics; estimation of binding free energies using additional sampling or analysis approaches	Conventional MD does not directly provide binding affinity; enhanced sampling may suffer from slow convergence and sampling limitations
Quantum mechanics	Estimation of protein–ligand interactions and binding affinities using electronic-structure calculations	High computational cost, particularly for large molecular systems
Machine learning	Prediction of binding poses and binding affinity from relationships learned from experimental and structural data	Performance and applicability depend on training-data quality and model validation

Despite major advances in structural biology and computational chemistry, accurate prediction of protein–ligand affinity and selectivity remains challenging [23–25]. A central goal of computational drug design is to predict binding affinity and selectivity rapidly and accurately, thereby enabling the identification of potent inhibitors while minimizing interactions with relevant off-targets. The research presented in this dissertation contributes to this goal by investigating the physical basis of protein–ligand recognition and relating molecular structure to binding thermodynamics, affinity, and selectivity.

1.2 Protein–Ligand Binding: Physical Basis and Thermodynamic Description

Protein–ligand binding arises from a complex interplay of hydrogen bonding, electrostatic interactions, hydrophobic effects, van der Waals contacts, conformational dynamics, and solvent-mediated processes. These contributions are highly interdependent, making molecular recognition difficult to interpret from static structural information alone. Consequently, thermodynamic and dynamic analyses are essential for understanding the energetic basis of binding [26, 27].

Human carbonic anhydrases and primary benzenesulfonamide inhibitors are used throughout this dissertation as a model system for investigating these relationships (Figure 1.2). The conserved binding of the primary sulfonamide group to the catalytic zinc ion provides a common structural anchor, while modifications of the benzenesulfonamide scaffold and differences between carbonic anhydrase isozymes allow the effects of relatively small structural changes on affinity, selectivity, and binding thermodynamics to be examined. Examples from this model system are therefore used throughout the following sections to illustrate general principles of protein–ligand recognition. The carbonic anhydrase family and its inhibition are described in detail in Section 1.3.

1.2.1 Interactions Governing Protein–Ligand Binding

Metal Coordination

Metal coordination is a distinct class of protein–ligand interaction in which a ligand directly interacts with a metal ion located within a protein binding site [28]. Compared with conventional noncovalent interactions, metal coordination exhibits mixed electrostatic and covalent character and is generally stronger and more directional than hydrogen bonds or van der Waals contacts [29, 30].

Catalytically active human carbonic anhydrases provide a well-characterized example of metal-assisted molecular recognition. Their active sites contain a catalytic Zn^{II} ion [13, 31]. Sulfonamide inhibitors bind through direct coordination of the deprotonated sulfonamide nitrogen to the Zn^{II} ion, displacing the zinc-bound water molecule and forming a tetrahedral complex. Because only the deprotonated sulfonamide

species can coordinate the catalytic metal ion, inhibitor binding is intrinsically linked to protonation equilibria [11]. Crystal structures reveal conserved Zn–N distances of approximately 1.9 Å to 2.2 Å and a hydrogen-bond network involving Thr199 [32–34].

The importance of this interaction is demonstrated by apo-carbonic anhydrases, where removal of the catalytic zinc ion decreases sulfonamide affinity by approximately $(10^4) - (10^6)$-fold, corresponding to a loss of 25 kJ mol^{-1} to 35 kJ mol^{-1} in binding energy [35]. Thermodynamic analyses further suggest that 60 % to 65 % of the stabilization

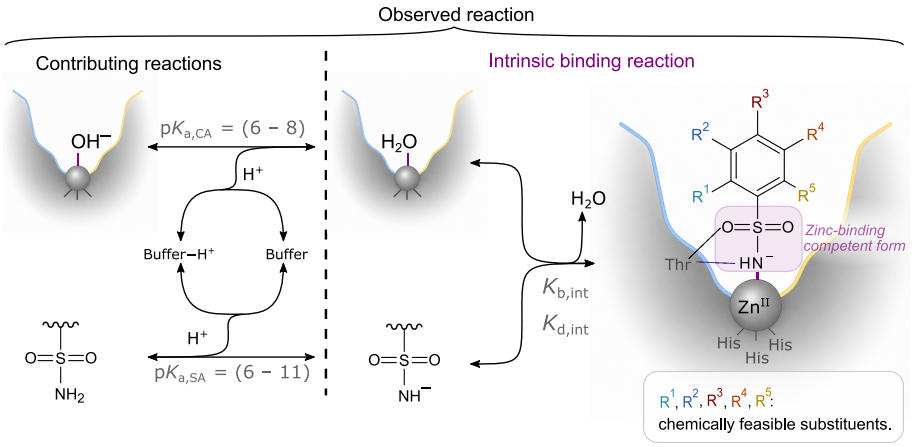

Figure 1.2: General scheme of carbonic anhydrase–primary sulfonamide recognition. The scheme summarizes the common features of primary sulfonamide (emphasis on benzenesulfonamides, which are the main focus of this work) binding to the catalytically active human carbonic anhydrase isozymes and introduces concepts discussed in the following sections. Binding is coupled to the protonation equilibria of both partners, with approximate $\mathrm{p}K_\mathrm{a}$ values indicated. The conserved zinc-binding motif involves coordination of the sulfonamide nitrogen to the catalytic $\mathrm{Zn}^{\mathrm{II}}$ ion and hydrogen-bonding interactions with Thr199. Located at the interface between the more hydrophobic and more hydrophilic sides of the active site (yellow and blue, respectively), this motif provides a common structural anchor. Beyond this motif, variation in sulfonamide substituents and the active-site environments of individual CA isozymes gives rise to diverse interaction patterns affecting affinity, selectivity, and binding thermodynamics. Experimentally observed binding additionally includes contributions from linked protonation equilibria; accounting for these enables determination of intrinsic binding parameters that directly reflect protein–ligand interactions.

energy of carbonic anhydrase–sulfonamide complexes originates from direct interaction with the catalytic Zn^{II} ion [13]. Thus, metal coordination serves as the primary anchoring interaction, while secondary interactions and solvent effects fine-tune affinity and selectivity.

Desolvation and Water-Network Reorganization

Protein–ligand binding occurs in aqueous solution and therefore involves not only direct protein–ligand interactions but also reorganization of surrounding solvent molecules and dissolved ions [7, 9, 36–38]. Both the protein and ligand are surrounded by hydration shells that stabilize exposed polar, charged, and hydrophobic groups. Complex formation requires partial removal and rearrangement of these solvent molecules, creating a desolvation penalty that must be compensated by favorable protein–ligand interactions [39]. Consequently, the energetic contribution of any protein–ligand interaction cannot be evaluated independently of the protein–water and ligand–water interactions displaced upon binding [37–39]. Water molecules within binding sites often differ substantially from bulk solvent: displacement of energetically unfavorable waters can enhance affinity, whereas retention of structurally important waters may stabilize hydrogen-bond networks and contribute to molecular recognition [38, 40, 41].

Carbonic anhydrases provide a notable example of the importance of solvent organization. Their active sites contain an extended hydrogen-bond network connecting the catalytic Zn^{II} ion, the zinc-bound water molecule, Thr199, His64, and several ordered water molecules involved in proton transfer [31, 42]. Binding of sulfonamide inhibitors displaces the zinc-bound water molecule and reorganizes the surrounding solvent network, contributing substantially to binding thermodynamics and enthalpy–entropy compensation [13, 43, 44]. Most current knowledge of active-site water organization in carbonic anhydrases originates from studies of CA II, which revealed a highly ordered network of water molecules involved in proton transfer and stabilization of the catalytic center [43, 45–51].

In addition to water, dissolved ions such as sodium, potassium, chloride, phosphate, and sulfate can influence molecular recognition through electrostatic screening and ion displacement. Although often absent from crystallographic models, these species contribute to experimentally measured binding thermodynamics and complicate interpretation of protein–ligand interactions [52, 53].

Hydrophobic Effect

The hydrophobic effect is one of the major driving forces of protein–ligand binding in aqueous environments. Unlike electrostatic interactions, hydrogen bonds, or metal coordination, it does not arise from a direct attractive force between nonpolar groups. Instead, it originates from the thermodynamic consequences of water reorganization around hydrophobic surfaces [37, 38, 54–56].

In aqueous solution, water molecules surrounding nonpolar groups adopt a more ordered arrangement than in bulk solvent. Upon ligand binding, burial of hydrophobic surfaces releases these constrained water molecules back into the bulk phase, resulting in a favorable increase in solvent entropy. Consequently, the hydrophobic effect often contributes substantially to the energy of binding and generally scales with the amount of nonpolar surface area buried upon complex formation [54, 57].

Hydrophobic interactions are closely coupled to desolvation and water-network reorganization. Therefore, their energetic contribution cannot always be separated from the thermodynamic effects associated with displacement of water molecules from the binding interface [37, 38]. In structure-based drug design, optimization of hydrophobic contacts is frequently used to enhance ligand affinity, although excessive hydrophobicity may compromise solubility and pharmacokinetic properties [30, 38].

In carbonic anhydrases, hydrophobic interactions contribute significantly to inhibitor affinity and isozyme selectivity. The hydrophobic region of the active site, formed primarily by residues Val121, Val143, Leu198, and Trp209 (CA II numbering), plays an important role in accommodation of aromatic inhibitor substituents. While the Zn^{II} coordination is highly conserved among isozymes, differences in hydrophobic regions surrounding the active-site cavity provide opportunities for selective recognition. Aromatic and fluorinated [58–60] substituents of sulfonamide inhibitors frequently occupy these regions, forming favorable contacts and displacing ordered water molecules, thereby enhancing binding affinity and selectivity [13, 34].

Hydrogen-Bond Networks

Hydrogen bonds are among the most important noncovalent interactions involved in protein–ligand recognition. Owing to their strong directionality, they contribute to ligand affinity, specificity, and orientation within the binding site [30, 61]. Although the energetic contribution of an individual hydrogen bond is typically estimated to range from $4\,\mathrm{kJ\,mol^{-1}}$ to $20\,\mathrm{kJ\,mol^{-1}}$, its net stabilizing effect depends strongly on geometry, solvent exposure, and desolvation effects [8, 30].

Hydrogen bonds frequently form cooperative networks involving protein residues, the ligand, and ordered water molecules, thereby stabilizing protein–ligand complexes and maintaining binding-site architecture [13, 38].

In carbonic anhydrases, a conserved hydrogen-bond network surrounds the catalytic $\mathrm{Zn^{II}}$ ion and contributes to both catalysis and inhibitor binding. The residue Thr199 plays a central role by forming hydrogen bonds with the sulfonamide group of bound inhibitors while simultaneously linking the catalytic center to the surrounding solvent network [13, 34]. Together with $\mathrm{Zn^{II}}$ coordination, these conserved interactions are major determinants of the affinity of sulfonamide inhibitors.

Electrostatic Interactions

Electrostatic interactions arise from attractive or repulsive forces between charged and polar groups and represent one of the longest-range contributors to protein–ligand recognition. They include ion–ion, ion–dipole, and dipole–dipole interactions, all of which can influence ligand orientation and binding-site recognition before direct molecular contact is established [30, 61].

The strength of electrostatic interactions depends strongly on the local environment. In aqueous solution, solvent screening substantially weakens interactions between charged groups, making their energetic contribution highly context dependent and closely coupled to desolvation effects [37, 38]. In buried binding sites, however, electrostatic interactions can contribute significantly to binding affinity owing to reduced dielectric screening.

In carbonic anhydrases, electrostatic interactions contribute to both catalysis and inhibitor binding. The catalytic $\mathrm{Zn^{II}}$ ion generates a strong

positive electrostatic potential that stabilizes the zinc-bound hydroxide ion and promotes binding of negatively charged ligands [13, 62]. In addition, interactions between charged or polar ligand substituents and residues lining the active-site cavity can influence ligand orientation and contribute to isozyme selectivity [34].

van der Waals and Packing Interactions

van der Waals interactions arise from transient fluctuations in electron density that generate temporary dipoles between neighboring atoms. Although individually weak, they are ubiquitous in protein–ligand complexes and can contribute substantially to binding through their cumulative effect [30, 61]. Because these interactions operate only over short distances, their contribution depends strongly on shape complementarity and efficient packing between the ligand and the protein binding site.

Optimal packing maximizes favorable contacts while avoiding steric clashes. Consequently, small structural modifications can markedly influence binding affinity by improving or disrupting local van der Waals interactions [30, 38]. In many cases, affinity improvements achieved during lead optimization arise from more efficient occupation of available space rather than the introduction of additional hydrogen bonds.

In carbonic anhydrases, van der Waals interactions stabilize inhibitors after primary anchoring interactions, such as Zn^{II} coordination and hydrogen bonding, have been established. Aromatic, heterocyclic, and fluorinated substituents frequently occupy hydrophobic regions of the active-site cavity, where favorable packing interactions enhance binding affinity [34, 63]. Because the architecture of the active-site entrance differs among isozymes, optimization of packing interactions in these regions is often exploited to improve inhibitor selectivity [63].

Conformational Effects

Protein–ligand binding is frequently accompanied by conformational changes in both the protein [64–66] and the ligand [10, 67]. Rather than existing as rigid structures, proteins populate dynamic ensembles of interconverting conformational states that differ in their ability to recognize and bind ligands [68, 69]. Molecular recognition is therefore

often associated with structural rearrangements that optimize protein–ligand interactions [70].

Two complementary models are commonly used to describe these processes. In the induced-fit model, ligand binding promotes structural changes that generate a favorable binding geometry, whereas in the conformational-selection model the ligand preferentially binds a pre-existing conformation and shifts the equilibrium toward the bound state [68, 71]. In practice, both mechanisms may contribute to molecular recognition.

Conformational changes influence binding through both enthalpic and entropic contributions. Structural rearrangements can improve shape complementarity and intermolecular interactions but are often accompanied by a loss of conformational freedom upon complex formation [38, 72].

Although carbonic anhydrases are generally considered structurally conserved enzymes [73], recent experimental and computational studies have demonstrated conformational flexibility of active-site residues and surface loops [74–78]. These motions can influence ligand binding, solvent organization, and isozyme selectivity, particularly near the active-site entrance, highlighting the importance of protein dynamics in molecular recognition.

1.2.2 Thermodynamic Description of Protein–Ligand Binding

The thermodynamic behavior of molecular systems can be described by a network of interrelated state functions and response properties. These include Gibbs energy, enthalpy, entropy, heat capacity, volume, compressibility, and thermal expansion coefficients, all of which provide complementary information about molecular interactions and structural changes. Figure 1.3 summarizes the thermodynamic relationships between several quantities most frequently used to characterize protein–ligand interactions. Among these, Gibbs energy (ΔG), enthalpy (ΔH), and entropy (ΔS) are the principal descriptors of molecular recognition because they directly characterize binding affinity and the energetic and dynamic processes accompanying complex formation [8]. Additional parameters, such as changes in heat capacity (ΔC_p) and volume (ΔV), can provide further insight into solvation, conformational rearrangements, and molecular packing [79, 80].

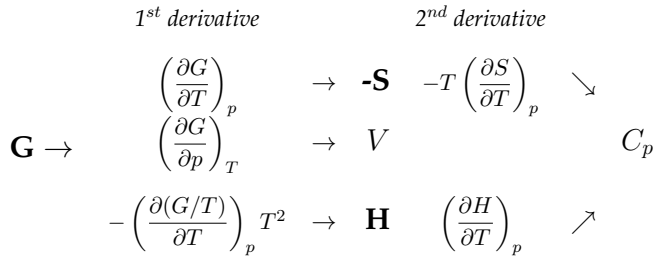

Figure 1.3: Derivative relationships between Gibbs energy (G), entropy (S), volume (V), enthalpy (H), and constant-pressure heat capacity (C_p). These quantities constitute the principal thermodynamic parameters used to describe protein–ligand interactions. Adapted from [79, 80].

Binding Equilibrium and Binding Constants

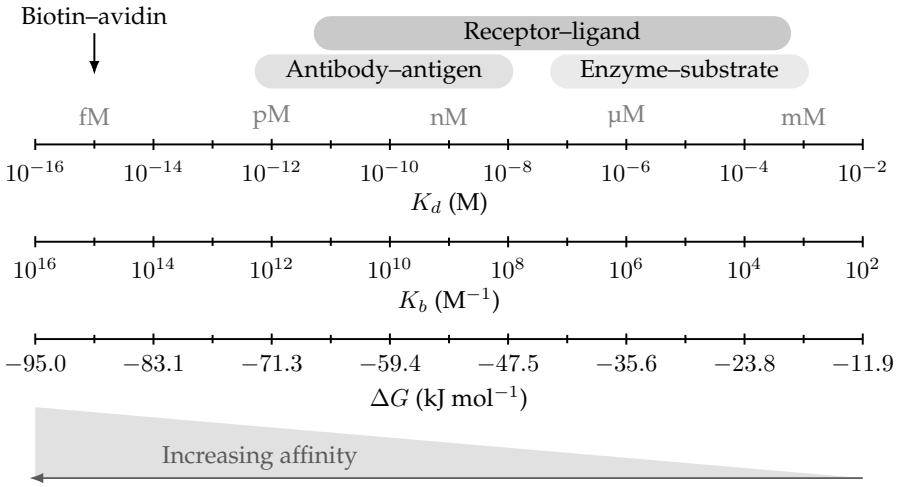

Figure 1.4: Relationship between the dissociation constant (K_d), binding constant (K_b), and Gibbs energy change (ΔG) for representative biomolecular interactions at 37 °C. Interaction classes are shown as approximate ranges. The figure was constructed based on data and concepts presented in [81].

Protein–ligand binding is typically described as a reversible equilibrium between the free protein (P), free ligand (L), and the protein–ligand complex (PL):

$$P + L \rightleftharpoons PL \tag{1.1}$$

The position of this equilibrium is quantified by the association (binding) constant, K_{b}, or equivalently by the dissociation constant, K_{d}, defined as:

$$K_{\mathrm{b}} = \frac{[PL]}{[P][L]} \qquad \text{and} \qquad K_{\mathrm{d}} = \frac{[P][L]}{[PL]} = \frac{1}{K_b} \tag{1.2}$$

where $[P]$, $[L]$, and $[PL]$ represent the equilibrium concentrations of free protein, free ligand, and the protein–ligand complex, respectively. High-affinity interactions are characterized by large K_{b} values and correspondingly low K_{d} values. Because binding constants directly reflect the extent of complex formation at equilibrium, they provide the fundamental quantitative measure of molecular recognition and form the basis for the thermodynamic description of protein–ligand interactions.

Gibbs Energy of Binding

The Gibbs energy of binding (ΔG) is the primary thermodynamic parameter describing the spontaneity and favorability of protein–ligand interactions. It is directly related to the equilibrium binding constant (Figure 1.4) according to:

$$\Delta G = -RT \ln K_{\mathrm{b}} \tag{1.3}$$

where R is the universal gas constant and T is the absolute temperature. More negative values of ΔG correspond to stronger binding affinities and greater stability of the protein–ligand complex. Because ΔG integrates all energetic contributions associated with binding, it provides a quantitative measure of the overall driving force for molecular recognition. Importantly, ligands with comparable binding affinities may display markedly different thermodynamic signatures, indicating that similar ΔG values can arise from different balances of intermolecular interactions, conformational changes, and solvent reorganization. The relationship between Gibbs energy, enthalpy, and entropy is described by:

$$\Delta G = \Delta H - T\Delta S \tag{1.4}$$

which forms the basis for thermodynamic analysis of protein–ligand binding.

Binding Enthalpy

Binding enthalpy (ΔH) reflects the energetic changes associated with formation and disruption of intermolecular interactions during protein–ligand complex formation. Favorable enthalpic contributions typically arise from hydrogen bonding, electrostatic interactions, metal coordination, van der Waals contacts, and other attractive interactions established between the protein and the ligand [82, 83]. However, the observed enthalpy change also includes contributions from desolvation, conformational rearrangements, and reorganization of solvent molecules surrounding the binding interface. Consequently, highly favorable binding enthalpies do not necessarily indicate a greater number of direct protein–ligand interactions, but rather reflect the overall energetic balance between interactions formed and interactions disrupted upon binding. In many systems, binding enthalpy provides valuable insight into the molecular determinants of ligand recognition and is frequently used to guide structure-based optimization of protein–ligand interactions.

Binding Entropy

Binding entropy (ΔS) reflects changes in molecular freedom and the distribution of accessible states accompanying protein–ligand complex formation. Binding is generally associated with unfavorable entropy due to restriction of translational, rotational, and internal conformational freedom of both the ligand and the protein. However, favorable entropy contributions may arise from desolvation and the release of ordered water molecules or ions from the binding interface into bulk solution [10, 64, 70]. Consequently, the observed entropy change reflects a balance between losses of molecular flexibility and gains in solvent entropy. Because many entropic contributions cannot be directly visualized in static structures, entropy provides important information about protein dynamics, conformational heterogeneity, and solvent reorganization that complements structural and enthalpic analyses of molecular recognition.

Enthalpy–Entropy Compensation

Enthalpy–entropy compensation refers to the tendency of favorable changes in binding enthalpy (ΔH) to be offset by less favorable entropy changes (ΔS), and vice versa [8, 36, 72]. Strong intermolecular interactions often increase ordering within the protein–ligand complex and reduce conformational freedom, leading to entropic penalties. Conversely, entropy-favorable processes such as desolvation and release of ordered water molecules may contribute less favorably to binding enthalpy. Consequently, large variations in ΔH and ΔS frequently result in relatively small changes in the overall Gibbs energy of binding (ΔG). This phenomenon explains why ligands with similar binding affinities can display markedly different thermodynamic signatures and highlights the importance of considering both enthalpic and entropic contributions during drug design.

1.3 Carbonic Anhydrases as a Model System

Carbonic anhydrases [84] (CAs; EC 4.2.1.1) constitute a family of metalloenzymes that catalyze the reversible hydration of carbon dioxide. These enzymes are widely distributed across all kingdoms of life and are classified into eight evolutionarily distinct families. They participate in a broad range of physiological processes, including pH regulation, respiration, and ion transport. [85, 86]

This thesis focuses on the human isozymes of the α-CA family, which includes 15 members, 12 of which are catalytically active. These isozymes display considerable variation in physiological roles, tissue distribution, expression levels, kinetic parameters, thermal stability, and inhibitor binding properties [13]. The subcellular localization of human CAs is presented in Figure 1.5. Three isozymes, CA VIII, CA X, and CA XI, are catalytically inactive due to the absence of zinc-coordinating histidine residues [87]. These are referred to as carbonic anhydrase-related proteins (CARPs); therefore, they are not considered further in this work.

1.3.1 Structural Features of Carbonic Anhydrases

Carbonic anhydrases belonging to the α-class share a highly conserved globular fold composed of a central twisted β-sheet surrounded

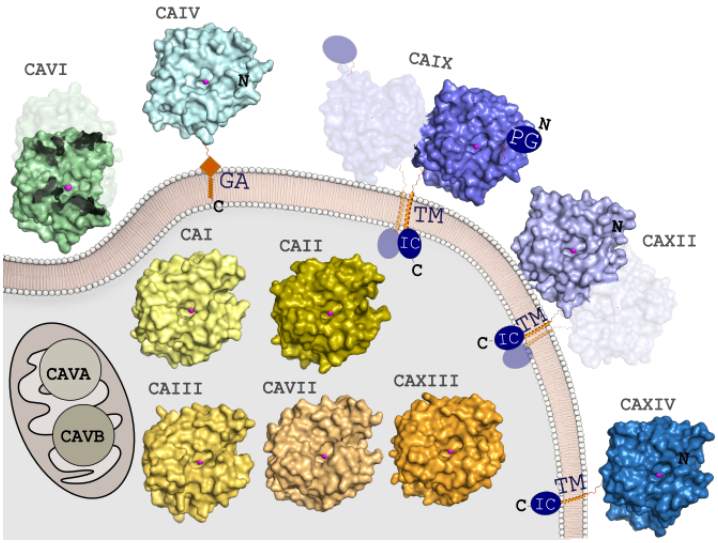

Figure 1.5: Schematic representation and cellular distribution of human carbonic anhydrases. Isozymes are cytosolic (CA I, CA II, CA III, CA VII, CA XIII), membrane-bound (CA IV, CA IX, CA XII, CA XIV), mitochondrial (CA VA, CA VB), or secreted (CA VI). Most are monomeric, whereas CA VI, CA IX, and CA XII form dimers with distinct interfaces. All contain a catalytic domain; CA IV additionally carries a glycosylphosphatidylinositol anchor (GA), CA XII and CA XIV contain a transmembrane region (TM) and intracellular tail (IC), and CA IX additionally contains a proteoglycan-like domain (PG). X-ray crystal structures of the catalytic domains are available for all shown isozymes except CA VA and CA VB. Structures with the following PDB IDs were used: CA I - 1AZM, CA II - 3HS4, CA III - 1Z93, CA IV - 5JN8, CA VI - 3FE4, CA VII - 3ML5, CA IX - 3IAI, CA XII - 1JD0, CA XIII - 3CZV, CA XIV - 4LU3.

by several α-helices and flexible loop regions. Despite substantial sequence diversity among individual isozymes, the overall catalytic architecture remains strongly conserved (Figure 1.6). The active site forms a conical cavity approximately 15 Å deep extending from the protein surface toward the catalytic Zn^{II} ion located at the bottom of the pocket. The zinc ion is tetrahedrally coordinated by three histidine residues (His94, His96, and His119) and a water molecule or hydroxide ion [88].

The active-site cavity contains distinct hydrophobic and hydrophilic regions that collectively regulate substrate binding, proton transfer, solvent organization, and inhibitor recognition. The hydrophobic region, formed primarily by residues Val121, Val143, Leu198, and Trp209, facili-

tates accommodation and orientation of CO_2 and aromatic fragments of inhibitors. The hydrophilic region contains an extended hydrogen-bonding network centered around Thr199, Glu106, and conserved ordered water molecules involved in stabilization of the zinc-bound solvent molecule, proton transfer and inhibitor-binding geometries.

Although the catalytic core remains strongly conserved among isozymes, subtle variations in amino acid composition surrounding the active-site entrance modify cavity geometry, hydrophobicity, solvent accessibility, and electrostatic surface properties. These differences generate distinct binding-site microenvironments that influence inhibitor affinity, selectivity, and binding thermodynamics.

Human CA II is used throughout as the reference structure for structural comparisons, and residue numbers refer to the corresponding CA II positions unless otherwise indicated. Figures 1.8 and 1.9 provide complementary comparisons of the active-site architectures of CAs, showing differences in amino acid composition relative to CA II and qualitative differences in active-site cavity shape and accessibility. The latter depend on the conformations of individual residues and should therefore not be interpreted as direct comparison of cavity size.

CA I

Human CA I adopts the conserved α-carbonic anhydrase fold and possesses an active-site architecture highly similar to that of CA II [89]. Despite strong conservation of the catalytic core, several amino acid substitutions near the active-site entrance distinguish CA I from CA II. In particular, Ala65, Asn67, and His200 replace Ser65, His67, and Thr200 of CA II, respectively. The Ser65$\rightarrow$Ala substitution removes a hydroxyl group, His67$\rightarrow$Asn replaces an imidazole side chain with a shorter amide, and Thr200$\rightarrow$His introduces a bulkier imidazole group. Additional differences surrounding residues Phe91, Ala121, Leu131, and Ala135 modify the hydrophobic region of the active site. Consequently, CA I exhibits lower catalytic activity and generally weaker inhibitor affinities than CA II. Differences in the organization of ordered water molecules surrounding Thr199 and the zinc-bound solvent may further contribute to isozyme-dependent binding thermodynamics.

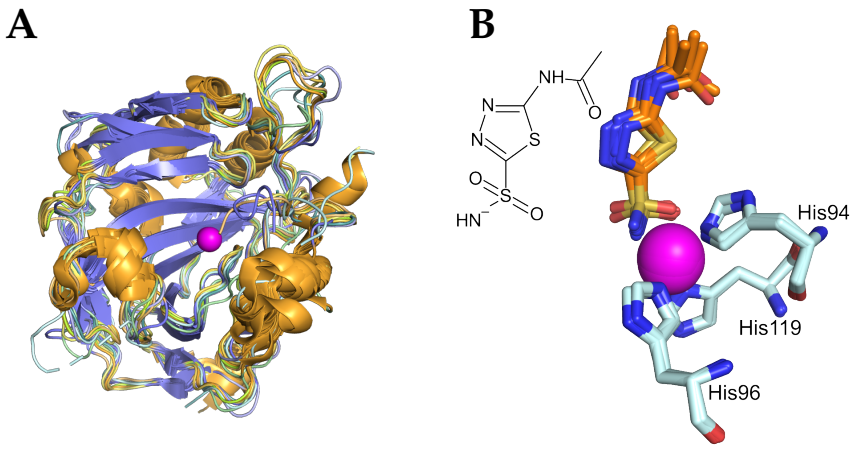

Figure 1.6: Structural conservation of human CAs. (A) Superposition of the catalytic domains of human carbonic anhydrases: CA I - 1AZM, CA II - 3HS4, CA III - 1Z93, CA IV - 5JN8, CA VI - 3FE4, CA VII - 3ML5, CA IX - 3IAI, CA XII - 1JD0, CA XIII - 3CZV, CA XIV - 4LU3. (B) Superposition of active-site regions from carbonic anhydrase isozymes for which crystal structures in complex with acetazolamide (AZM), a classical sulfonamide carbonic anhydrase inhibitor, are available in the Protein Data Bank. The catalytic zinc ion (magenta sphere), AZM, and the three zinc-coordinating histidine residues are shown. The high degree of conservation of the zinc-binding site and surrounding active-site architecture explains the broad inhibitory activity of primary sulfonamides.

CA II

Human CA II is the most extensively investigated member of the carbonic anhydrase family and one of the best structurally characterized metalloenzymes. Owing to its exceptionally high catalytic activity, stability, and the availability of abundant structural and kinetic data, CA II has become the principal model protein for studies of carbonic anhydrases, and structural as well as mechanistic features of other CA isozymes are commonly interpreted and compared relative to CA II. Research on its structural features has evolved from early crystallographic characterization toward detailed mechanistic analyses of catalysis, proton transfer, and active-site dynamics. The first crystal structure of CA II (historically termed carbonic anhydrase C) established the overall architecture of the enzyme and provided the initial description of the catalytic zinc environment and active-site organization [32]. High-resolution refinement studies later improved the accuracy of the active-site geometry

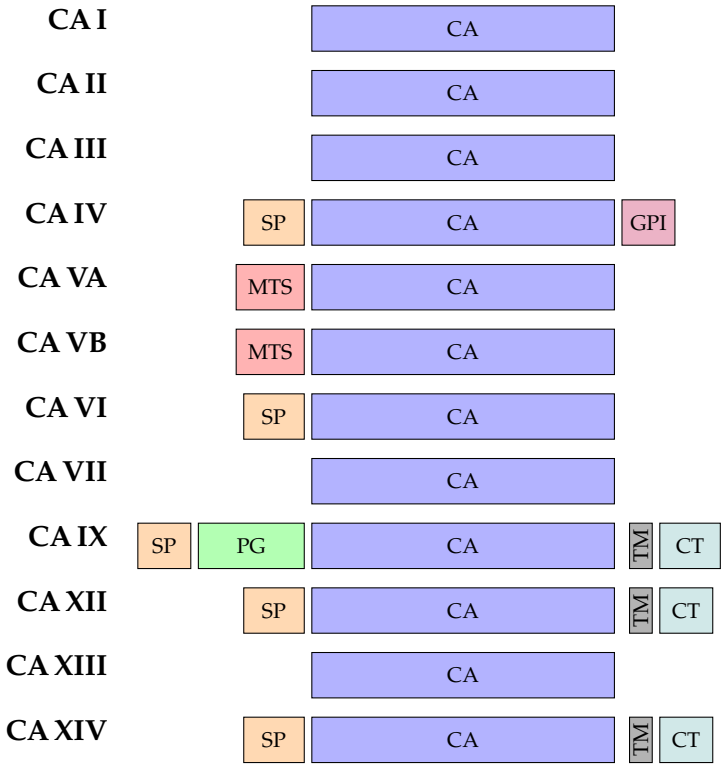

Figure 1.7: Domain organization of catalytically active human CAs. Catalytic carbonic anhydrase domains (CA) are shown together with signal peptides (SP), mitochondrial targeting sequences (MTS), the proteoglycan-like domain (PG), transmembrane helices (TM), cytoplasmic tails (CT), and the GPI-anchor region. Carbonic anhydrase-related proteins (CARPs) are not shown; despite retaining the carbonic anhydrase domain architecture, substitutions of residues required for catalytic zinc coordination render them catalytically inactive.

and solvent structure, providing the basis for mechanistic interpretation of catalysis [90]. Subsequent structural and kinetic investigations identified the central role of His64 as a proton shuttle and characterized the conserved hydrogen-bond network involved in proton transfer and stabilization of the zinc-bound solvent molecule [42, 91, 92]. Mutagenesis combined with crystallographic analysis further clarified the contributions of active-site residues to catalysis, inhibitor binding, and stabilization of the catalytic water network [93, 94]. More recent ultrahigh-resolution X-ray and neutron diffraction studies provided direct insight into protonation states, hydrogen-bonding patterns, and active-site water organization, substantially advancing understanding of

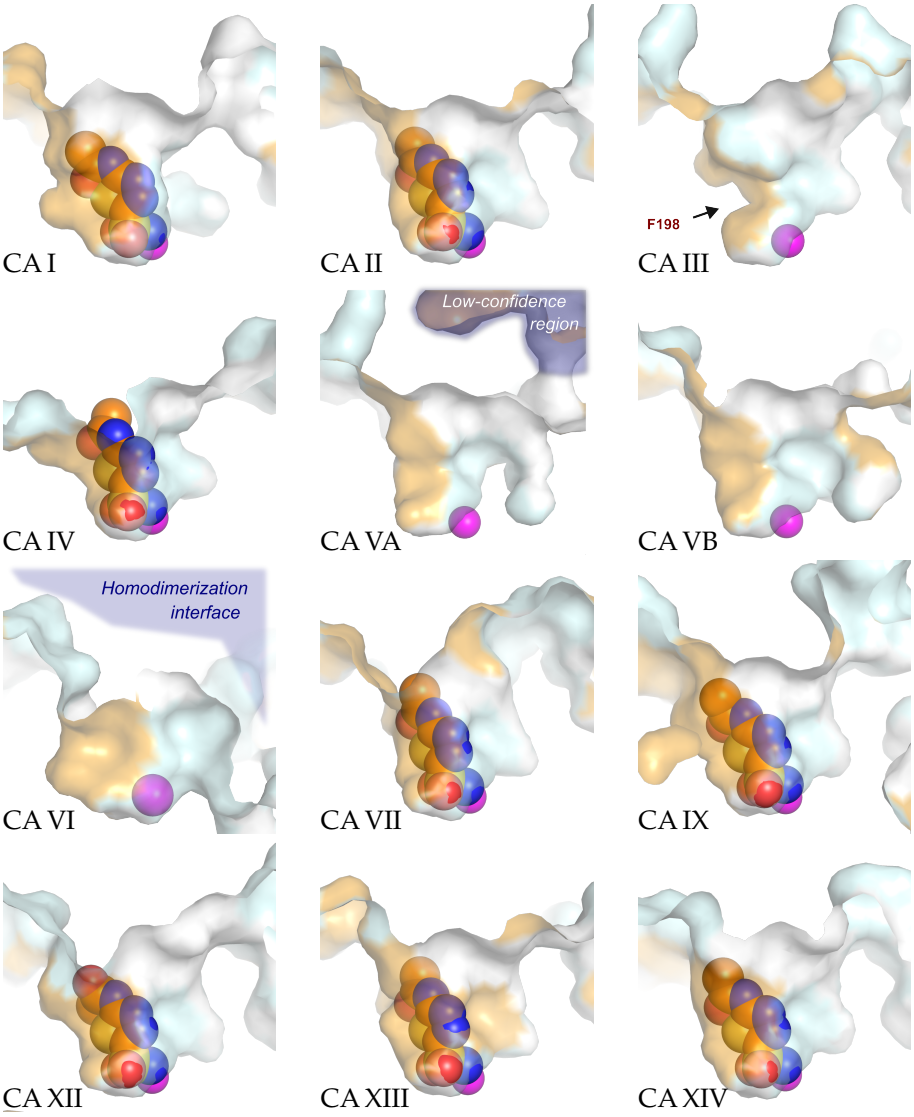

Figure 1.8: Surface representations of active-site cavities in CA isozymes (hydrophobic: orange, hydrophilic: cyan, zinc: magenta sphere). AZM, where available in the experimental structure, indicates the sulfonamide-binding region. In CA III, the bulky Phe198 residue partially occludes the active-site cavity and contributes to its reduced affinity for sulfonamide inhibitors. CA VI forms a homodimer with the dimer interface located adjacent to the active-site entrance, while the catalytic site remains accessible. Experimental structures and PDB IDs are the same as in Figure 1.5. Representations of CA VA and CA VB were generated from AlphaFold-predicted structures (AF-A0A3B3ITA6-F1 and AF-Q9Y2D0-F1, respectively); a low-confidence region of the CA VA model is marked, as it overlaps with the active-site entrance and may lead to a misleading interpretation of ligand access.

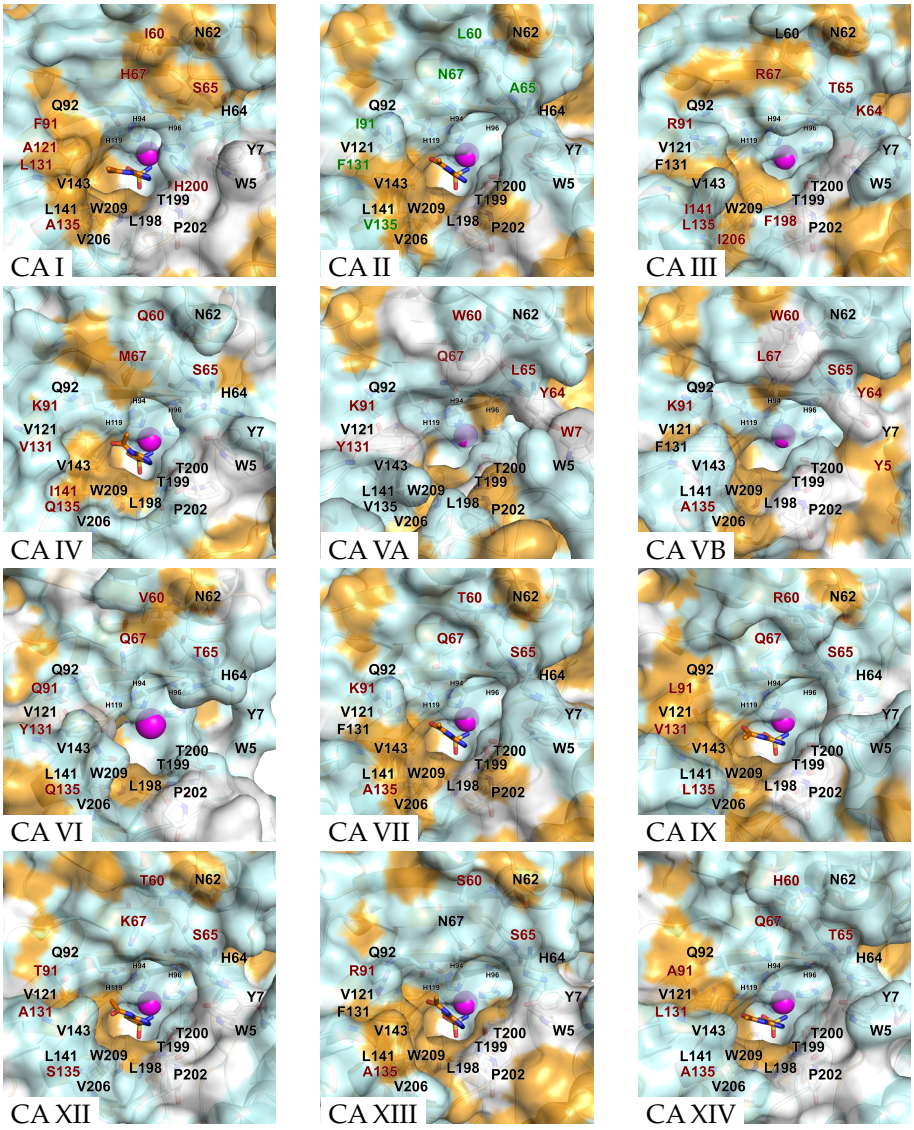

Figure 1.9: Detailed surface representations of the region surrounding the catalytic Zn^{II} ion (magenta sphere) in CAs. Hydrophobic and hydrophilic surface regions are colored orange and cyan, respectively. Residues are numbered according to CA II, which is the most extensively characterized and is used as the reference isozyme for comparison. In CA II, residues shown in green indicate positions exhibiting sequence variability among CAs. In the other isozymes, residues shown in red differ from the corresponding residues of CA II. These variable positions may contribute to differences in inhibitor recognition and isozyme selectivity. Structural models and PDB/AlphaFold entries are the same as those used previously in Figure 1.5 and Figure 1.8.

the catalytic mechanism and solvent dynamics in CA II [45, 95]. Recent work has additionally highlighted the importance of active-site water dynamics for efficient catalysis and product release [51].

CA III

Among the cytosolic carbonic anhydrases, CA III possesses one of the most distinctive active-site environments. The most characteristic substitution is Lys64 replacing the proton shuttle residue His64 of CA II, which substantially reduces proton-transfer efficiency and catalytic turnover [96]. Another important substitution is Phe198 replacing Leu198 near the active-site entrance. The bulky phenylalanine side chain partially restricts access to the active-site cavity and introduces steric hindrance that affects accommodation of sulfonamide inhibitors, contributing to weaker inhibitor affinities compared with CA II. In addition, CA III contains reactive surface-exposed cysteine residues, particularly Cys181 and Cys186, which are susceptible to oxidative modification and are implicated in redox regulation and protection against oxidative stress.

CA IV

CA IV is an extracellular membrane-associated isozyme attached to the cell surface through a glycosylphosphatidylinositol (GPI) anchor [97]. The catalytic domain is additionally stabilized by a disulfide bond between Cys6 and Cys11 and by several glycosylation sites that influence hydration properties near the active-site entrance. Compared with cytosolic isozymes, CA IV exhibits a narrower and less solvent-accessible catalytic cavity, with substitutions including Gln60, Met67, Lys91, Val131, Ile141, and Gln135 around the active-site cavity. Relative to CA II, substitutions around the active-site cavity include Leu60→Gln, Asn67→Met, Ile91→Lys, Phe131→Val, Leu141→Ile, and Ala135→Gln. Leu60→Gln and Ala135→Gln introduce polar amide groups, Asn67→Met removes an amide group and introduces a hydrophobic thioether side chain, and Ile91→Lys introduces a positively charged side chain. Phe131→Val removes a bulky aromatic ring while retaining hydrophobic character, whereas Leu141→Ile represents a comparatively conservative hydrophobic substitution.

CA VA and CA VB

No experimentally determined structures are currently available for the mitochondrial isozymes CA VA and CA VB. Structural insights are therefore derived from sequence analysis and homology models based on structurally characterized human carbonic anhydrases, particularly CA II [98]. These models indicate that both isozymes retain the catalytic zinc-coordinating residues His94, His96, and His119, suggesting conservation of the canonical catalytic mechanism. Despite the highly conserved catalytic core, several substitutions surrounding the active-site cavity distinguish CA VA and CA VB from CA II. In CA VA, Leu60→Trp, His64→Tyr, Ser65→Leu, Asn67→Gln, Ile91→Lys, Phe131→Tyr, and Ala135→Val are observed, whereas CA VB contains Leu60→Trp, His64→Tyr, Asn67→Leu, and Ile91→Lys, while Ser65, Phe131, and Ala135 are conserved relative to CA II. Leu60→Trp introduces a substantially bulkier aromatic side chain in both mitochondrial isozymes, while His64→Tyr replaces the proton-shuttling imidazole group with a phenolic aromatic side chain. Ile91→Lys replaces a hydrophobic side chain with a positively charged one. In CA VA, Ser65→Leu removes a hydroxyl group and introduces a larger hydrophobic side chain, Phe131→Tyr adds a hydroxyl group while retaining the aromatic ring, and Ala135→Val increases the size and hydrophobic character of the side chain. In CA VB, Asn67→Leu removes a polar amide group and introduces a hydrophobic aliphatic side chain. Both isozymes additionally contain N-terminal mitochondrial targeting sequences that are removed during mitochondrial import, yielding mature enzymes localized within the mitochondrial matrix.

CA VI

CA VI is the only secreted member of the human α-carbonic anhydrase family and forms a homodimer [99]. In addition, several N-glycosylation sites, including Asn67 and Asn256 (CA VI numbering), contribute to extracellular stability and hydration of the protein surface. Compared with CA II, the active-site entrance of CA VI is wider and more solvent exposed, altering the organization of active-site water molecules and accommodation of aromatic inhibitor fragments. The active-site cavity also contains several substitutions relative to CA II: Leu60→Val, Ser65→Thr, Asn67→Gln, Ile91→Gln, Phe131→Tyr, and Ala135→Gln. Leu60→Val represents a conservative hydrophobic substitution with a smaller side chain, whereas Ser65→Thr adds a

methyl group while retaining the hydroxyl functionality. Asn67→Gln extends the amide-containing side chain by one methylene group. More pronounced changes occur at positions 91 and 135, where Ile91→Gln and Ala135→Gln replace hydrophobic side chains with polar amide-containing groups. Phe131→Tyr retains the aromatic ring but introduces a hydroxyl group capable of hydrogen bonding.

CA VII

CA VII is among the most catalytically active cytosolic carbonic anhydrases and retains the proton shuttle residue His64 responsible for efficient proton transfer (Ugochukwu *et. al.*, PDB ID: 3MDZ). The active-site cavity contains an extended hydrophobic cluster formed by Phe131, Val143, Leu198, and Trp209, facilitating accommodation of both CO_2 and hydrophobic ligand fragments. Relative to CA II, the active-site region of CA VII contains the substitutions Leu60→Thr, Asn67→Gln, and Ile91→Lys, while Ala135 and Phe131 are conserved. Leu60→Thr replaces a hydrophobic side chain with a smaller hydroxyl-containing residue, whereas Asn67→Gln extends the amide-containing side chain by one methylene group. Ile91→Lys represents the most pronounced change, replacing a hydrophobic side chain with a positively charged lysine side chain. In addition, reactive cysteine residues, particularly Cys183 and Cys217, may undergo oxidative modifications that affect enzyme activity and structural stability.

CA IX

CA IX is a multidomain transmembrane carbonic anhydrase composed of an N-terminal proteoglycan-like (PG) domain, catalytic domain, transmembrane (TM) segment, and short intracellular (IC) tail [100, 101]. The PG domain forms a highly hydrated and negatively charged extracellular region that contributes to enzyme stability and interactions with the tumor microenvironment, while the extracellular catalytic domains form a homodimer [100, 101]. Crystal structures of the catalytic domain revealed several active-site substitutions relative to CA II, including Leu60→Arg, Ile91→Leu, Phe131→Val, and Ala135→Leu. Leu60→Arg replaces a hydrophobic side chain with a positively charged guanidinium-containing group. The Ile91→Leu substitution preserves a hydrophobic side chain but changes its branching

and local steric profile, whereas Phe131→Val removes the bulky aromatic phenyl group while retaining hydrophobic character. The latter substitution therefore increases the available space adjacent to position 131. Ala135→Leu introduces a larger hydrophobic side chain at the cavity wall. These substitutions generate a more hydrophobic and sterically accessible selective pocket capable of accommodating bulky tail-containing sulfonamide inhibitors and represent key determinants of CA IX selectivity [63]. CA IX additionally contains an intramolecular disulfide bond (Cys119–Cys299) and an N-glycosylation site at Asn309 that contribute to extracellular stability and hydration. The TM segment anchors the enzyme to the plasma membrane, whereas the IC tail contains phosphorylation sites implicated in regulation of enzyme activity and cellular signaling under hypoxic conditions.

CA XII

CA XII is a membrane-associated carbonic anhydrase that forms extracellular homodimers and contains a catalytic domain connected to a single-pass transmembrane segment through a flexible stalk region [98, 102]. Compared with CA IX, the active-site cavity of CA XII is narrower and more hydrophilic. Relative to CA II, the active-site region contains the substitutions Asn67→Lys, Ile91→Thr, Phe131→Ala, and Ala135→Ser. Asn67→Lys replaces a neutral amide-containing side chain with a positively charged amino group, while Ile91→Thr replaces a hydrophobic side chain with a smaller hydroxyl-containing residue. Phe131→Ala removes the bulky aromatic phenyl group and substantially reduces side-chain volume, whereas Ala135→Ser introduces a hydroxyl group with only a small increase in side-chain size. Consequently, the selective pocket of CA XII is less hydrophobic than that of CA IX, contributing to differences in inhibitor specificity and binding thermodynamics [102]. Several extracellular glycosylation sites, including Asn28 and Asn80, contribute to protein stability and hydration, while the short intracellular tail contains phosphorylation sites implicated in regulation of catalytic activity and membrane-associated signaling.

CA XIII

CA XIII exhibits active-site properties intermediate between highly active CA II and low-activity CA III [103]. Unlike CA III, it retains the

proton shuttle residue His64, allowing efficient proton-transfer activity. Relative to CA II, the active-site region contains the substitutions Leu60→Ser, Asn67→Ser, and Ile91→Arg, while Ser65 is conserved. Leu60→Ser replaces a hydrophobic side chain with a smaller hydroxyl-containing residue, and Asn67→Ser replaces an amide group with a shorter hydroxyl-containing side chain. Ile91→Arg represents the most pronounced change, replacing a hydrophobic side chain with a larger, positively charged guanidinium-containing side chain. Compared with CA II, the active-site cavity of CA XIII is slightly narrower and exhibits altered surface electrostatics near the active-site entrance. Differences in the arrangement of ordered water molecules surrounding Thr199 and the zinc-bound solvent further influence inhibitor orientation and binding thermodynamics, contributing to catalytic and inhibitor-binding properties distinct from those of both CA II and CA III [103].

CA XIV

CA XIV is a transmembrane carbonic anhydrase with a compact extracellular catalytic domain [104]. Compared with CA IX and CA XII, its active-site cavity is narrower, more sterically constrained, and less solvent accessible. Relative to CA II, the active-site region contains the substitutions Leu60→His, Ser65→Thr, Asn67→Gln, Ile91→Ala, and Phe131→Leu, while Ala135 is conserved. Leu60→His replaces a hydrophobic side chain with an imidazole-containing residue, whereas Ser65→Thr adds a methyl group while retaining the hydroxyl functionality. Asn67→Gln extends the amide-containing side chain by one methylene group. Ile91→Ala substantially reduces the size of the hydrophobic side chain, while Phe131→Leu removes the aromatic phenyl group but retains a hydrophobic side chain. In addition, extracellular glycosylation sites contribute to surface hydration and structural stability. Differences in loop organization and electrostatic surface properties surrounding the active-site cavity further contribute to isozyme-dependent inhibitor selectivity and binding thermodynamics [104].

Catalytic Mechanism

The active-site environment lowers the $\mathrm{p}K_{\mathrm{a}}$ of the zinc-bound water molecule, favoring formation of the catalytically active hydroxide ion under physiological conditions (Figure 1.10). Classical mechanistic

studies [105] highlighted the importance of both hydration/dehydration reaction steps and proton-transfer processes.

The catalytic cycle is generally described as a two-step ping-pong mechanism [62]: (i) **Hydration of CO_2:** CO_2 binds within a hydrophobic pocket near the zinc-bound hydroxide ion. The hydroxide ion attacks the CO_2, forming a zinc-bound bicarbonate, which is subsequently displaced by a water molecule. (ii) **Proton transfer (enzyme regeneration):** the zinc-bound water molecule must be deprotonated to regenerate the catalytically active hydroxide ion. This proton transfer step is generally considered rate-limiting.

The residue His64 (in CA II) plays a central role as a proton shuttle. Its imidazole side chain alternates between inward and outward conformations, thereby transferring protons between the active site and the bulk solvent. Mutagenesis and structural studies demonstrated that substitution of His64 significantly reduces catalytic efficiency.

Additionally, networks of hydrogen-bonded water molecules in the active-site cavity connect the zinc-bound water to His64. These ordered networks are stabilized by surrounding hydrophilic residues and serve as proton transfer pathways (Figure 1.10). Neutron crystallography and computational simulations have provided further insights into protonation states, hydrogen atom positions, and alternative proton-transfer mechanisms, emphasizing the importance of protein dynamics in catalysis [106, 107].

1.3.2 Sulfonamides as Carbonic Anhydrase Inhibitors

Among the diverse classes of CA inhibitors, sulfonamides remain the most thoroughly investigated and clinically relevant [110–113]. Primary sulfonamides contain a sulfonamide group (-SO_2NH_2) that, upon deprotonation, coordinates directly to the catalytic zinc ion. The sulfonamide nitrogen displaces the zinc-bound water molecule, forming a tetrahedral complex that prevents substrate access and effectively halts catalysis (Figure 1.10). The primary sulfonamide group therefore provides a conserved zinc-binding anchor, whereas the remainder of the molecule can be modified to establish additional interactions within the active-site cavity. These interactions can modulate both binding affinity and isozyme selectivity.

Clinically used CA inhibitors containing sulfonamide or related zinc-binding groups encompass considerable structural diversity, including

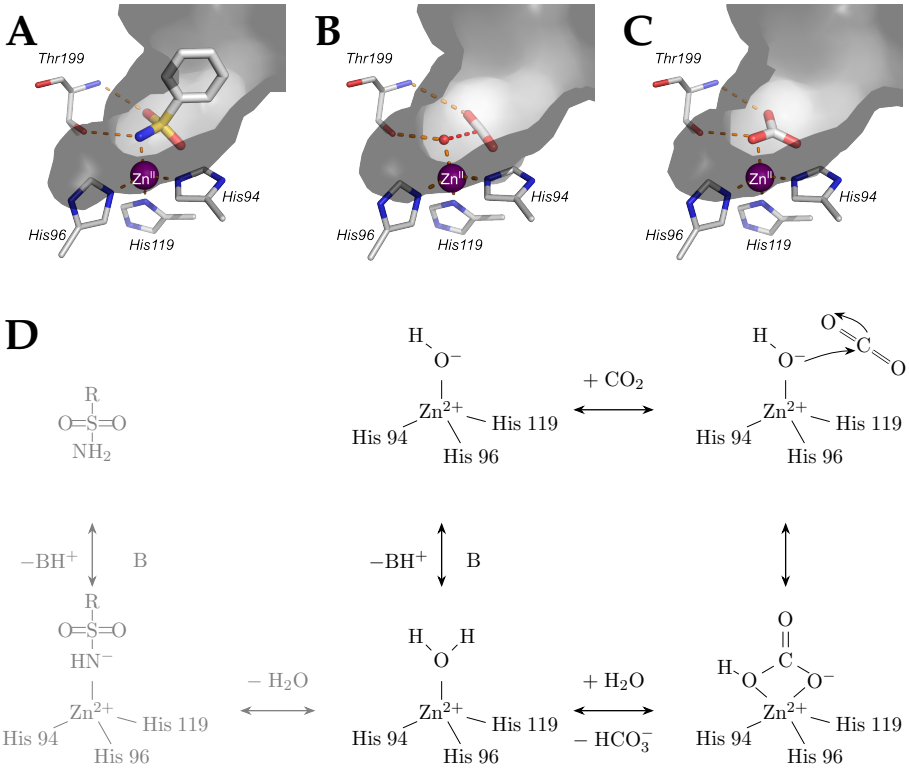

Figure 1.10: Structural and mechanistic views of catalysis and inhibition in human CA II. The catalytic Zn^{II} ion (magenta) is coordinated by His94, His96, and His119; Thr199 participates in the interaction network. Dashed lines indicate zinc coordination and H-bonds. (A) Benzenesulfonamide bound to Zn^{II} (PDB ID: 6GDC; closely mimics the transition state of the substrate hydration reaction [108]). (B) CO_2 adjacent to zinc-bound hydroxide (PDB ID: 2VVA). (C) Bicarbonate bound to Zn^{II} (PDB ID: 2VVB). (D) The catalytic cycle shows CO_2 hydration and enzyme regeneration via proton transfer. Inhibition (grey) illustrates sulfonamide coordination to Zn^{II} and the associated proton-linked equilibria. These proton-linked events (B/BH^+) must be accounted for to determine intrinsic thermodynamic parameters that reflect protein–ligand interaction energetics.

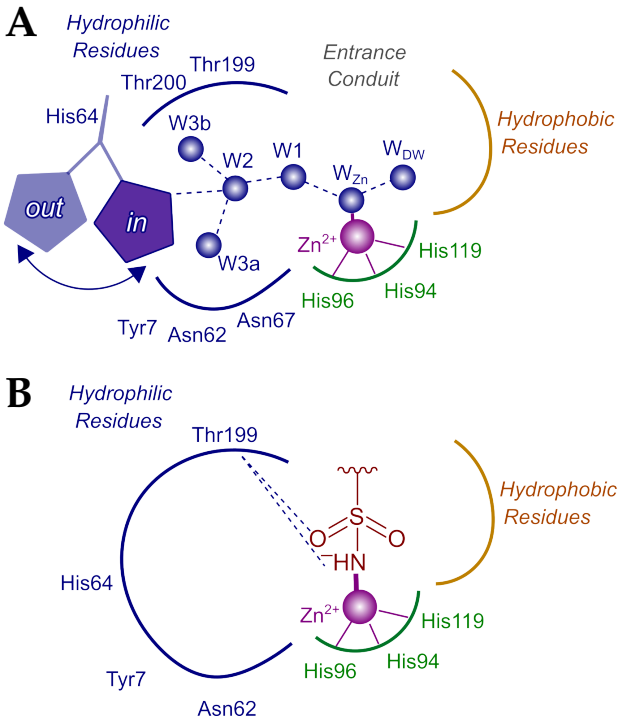

Figure 1.11: Active-site water network and general sulfonamide binding in carbonic anhydrases. (A) Schematic representation of the active-site water network in CA II, based on recent structural studies of CA II water dynamics [51]. The catalytic Zn^{II} ion is coordinated by His94, His96, and His119, while an ordered network of water molecules (W_{Zn}, W1, W2, W3a, and W3b) connects the catalytic center to the proton-shuttling residue His64 through a hydrophilic region formed by Tyr7, Asn62, Asn67, Thr199, and Thr200. This water network plays a central role in proton transfer and catalysis. Similar water-mediated architectures likely exist in other α-carbonic anhydrases, but none have been characterized in comparable detail to CA II. (B) General binding mode of sulfonamide inhibitors in carbonic anhydrases. The sulfonamide zinc-binding group forms conserved interactions with Zn^{II} and Thr199 and occupies a highly conserved position. In contrast, the attached substituents can adopt markedly different orientations and interaction patterns depending on their size, flexibility, and chemical composition, often extending toward distinct regions of the active-site cavity.

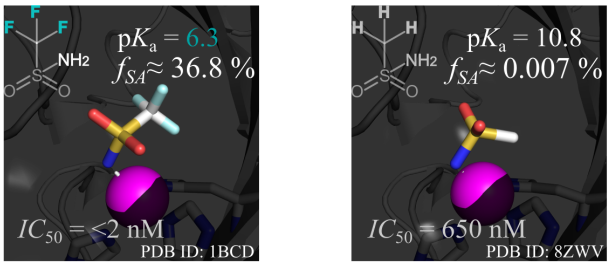

Figure 1.12: Influence of sulfonamide acidity on carbonic anhydrase observed inhibition and binding. Comparison of trifluoromethanesulfonamide (TFMSA, left) and methanesulfonamide (MSA, right) bound to human CA II. The two inhibitors adopt similar binding modes, coordinating the catalytic Zn^{II} ion through the deprotonated sulfonamide nitrogen. Replacement of the methyl group with the strongly electron-withdrawing trifluoromethyl group lowers the sulfonamide $pK_{a,SA}$ from 10.8 to 6.3, increasing the fraction of the zinc-binding sulfonamide anion (f_{SA}) at pH 7.0 from approximately $0.007\,\%$ to $36.8\,\%$. Consequently, the markedly improved inhibitory potency of TFMSA ($IC_{50} < 2\,nM$) relative to MSA ($IC_{50} = 650\,nM$) arises primarily from a greater population of the active, deprotonated zinc-binding species rather than from substantial differences in protein–ligand interactions. Structures are shown from PDB entries 1BCD (TFMSA) and 8ZWV (MSA); pK_a and IC_{50} values were taken from the literature [109].

compounds developed specifically as CA inhibitors as well as compounds developed primarily for other therapeutic targets (Figure 1.13). Despite their structural diversity, these compounds generally show limited selectivity among individual CA isozymes.

An important consequence of this binding mechanism is its dependence on protonation equilibria. Because binding of sulfonamide inhibitors to carbonic anhydrases is coupled to protonation and deprotonation equilibria, experimentally observed binding parameters do not directly reflect the intrinsic protein–ligand interaction strength. The equations used to eliminate the contributions of linked protonation reactions and calculate intrinsic binding parameters are provided in the Methods section. Figure 1.12 illustrates one of the most striking examples of the importance of considering intrinsic rather than observed parameters: despite nearly identical binding modes, methanesulfonamide and trifluoromethanesulfonamide differ dramatically in apparent potency owing primarily to differences in sulfonamide acidity and the resulting population of the zinc-binding anionic species. This example

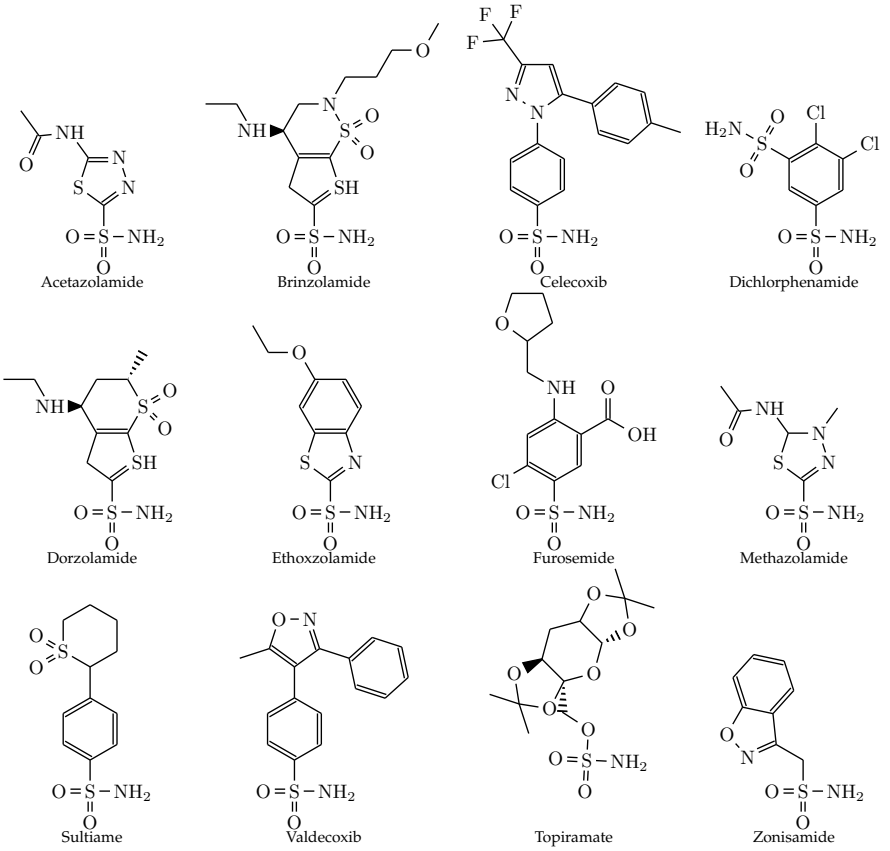

Figure 1.13: Chemical structures of selected clinically relevant sulfonamide and sulfamate carbonic anhydrase inhibitors. A more comprehensive review of CA inhibitors was provided by Kojis *et al.* [114]. Acetazolamide, one of the earliest systemic CA inhibitors, was introduced into clinical practice in the 1950s and remains in use for several indications. Methazolamide is also a systemic CA inhibitor, whereas dorzolamide and brinzolamide were developed for topical treatment of glaucoma. Dichlorphenamide, another early systemic CA inhibitor, is currently used for the treatment of primary periodic paralysis, while ethoxzolamide has little current clinical use. Sulthiame, topiramate, and zonisamide are antiepileptic drugs with CA-inhibitory activity, whereas furosemide, celecoxib, and valdecoxib were developed primarily for pharmacological targets other than CAs but also inhibit CA isozymes. Together, these compounds illustrate the structural and pharmacological diversity of CA-inhibiting drugs, many of which show limited selectivity among individual CA isozymes.

highlights the importance of intrinsic binding parameters for correctly assessing binding strength and guiding compound design.

In addition to direct coordination, sulfonamide inhibitors frequently engage in secondary hydrophobic and hydrogen-bonding interactions with residues lining the active site. These interactions substantially enhance both binding affinity and isozyme selectivity. Structural modifications of the aromatic or heterocyclic substituents have been shown to influence selectivity, which remains a critical challenge in the development of clinically useful CA inhibitors.

The therapeutic applications of sulfonamide-based CA inhibitors are extensive and include the treatment of glaucoma, epilepsy, edema, while inhibition of tumor-associated CA isozymes, particularly CA IX and CA XII, is being investigated as a therapeutic strategy for hypoxic solid tumors [86]. For example, inhibition of CA isozymes in the ciliary body of the eye reduces aqueous humor secretion, thereby lowering intraocular pressure in glaucoma patients. A detailed overview of clinically used CA inhibitors, their therapeutic applications, and emerging CA-targeted drugs is provided elsewhere [114].

Acetazolamide (AZM) is the classical and most extensively studied sulfonamide carbonic anhydrase inhibitor and has been widely used both clinically and as a model compound in structural and mechanistic studies of CA inhibition. Although AZM exhibits high affinity toward carbonic anhydrases and is often described as a selective CA inhibitor relative to other classes of proteins, it displays limited selectivity among CA isozymes, inhibiting a broad range of isozymes with comparable potency. Consequently, AZM is frequently employed as a reference inhibitor in structure-based drug design, serving as a starting point for the development of next-generation inhibitors with improved isozyme selectivity. The combination of a conserved sulfonamide–zinc binding mode and variable interactions with the surrounding active-site environment makes CA–sulfonamide complexes a particularly useful model system for investigating the structural determinants of ligand affinity, selectivity, and binding thermodynamics.

Chapter 2

Methods

Figure 2.1 summarizes the experimental and analytical workflow used in this dissertation. Recombinant carbonic anhydrases and sulfonamide inhibitors constituted the primary study materials.

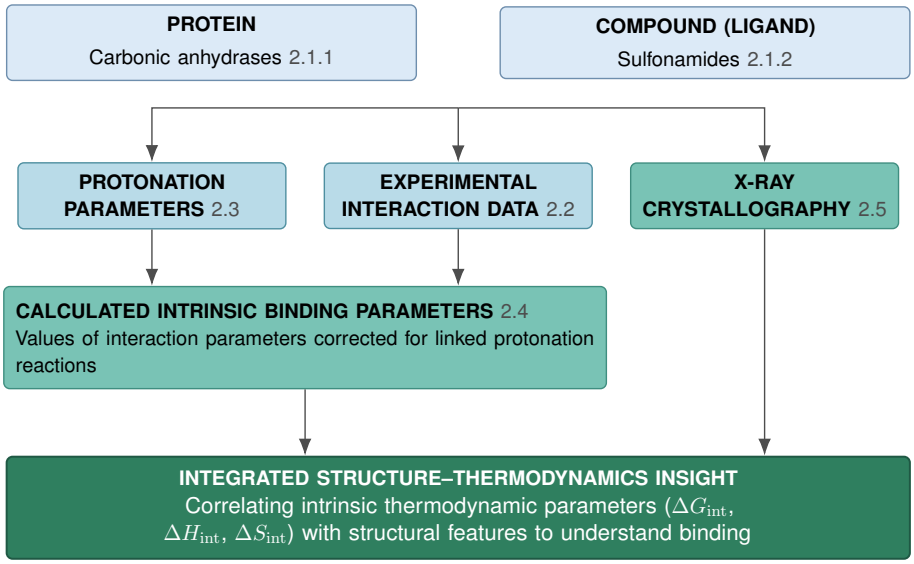

Figure 2.1: Workflow of the main experimental and computational approaches used in this dissertation. Observed protein–ligand interaction data and protonation parameters were combined to calculate intrinsic thermodynamic parameters, which were subsequently integrated with structural information obtained by X-ray crystallography.

Protein–ligand interactions were characterized using biophysical

methods, primarily FTSA and ITC, yielding observed binding constants and thermodynamic parameters. In parallel, protonation parameters of the ligands were determined experimentally, while corresponding protonation parameters of carbonic anhydrase isozymes were obtained from previous studies.

Observed binding parameters were subsequently corrected for linked protonation reactions to derive intrinsic thermodynamic parameters that are independent of experimental conditions and therefore more suitable for comparison across systems. Structural information on protein–ligand complexes was obtained by X-ray crystallography. Finally, intrinsic thermodynamic parameters were integrated with structural data to identify correlations between binding energetics, and molecular recognition, providing insights relevant to inhibitor design. Together, these approaches enabled analysis of relationships between protein–ligand binding thermodynamics and structural features of carbonic anhydrase–inhibitor complexes.

2.1 Materials

2.1.1 Carbonic Anhydrase Isozymes

The CA expression and purification platform used in this work was developed and maintained through the contributions of numerous laboratory members and collaborators over many years. The author gratefully acknowledges these contributions and the protein resources made available for this study.

Twelve CA isoforms were produced recombinantly as full-length proteins or truncated constructs retaining the catalytic domain. Most isoforms were expressed in *Escherichia coli*, using expression strains selected according to the requirements of individual proteins, including BL21(DE3), Rosetta 2(DE3), and Origami B(DE3) [115]. Because stable recombinant CA IX could not be obtained in bacterial cells, its catalytic domain was produced using mammalian expression systems (FreeStyle 293-F or Expi293F) [115]. Proteins were purified using isozyme-specific combinations of Ni^{2+}-chelation, ion-exchange, and sulfonamide-based ligand-affinity chromatography. Protein purity, molecular mass, and catalytic activity were assessed by SDS-PAGE, high-resolution mass spectrometry (HR-MS), and stopped-flow CO_2 hydration assays, respectively. Detailed construct sequences, expression conditions, and

purification procedures are provided in [115].

Information on the recombinant proteins can be also accessed through the PLBD: https://plbd.org/db/main/protein. Experimental datasets and the corresponding protein batches used in the experiments are linked and described within the database.

Protein samples were stored at $-80\,^{\circ}\mathrm{C}$. Prior to experiments, proteins were buffer-exchanged into the corresponding experimental buffers when necessary. The concentrations of CA isozymes were determined spectrophotometrically using their respective molar extinction coefficients at $280\,\mathrm{nm}$.

2.1.2 Sulfonamide Inhibitors

Sulfonamide compounds investigated in this work were synthesized in-house by laboratory collaborators. Different synthetic strategies were employed depending on the compound series, including nucleophilic substitution, alkylation, amidation, and oxidation reactions. Compound identity and purity were confirmed using appropriate analytical methods, primarily NMR spectroscopy and mass spectrometry. Detailed synthesis, purification, and characterization procedures are described in the corresponding publications on which this dissertation is based. Information on the synthesized compounds, including their laboratory identifiers, is available through PLBD (https://plbd.org/db/main/compound).

Stock solutions of all compounds were prepared in DMSO at concentrations of $10\,\mathrm{mM}$ to $50\,\mathrm{mM}$ and subsequently diluted in the appropriate experimental buffers prior to use.

2.2 Experimental Determination of Protein–Ligand Interactions

A combination of biophysical, biochemical, and structural methods was employed to characterize carbonic anhydrase–ligand interactions and to establish relationships between binding energetics and molecular recognition. The overall strategy of this dissertation was to obtain experimental binding parameters, correct them for linked protonation reactions to derive intrinsic thermodynamic parameters, and subsequently

integrate these data with structural information obtained by X-ray crystallography (Section 2.5). These included fluorescent thermal shift assay (FTSA) [116, 117], isothermal titration calorimetry (ITC) [118], X-ray crystallography [119–121], stopped-flow measurements of CO_2 hydration activity [122], and other complementary approaches described in the corresponding publications included in the dissertation.

The Methods section summarizes the experimental approaches and procedures relevant to the interpretation of the results presented in this dissertation. Complete experimental protocols, study-specific conditions, instrumentation, and data analysis procedures are reported in the corresponding publications included. Further methodological details and comparisons between the experimental approaches are provided in the corresponding reviews and standard operating procedures (SOPs) [20, 26, 123, 124].

To ensure data traceability and reproducibility, experimental datasets and associated metadata were recorded in the Protein–Ligand Binding Database (PLBD; https://plbd.org) [125]. Structural data obtained by X-ray crystallography were deposited in the Protein Data Bank (PDB).

2.2.1 Fluorescent Thermal Shift Assay

FTSA served as the primary method for determining observed binding constants for large numbers of carbonic anhydrase–inhibitor complexes included in this dissertation. The resulting observed binding constants were subsequently corrected for linked protonation reactions to obtain intrinsic binding constants, as described in Section 2.4.

Protein thermal stability was monitored using FTSA, which detects heat-induced protein unfolding using environmentally sensitive fluorescent dyes. As the protein unfolds, hydrophobic regions become exposed and interact with the fluorescent dye, resulting in changes in fluorescence intensity that can be monitored as a function of temperature [126, 127].

Ligand binding alters protein thermal stability and shifts the protein melting temperature (T_m). Protein–ligand binding constants were derived from ligand-induced thermal stabilization curves using thermodynamic models implemented in Microsoft Excel and later in the Thermott web server (thermott.com) [128] developed in our laboratory.

2.2.2 Isothermal Titration Calorimetry

Isothermal titration calorimetry (ITC) was used to directly measure the heat released or absorbed during protein–ligand binding [129]. The method provided observed binding enthalpies, binding constants, and binding stoichiometries, from which Gibbs energy and entropy changes were calculated. These observed thermodynamic parameters were subsequently corrected for linked protonation reactions to obtain intrinsic binding parameters (see Section 2.4).

To evaluate linked protonation reactions accompanying ligand binding, selected experiments were performed in buffers with different ionization enthalpies [11]. The resulting thermodynamic parameters were subsequently used for the calculation of intrinsic binding constants and intrinsic thermodynamic parameters.

Analysis of ITC datasets involved baseline determination, peak integration, model fitting, and thermodynamic parameter extraction. Depending on the study, calorimetric data were analyzed using manufacturer-provided software and/or specialized ITC software packages, including NITPIC [130, 131], SEDPHAT [131, 132], and GUSSI [133]. Particular attention was devoted to the quality assessment and fitting of calorimetric data, as accurate determination of binding enthalpies was essential for subsequent correction of linked protonation reactions.

2.3 Determination of Protonation Parameters

2.3.1 Sulfonamide $\mathrm{p}K_\mathrm{a}$ Measurements

The acid dissociation constants ($\mathrm{p}K_\mathrm{a}$) of sulfonamide inhibitors were determined experimentally using UV–Vis spectrophotometric titration [56]. The measurements rely on changes in the absorption spectra accompanying protonation and deprotonation of the sulfonamide group. Spectra were recorded at different pH values, and the resulting pH-dependent absorbance changes were fitted to obtain $\mathrm{p}K_\mathrm{a}$ values.

The experimentally determined $\mathrm{p}K_\mathrm{a}$ values were subsequently used to calculate the fractions of binding-ready ligand species required for correction of observed thermodynamic parameters and to derive intrinsic thermodynamic parameters of carbonic anhydrase–sulfonamide binding.

2.3.2 Sulfonamide Protonation Enthalpy Measurements

The protonation enthalpies of sulfonamide inhibitors were determined by isothermal titration calorimetry (ITC). The measurements were based on the heat associated with protonation of the deprotonated sulfonamide group during titration with a strong acid. The resulting calorimetric data were analyzed to obtain the protonation enthalpy ($\Delta H_{\mathrm{pr,SA}}$) of each compound.

The experimentally determined protonation enthalpies were subsequently used to correct observed binding enthalpies and calculate intrinsic thermodynamic parameters of carbonic anhydrase–sulfonamide interactions.

2.4 Calculation of Intrinsic Thermodynamic Parameters

Intrinsic thermodynamic parameters reflect the energetic contributions of the protein–ligand interaction itself and therefore provide a more suitable basis for comparison of structurally diverse complexes than the experimentally observed parameters.

Structural studies have demonstrated that sulfonamide inhibitors bind in their deprotonated form by coordinating the active-site $\mathrm{Zn^{II}}$ ion and displacing the zinc-bound water molecule [107]. Because only a fraction of both the ligand and the enzyme is present in the binding-competent form under a given set of experimental conditions, the measured binding constants and enthalpies represent observed thermodynamic parameters that depend on pH, buffer composition, and protonation equilibria [11, 12].

To enable direct comparison of thermodynamic and structural data, observed binding parameters were converted into intrinsic thermodynamic parameters by correcting for linked protonation reactions. Figure 1.12 provides one of the most striking examples of the importance of intrinsic over observed parameters in carbonic anhydrase inhibition and binding.

2.4.1 Correction of Binding Constants

The intrinsic binding constant, $K_{\mathrm{b,int}}$, was calculated from the observed binding constant, $K_{\mathrm{b,obs}}$, and the fractions of the binding-competent forms of the protein (f_{CA}) and ligand (f_{SA}):

$$K_{\mathrm{b,int}} = \frac{K_{\mathrm{b,obs}}}{f_{\mathrm{CA}} \cdot f_{\mathrm{SA}}} \tag{2.1}$$

The fraction of the protonated enzyme was calculated as

$$f_{\mathrm{CA}} = \frac{10^{\mathrm{p}K_{\mathrm{a,CA}} - \mathrm{pH}}}{1 + 10^{\mathrm{p}K_{\mathrm{a,CA}} - \mathrm{pH}}} \tag{2.2}$$

and the fraction of the deprotonated sulfonamide inhibitor as

$$f_{\mathrm{SA}} = \frac{10^{\mathrm{pH} - \mathrm{p}K_{\mathrm{a,SA}}}}{1 + 10^{\mathrm{pH} - \mathrm{p}K_{\mathrm{a,SA}}}}. \tag{2.3}$$

Here, $\mathrm{p}K_{\mathrm{a,CA}}$ denotes the acid dissociation constant of the zinc-bound water molecule in the enzyme active site and $\mathrm{p}K_{\mathrm{a,SA}}$ the acid dissociation constant of the sulfonamide group.

The intrinsic Gibbs energy of binding, ΔG_{int}, was then calculated from $K_{\mathrm{b,int}}$ using the standard thermodynamic relationship

$$\Delta G_{\mathrm{int}} = -RT \ln(K_{\mathrm{b,int}}). \tag{2.4}$$

2.4.2 Correction of Binding Enthalpies and Entropies

The intrinsic binding enthalpy, ΔH_{int}, was obtained by correcting the observed binding enthalpy, ΔH_{obs}, for proton transfer reactions associated with ligand deprotonation, deprotonation of the zinc-bound water molecule, and protonation of the experimental buffer:

$$\Delta H_{\mathrm{int}} = \Delta H_{\mathrm{obs}} - n_1 \Delta H_{\mathrm{pr,SA}} - n_2 \Delta H_{\mathrm{pr,CA}} + (n_1 + n_2) \Delta H_{\mathrm{pr,buf}} \tag{2.5}$$

where

$$n_1 = f_{\mathrm{SA}} - 1 \tag{2.6}$$

$$n_2 = 1 - f_{\mathrm{CA}}. \tag{2.7}$$

The parameters n_1 and n_2 correspond to the numbers of protons released or accepted during the binding process.

Values of $\mathrm{p}K_{\mathrm{a,CA}}$ and $\Delta H_{\mathrm{pr,CA}}$ for individual carbonic anhydrase isozymes were determined previously in our laboratory and published in [134]. Buffer protonation enthalpies ($\Delta H_{\mathrm{pr,buf}}$) were obtained from published thermodynamic data [135]. The values of $\mathrm{p}K_{\mathrm{a,SA}}$ and $\Delta H_{\mathrm{pr,SA}}$ were determined experimentally as described in Section 2.3.

Observed binding constants were determined by fluorescent thermal shift assay, whereas observed binding enthalpies were measured by isothermal titration calorimetry. These parameters were subsequently used to calculate intrinsic binding constants and thermodynamic parameters that are independent of linked protonation equilibria and therefore more suitable for comparison with structural data.

Intrinsic entropy changes were calculated from intrinsic Gibbs energies and intrinsic enthalpies according to Eq. S.8.

$$\Delta S_{\mathrm{int}} = \frac{\Delta H_{\mathrm{int}} - \Delta G_{\mathrm{int}}}{T}. \tag{2.8}$$

2.5 Structural Studies

Structural information for carbonic anhydrase–ligand complexes was obtained by X-ray crystallography. Crystals of CA isozymes were grown at room temperature using the sitting-drop vapor diffusion method. Recombinant protein samples were concentrated via ultrafiltration to final concentrations ranging from $15\,\mathrm{mg\,mL^{-1}}$ to $50\,\mathrm{mg\,mL^{-1}}$. Crystallization drops ($0.1\,\mu\mathrm{L}$ to $5\,\mu\mathrm{L}$) were prepared by mixing the protein stock with the reservoir solution and equilibrated against $0.1\,\mathrm{mL}$ to $0.5\,\mathrm{mL}$ of the same reservoir solution. Optimized crystallization conditions typically involved $0.1\,\mathrm{M}$ Tris-HCl (pH 8.5) with $0.2\,\mathrm{M}$ salts (NaCl or amonium sulfate) and $20\,\%$ to $28\,\%$ PEG (4000, 3350, or 8000) for CA I; $0.1\,\mathrm{M}$ sodium

bicine (pH 9.0) and $2.0\,\mathrm{M}$ sodium malonate (pH 7.0) for CA II; $0.1\,\mathrm{M}$ ammonium citrate (pH 7.0–7.2) and $26\,\%$ to $30\,\%$ PEG 4000 for CA XII; and sodium citrate or acetate buffers (pH 4.5–5.5) with $26\,\%$ to $30\,\%$ PEG 4000 for CA XIII. Protein–ligand complexes were primarily obtained by soaking pre-grown crystals in reservoir solutions supplemented with $0.5\,\mathrm{mM}$ to $1.0\,\mathrm{mM}$ ligand (diluted from $50\,\mathrm{mM}$ DMSO stocks) for up to one week, while co-crystallization was specifically employed for CA I complexes. CA I and CA II crystals were flash-cooled directly from the mother liquor, while CA XII and CA XIII crystals were transferred to a cryoprotectant solution containing $15\,\%$ to $20\,\%$ ethylene glycol.

Diffraction data were collected either at the macromolecular crystallography beamlines P13 and P14 at the DESY synchrotron (Hamburg, Germany) or using a Rigaku MM007-HF diffractometer at the Life Sciences Center of Vilnius University. Diffraction datasets were processed using standard crystallographic procedures, and structures were solved by molecular replacement using previously determined carbonic anhydrase structures as search models. Iterative cycles of model building and refinement were performed until satisfactory agreement between the atomic model and experimental electron density was achieved.

The majority of crystal structures included in this dissertation were determined by the author. A subset of CA IX and CA XII structures was determined by collaborators Dr. Jānis Leitāns and Prof. Dr. Kaspars Tars (Latvian Biomedical Research and Study Centre, Latvia). All structures included in this dissertation were subsequently analyzed by the author to identify protein-ligand interactions, binding-site hydration patterns, and structural features relevant to thermodynamic binding parameters.

Detailed crystallization conditions, data collection parameters, refinement statistics, structure validation metrics, and software used for structure determination are reported in the corresponding publications included in this dissertation.

Chapter 3

Summary of Results

3.1 Determinants of Protein–Ligand Recognition

The studies presented in this section investigate the molecular determinants governing protein–ligand recognition in carbonic anhydrases. Particular emphasis is placed on understanding how thermodynamic mechanisms, ligand structure, and protein environment contribute to binding affinity and isozyme selectivity. First, the phenomenon of enthalpy–entropy compensation is examined to reveal how similar binding affinities can arise through distinct energetic mechanisms. Subsequently, the influence of minor ligand modifications on affinity and selectivity is investigated. Finally, structural and thermodynamic data are integrated to establish relationships between protein–ligand structure and binding energy.

3.1.1 Enthalpy-Entropy Compensation

This subsection summarizes the results of the publication Paketuryte-Latve et al. 2026:

Vaida Paketurytė-Latvė, Audrius Zakšauskas, Visvaldas Kairys, Edita Čapkauskaitė, Martynas Bagdonas, Alexey Smirnov, Elena Manakova, Saulius Gražulis, Daumantas Matulis

Enthalpy–Entropy Compensation in Inhibitor Binding to Carbonic Anhydrase Isozymes
Manuscript under review at the time of dissertation submission. The manuscript was subsequently accepted for publication in Biophysical Journal, after the dissertation had been printed, and is available under DOI: 10.1016/j.bpj.2026.09.032.

My contribution included development of the study concept, experimental determination of binding thermodynamics by ITC, calculation and analysis of intrinsic thermodynamic parameters, X-ray crystallographic studies, interpretation of enthalpy–entropy compensation phenomena, and manuscript preparation.

To investigate the molecular origins of enthalpy–entropy compensation, a matched series of sulfonamide inhibitors (specifically, the series of six *ortho*, *meta*-disubstituted benzenesulfonamides 4a–4d, 4h, and 7h) was characterized in complex with CA II, CA XII, and CA XIII. Binding affinities were determined by FTSA and ITC, while ITC additionally provided binding enthalpies. High-resolution X-ray structures were determined for selected protein–ligand complexes yielding seven atomic-resolution structures of complexes with CA II (PDB: 3OEN, 3OEO, 3OIC), CA XII (PDB: 3OFA, 3OFB), and CA XIII (PDB: 3OFP, 3OFN) to relate the measured thermodynamic differences to specific features of the active sites.

Observed thermodynamic parameters were corrected for proton-linked equilibria involving sulfonamide deprotonation, protonation of the zinc-bound hydroxide, and buffer ionization. This deconvolution relied on experimentally determined ligand-scaffold parameters, including a $\mathrm{p}K_{\mathrm{a,SA}}$ of 9.8 and a protonation enthalpy ($\Delta H_{\mathrm{pr,SA}}$) of $-35.2\,\mathrm{kJ\,mol^{-1}}$ for compounds 4a–4d and 4h, and a $\mathrm{p}K_{\mathrm{a,SA}}$ of 8.9 and $\Delta H_{\mathrm{pr,SA}}$ of $-30.4\,\mathrm{kJ\,mol^{-1}}$ for compound 7h, using TRIS as the measurement buffer ($\Delta H_{\mathrm{pr,buf}} = -46.56\,\mathrm{kJ\,mol^{-1}}$). The resulting intrin-

sic Gibbs energies were generally similar among the three isozymes, whereas their enthalpic and entropic contributions differed substantially. For example, compound 4a exhibited intrinsic Gibbs energies of $-59.3\,\mathrm{kJ\,mol^{-1}}$ $-61.4\,\mathrm{kJ\,mol^{-1}}$ for CA II and CA XIII, respectively, while the corresponding intrinsic enthalpies were $-26.8\,\mathrm{kJ\,mol^{-1}}$ and $-64.0\,\mathrm{kJ\,mol^{-1}}$. Thus, a difference of only $2.1\,\mathrm{kJ\,mol^{-1}}$ in binding Gibbs energy was accompanied by a difference of $37.2\,\mathrm{kJ\,mol^{-1}}$in enthalpy, compensated by an opposing change in the entropic contribution (with $-T\Delta S_{\mathrm{int}}$ shifting from a highly favorable $-32.5\,\mathrm{kJ\,mol^{-1}}$ in CA II to an unfavorable $2.6\,\mathrm{kJ\,mol^{-1}}$ in CA XIII).

This behavior was observed across the investigated series. Binding to CA II was generally more entropy-favored, whereas binding to CA XIII was more enthalpy-favored, with CA XII displaying intermediate thermodynamic profiles. Specifically, the average relative partitioning of the binding Gibbs energy across the compounds demonstrated that binding to CA II was $70\,\%$ entropy-favored ($30\,\%$ enthalpy), CA XII was intermediate ($70\,\%$ enthalpy, $30\,\%$ entropy), whereas binding to CA XIII was entirely enthalpy-driven ($100\,\%$ enthalpy, $0\,\%$ entropy). Differences between isozymes were generally larger than those produced by modifications within the ligand series. Correction for proton-linked equilibria was essential for this comparison, as the observed thermodynamic profiles differed substantially from the intrinsic profiles.

Despite these pronounced thermodynamic differences, the crystallographic binding modes were highly conserved. In all structures, the deprotonated sulfonamide nitrogen coordinated the catalytic $\mathrm{Zn^{II}}$ ion, and the sulfonamide group formed conserved hydrogen bonds with Thr199. Differences were observed farther from this conserved anchoring region. At position 62, Asn in CA II and CA XII could form a direct hydrogen bond with the ligand, whereas the shorter Ser62 in CA XIII resulted in indirect, water-mediated interactions. At position 131, CA II and CA XIII contain Phe, while CA XII contains Ala; Phe131 showed conformational variability in response to different ligands. Another notable difference occurred at position 200, which is occupied by Thr in CA II and CA XII but by Val in CA XIII, altering the local hydration environment adjacent to the benzenesulfonamide group.

Comparison of the structural and thermodynamic data therefore showed that similar ligand poses and binding Gibbs energies do not imply similar enthalpic and entropic contributions. The largest differences were associated with the protein isozyme rather than with relatively small modifications of the ligand. These differences are consistent with isozyme-specific active-site hydration, where differences in water or-

ganization and the energetic cost of dehydration upon ligand binding may contribute to the distinct thermodynamic profiles. Specifically, in CA II, Thr200 stabilizes the ordered W1 water molecule via a short hydrogen bond, and its displacement upon ligand binding yields a highly favorable solvent-entropy contribution. In contrast, Val200 in CA XIII cannot form this stabilizing hydrogen bond, leading to a less ordered, unconstrained active-site water network that provides a negligible solvent-entropy change during ligand binding, thereby shifting the thermodynamic profile to be entirely enthalpy-driven.

3.1.2 Affinity and Selectivity

This subsection summarizes the results of the publication [136]:

Audrius Zakšauskas, **Vaida Paketurytė-Latvė**, Alberta Jankūnaitė, Edita Čapkauskaitė, Yann Becart, Alexey Smirnov, Klára Pospíšilová, Janis Leitans, Jiří Brynda, Andris Kazaks, Lina Baranauskienė, Elena Manakova, Saulius Gražulis, Visvaldas Kairys, Kaspars Tars, Pavlína Řezáčová, Daumantas Matulis

Affinity and Selectivity of Protein-Ligand Recognition: A Minor Chemical Modification Changes Carbonic Anhydrase Binding Profile
J. Med. Chem., 2025, 68 (16), 17752–17773.
DOI: 10.1021/acs.jmedchem.5c01421

My contribution included experimental determination of binding affinities by FTSA, analysis of intrinsic binding thermodynamics, X-ray crystallographic studies, interpretation of selectivity trends, data analysis, and manuscript preparation. A significant contribution to this publication was also provided by the organic synthesis of the studied compounds performed by Dr. A. Zakšauskas, Dr. A. Jankūnaitė, Dr. E. Čapkauskaitė, and Yann Becart. It is important to note that independent enzyme inhibition experiments were carried out by K. Pospíšilová. This enabled the demonstration of a strong correlation between independently obtained binding (FTSA) and inhibition (SFA) data.

This study systematically investigated how minor chemical modifications of *ortho*-substituted benzenesulfonamides dramatically alter binding affinity and selectivity toward human carbonic anhydrase (CA) isozymes. Nearly 50 compounds were synthesized, representing seven

chemical classes based on sulfur oxidation state and linker heteroatoms (including 4-sulfanyl, 4-sulfinyl, and 4-sulfonyl esters and benzamides, along with 4-amino benzamides). Binding affinities were quantified for all 12 catalytically active human CA isozymes using fluorescence-based thermal shift assay (FTSA), complemented by stopped-flow enzymatic inhibition assays and structural characterization by X-ray crystallography.

Small structural changes produced affinity differences spanning several orders of magnitude. In particular, 4-sulfanyl-substituted benzenesulfonamides exhibited exceptionally strong and selective binding to CA IX, with intrinsic dissociation constants reaching the picomolar range. Specifically, the cyclohexylsulfanyl ester 4b displayed an outstanding intrinsic K_{d} of $1\,\mathrm{pM}$ ($0.0010\,\mathrm{nM}$) for CA IX, while binding hundreds of times more weakly to the off-target isozyme CA II ($K_{\mathrm{d,int}}$ = $0.49\,\mathrm{nM}$). Furthermore, while the bulky adamantylsulfanyl ester 4g achieved a similar CA IX affinity ($K_{\mathrm{d,int}}$ = $3\,\mathrm{pM}$) with several hundred-fold selectivity over CA II, the smaller methylsulfanyl analogue 4h lost this selectivity. In contrast, oxidation of the sulfanyl group to sulfinyl or sulfonyl markedly reduced affinity and largely abolished CA IX selectivity; for instance, the sulfinyl derivative 7b and sulfonyl derivative 9b displayed dramatically reduced CA IX affinities of $28\,\mathrm{nM}$ and $320\,\mathrm{nM}$, respectively, despite minimal changes to the overall molecular scaffold.

Intrinsic binding constants were derived from observed affinities by correcting for pH-dependent protonation equilibria of both the sulfonamide group and the zinc-bound water molecule. This analysis demonstrated that enhanced binding was not solely attributable to favorable $\mathrm{p}K_{\mathrm{a}}$ shifts, but instead reflected genuine improvements in protein-ligand interactions. This correction is crucial because, although the strong electron-withdrawing effect of sulfinyl and sulfonyl groups lowered the sulfonamide $\mathrm{p}K_{\mathrm{a,SA}}$ by nearly a full pH unit (from 9.8 for sulfanyl compounds to 8.9 for sulfoxides) and increased the fraction of deprotonated ligand ready to coordinate the zinc ion at pH 7.0, their intrinsic binding affinities were actually hundreds of thousands of times weaker. These findings emphasize the importance of intrinsic thermodynamic parameters for reliable structure–affinity relationships in CA inhibitor design.

Comparison between ester and benzamide analogues showed that benzamides generally bound more weakly to CA isozymes, although several retained notable selectivity for CA IX since most benzamides exhibited no detectable binding against off-target CAs. Substituent size and hydrophobicity played a critical role: bulky hydrophobic groups op-

timized interactions within the enlarged CA IX active site while causing steric clashes in smaller isozymes, thereby driving selectivity. Additionally, comparing sulfanyl linkers to amino linkers showed similar potencies, where the cyclooctyl-substituted 4-amino-benzamide 6e selectively bound CA IX ($K_{\mathrm{d,int}}$ = $0.53\,\mathrm{nM}$) and showed no binding to smaller active-site isozymes.

X-ray crystal structures and molecular docking provided structural explanations for the affinity trends. High-affinity sulfanyl-substituted ligands adopted binding poses that optimized hydrophobic packing and water-mediated hydrogen bonding networks; specifically, the nine newly determined structures (including CA II-4c, CA IX-4d, and CA XIII-4d; PDB IDs: 9FPQ, 9R8X, 9FPW, respectively) showed that the ligand ester group formed a direct hydrogen bond with Asn62 in CA II, but transitioned to a water-mediated hydrogen bond network with Gln70/Asn65 in CA IX and Ser64/Asn69 in CA XIII. Furthermore, crystallographic analysis of compound 4h bound to CA II (PDB ID: 9FPS) revealed an atypical binding mode containing two ligand molecules, where the second molecule bound non-classically at the active-site periphery via hydrophobic and water-mediated interactions. In contrast sulfinyl and sulfonyl derivatives exhibited unfavorable intramolecular clashes that distorted binding geometries. Density Functional Theory (DFT) calculations revealed that the docked conformer of sulfonyl derivative 9a undergoes a severe intramolecular oxygen-oxygen clash, resulting in a conformational energy penalty of $53.8\,\mathrm{kJ\,mol^{-1}}$ relative to its low-energy solution state conformation, whereas the sulfanyl analogue 4a remains highly stable and free of clashes. Molecular docking reproduced several experimental trends for sulfanyl compounds but failed to account for the behavior of sulfonyl derivatives due to the scoring function's inability to calculate ligand conformational strain.

Overall, the results demonstrate that the oxidation state and conformational flexibility of a single *ortho* substituent can dictate CA isozyme affinity and selectivity over several orders of magnitude. This work establishes a clear mechanistic link between subtle chemical modifications, ligand conformational energetics, and selective recognition of CA IX, providing valuable guidance for the rational design of highly selective carbonic anhydrase inhibitors.

The pronounced effects of minor structural modifications prompted a broader investigation into how structural information and thermodynamic parameters can be integrated to explain protein–ligand recognition.

3.1.3 Structure-Thermodynamics Relationships

This subsection summarizes the results of the publication[137]:

Vaida Paketurytė-Latvė, Alexey Smirnov, Elena Manakova, Lina Baranauskienė, Vytautas Petrauskas, Asta Zubrienė, Jurgita Matulienė, Virginija Dudutienė, Edita Čapkauskaitė, Audrius Zakšauskas, Janis Leitans, Saulius Gražulis, Kaspars Tars, Daumantas Matulis

From X-ray crystallographic structure to intrinsic thermodynamics of protein-ligand binding using carbonic anhydrase isozymes as a model system
IUCrJ, 2024, 11 (4), 556–569.
DOI: 10.1107/S2052252524004627

My contribution included conceiving the publication idea, thermodynamic analysis of protein–ligand interactions, integration of structural and thermodynamic data, and preparation of the manuscript. The majority of the binding thermodynamic parameters were determined by Dr. A. Zubrienė and Dr. L. Baranauskienė, while some of the crystal structures cited in the article were solved by Dr. A. Smirnov, Dr. E. Manakova, and Dr. J. Leitans. The cell-based assays were carried out by Dr. J. Matulienė.

To establish correlations between protein–ligand structure and binding thermodynamics, X-ray crystallographic data for carbonic anhydrase–sulfonamide complexes were combined with binding measurements obtained by FTSA, ITC, enzymatic inhibition, and cell-based assays. The analysis focused on structurally related sulfonamide inhibitors (specifically the fluorinated and chlorinated benzenesulfonamide series) exhibiting markedly different affinities and selectivities toward human carbonic anhydrase isozymes, particularly CA IX. To overcome the crystallization challenges associated with native CA IX, a chimeric CA IX (chCA IX) was utilized as a highly accurate mimic, containing six active-site mutations (A65S, N67Q, I91L, F130V, V134L, L203A) introduced into the CA II.

Crystal structures revealed a conserved binding mode for sulfonamide inhibitors, with coordination of the catalytic zinc ion via the negatively charged deprotonated nitrogen and formation of similar interactions within the active site. However, ligands exhibiting nearly identical binding poses often differed in affinity by several orders of

magnitude. For instance, structurally highly similar inhibitors EA3-3 and EA5-3 in complexes with chCA IX and CA II (both crystallizing in the space group $P2_1$ with nearly identical unit-cell parameters) adopted conserved binding conformations but demonstrated vastly divergent affinities. These observations demonstrated that structural information alone is insufficient to explain binding affinity or isozyme selectivity.

Comparison of different experimental approaches highlighted the strengths and limitations of individual binding assays. FTSA provided the broadest affinity range, extending from millimolar to picomolar dissociation constants, whereas enzymatic inhibition assays and ITC were restricted to narrower measurement windows. The use of multiple orthogonal methods enabled more reliable characterization of protein–ligand interactions.

A central finding of this work was the importance of intrinsic thermodynamic parameters. Correction of observed binding data for linked protonation equilibria yielded intrinsic Gibbs energies, enthalpies, and entropies of binding. This deconvolution accounted for the simultaneous protonation of the zinc-bound hydroxide in the enzyme active site (with a $\mathrm{p}K_{\mathrm{a,CA}}$ of 6–7, or up to 8 for CA I and CA XIII) and the deprotonation of the benzenesulfonamide group (with a $\mathrm{p}K_{\mathrm{a,SA}}$ typically between 8 and 11). These intrinsic parameters more accurately reflected the energetic consequences of protein–ligand interactions and enabled meaningful structure–thermodynamics correlations.

The combined analysis showed that ligand affinity and selectivity arise from a complex interplay of structural, solvation, and thermodynamic effects. Minor chemical modifications often produced substantial changes in binding energetics despite only subtle differences in crystallographic structures. Specifically, substituting a tail methyl group (VD12-05) with a hydroxy tail (VD10-35) resulted in a systematic loss of 7.5–$10.7\,\mathrm{kJ\,mol^{-1}}$ of intrinsic Gibbs energy across CA isozymes, as the polar hydroxy group preferentially formed hydrogen bonds with bulk solvent rather than the protein. Conversely, adding a cyclooctyl amino ring at the *meta*-position (VD11-4-2) caused steric clashes that reduced CA I affinity by $18.0\,\mathrm{kJ\,mol^{-1}}$ (a 1000-fold decrease), but achieved a $21.9\,\mathrm{kJ\,mol^{-1}}$ gain (4000-fold increase) for CA IX and $14.9\,\mathrm{kJ\,mol^{-1}}$ for CA XII, driving a 100,000-fold selectivity for CA IX over CA I. Furthermore, cyclohexane substitution in compound EA2-3 optimized hydrophobic interactions within the enlarged CA IX pocket, yielding an exceptionally strong intrinsic Gibbs energy of $-75.0\,\mathrm{kJ\,mol^{-1}}$ (femtomolar range). These results emphasize that reliable interpretation of protein–ligand recognition requires integration of structural information

with intrinsic thermodynamic analysis.

Overall, this work emphasized a framework for connecting X-ray crystallographic structures with intrinsic thermodynamic parameters and demonstrated how such integration can improve the understanding of molecular recognition and support rational drug design. This is clearly illustrated by the opposing thermodynamic driving forces governing potent binders: while the binding of VD10-35 to CA I is purely enthalpy-driven ($\Delta H_{\mathrm{int}} = -76.8\,\mathrm{kJ\,mol^{-1}}$), the selective binding of VD11-4-2 to CA IX is heavily entropy-driven ($-T\Delta S_{\mathrm{int}} = -47.5\,\mathrm{kJ\,mol^{-1}}$) despite its lower enthalpic contribution ($\Delta H_{\mathrm{int}} = -24.3\,\mathrm{kJ\,mol^{-1}}$), together forming an exceptionally strong complex ($\Delta G_{\mathrm{int}} = -71.8\,\mathrm{kJ\,mol^{-1}}$).

3.2 Reliability of Thermodynamic Measurements

Reliable interpretation of protein–ligand recognition depends not only on the quality of structural and thermodynamic data, but also on the methods used to obtain and analyze these data. Experimental limitations, parameter correlations, and statistical uncertainty can substantially influence the accuracy and interpretation of binding constants and thermodynamic parameters. The studies presented in this section address two complementary aspects of this problem: standardization of fluorescent thermal shift assay measurements and rigorous quantification of uncertainty in protein–ligand binding parameters.

3.2.1 FTSA Standardization

This subsection summarizes the results of the publication[116]:

Egidijus Kazlauskas, Vytautas Petrauskas, **Vaida Paketurytė**, Daumantas Matulis

Standard Operating Procedure for Fluorescent Thermal Shift Assay (FTSA) for Determination of Protein-Ligand Binding and Protein Stability
Eur. Biophys. J., 2021, 50 (5), 707–714.
DOI: 10.1007/s00249-021-01537-1

My contribution included the analysis and interpretation of data, the preparation of figures and manuscript text focused on the FTSA standard operating procedure for protein stability and binding.

This standard operating procedure (SOP) demonstrated that FTSA provides reproducible, high-quality melting curves suitable for determining both protein stability and ligand binding affinities across a wide dynamic range (10^3 to $10^{13}\,\mathrm{M}^{-1}$). The melting temperature (T_m) is determined at the inflection point of the sigmoidal denaturation transition, where ligand-induced thermal shifts (ΔT_m) across varied concentrations are fitted to calculate the equilibrium binding constant (K_b). Using CA II (specifically, the binding of acetazolamide up to $200\,\mu\mathrm{M}$ with $5\,\mu\mathrm{M}$ CA II, $2\,\%$ v/v DMSO, and $50\,\mu\mathrm{M}$ ANS) and Hsp90α N-terminal domain (screened across pH 5.0 to 10.5 in a multicomponent acetate-borate-phosphate buffer) as examples on qPCR equipment (relying on centrifugal rotary spectrofluorimeters and $10\,\mu\mathrm{L}$-$20\,\mu\mathrm{L}$ volumes for optimal temperature uniformity), the assay reliably detected ligand-induced thermal shifts and pH-dependent stability changes. The work also showed that assay quality depends on temperature-insensitive buffer composition (utilizing phosphate or HEPES instead of TRIS to avoid temperature-dependent pH shifts), DMSO levels (safe at $2\,\%$ v/v, but destabilizing at $\geq 4\,\%$), protein structure (favoring mono-domain proteins over complex multi-domain assemblies that yield overlapping peaks), and reporter dye selection (recommending ANS with $\lambda_{EX/EM} \approx 350\,\mathrm{nm}/470\,\mathrm{nm}$ over SYPRO Orange due to weaker baseline binding, or utilizing label-free tryptophan fluorescence). Overall, the results validated FTSA as a robust, low sample, high throughput method for routine protein-ligand characterization.

3.2.2 Uncertainty Quantification

This subsection summarizes the results of the publication [138]:

Vaida Paketurytė, Vytautas Petrauskas, Asta Zubrienė, Olga Abian, Margarida Bastos, Wen-Yih Chen, Maria João Moreno, Georg Krainer, Vaida Linkuvienė, Arthur Sedivy, Adrian Velazquez-Campoy, Mark A. Williams, Daumantas Matulis

Uncertainty in protein-ligand binding constants: asymmetric

confidence intervals versus standard errors
Eur. Biophys. J., 2021, 50 (3–4), 661–670.
DOI: 10.1007/s00249-021-01518-4

This work was a task of the COST Action CA15126 (MOBIEU), emerging from collaborative discussions within the European biophysics community to improve uncertainty reporting in molecular interactions. My contribution to this effort involved participation in scientific discussions, experimental planning, data analysis, and the preparation of the manuscript.

The study demonstrates that symmetric standard errors, commonly reported as $\pm x$, substantially underestimate the true uncertainty of protein–ligand binding constants. Through the analysis of simulated and experimental datasets, the work shows that the distributions of the equilibrium binding constant (K_b), dissociation constant (K_d), and Gibbs energy change (ΔG) are inherently asymmetric due to their logarithmic, exponential, and reciprocal mathematical relationships. Specifically, in Case 1, assuming a normal distribution for K_b with a mean of $2.0\times10^7\,\mathrm{M}^{-1}$ and a standard deviation of $0.6\times10^7\,\mathrm{M}^{-1}$ leads, upon transformation to K_d, to a strongly skewed distribution (skewness 4.3). Moreover, because a normal distribution has unbounded support, it assigns a nonzero probability to physically impossible negative values of K_b. In contrast, if normality is assumed for ΔG, with a mean of $-41.67\,\mathrm{kJ\,mol}^{-1}$ at $25\,^\circ\mathrm{C}$ and a standard deviation of $0.77\,\mathrm{kJ\,mol}^{-1}$, the symmetric $95\,\%$ confidence interval is $-43.18\,\mathrm{kJ\,mol}^{-1}$ to $-40.16\,\mathrm{kJ\,mol}^{-1}$. Direct transformation of these limits using the thermodynamic relation between ΔG and K_b preserves the corresponding uncertainty structure and gives the asymmetric K_b $95\,\%$ confidence interval $[1.09,\ 3.68]\times10^7\,\mathrm{M}^{-1}$. Transformations between these parameters amplify skewness, making symmetric error reporting statistically inappropriate and potentially leading to physically impossible results, such as negative binding constants. Monte Carlo simulations of 1:1 binding titrations reveal that fitted K_b values become increasingly positively skewed at higher affinities, whereas ΔG remains closer to a normal distribution only under reasonably optimal experimental conditions. To evaluate experimentally realistic titrations, Case 2 modeled VP-ITC experiments consisting of $20\times15\,\mu\mathrm{L}$ injections of $200\,\mu\mathrm{M}$ ligand into $20\,\mu\mathrm{M}$ protein, with $\Delta H = -10\,\mathrm{kJ\,mol}^{-1}$ and a constant injection-heat noise of $3\,\mu\mathrm{J}$. Under these conditions, increasing the true K_b from $2\times10^5\,\mathrm{M}^{-1}$ (Wiseman parameter $c=4$) to $2\times10^7\,\mathrm{M}^{-1}$ ($c=400$) markedly increased the skewness of the fitted K_b distribution from 1.3 ($\mathrm{CI}_{95}=[0.78,\ 5.8]\times10^5\,\mathrm{M}^{-1}$) to 23 ($\mathrm{CI}_{95}=[0.51,\ 22]\times10^7\,\mathrm{M}^{-1}$). At the high-$c$ value, only 3–4 data points sample the transition region

of the binding isotherm. Consequently, the curvature that constrains K_b is poorly resolved, making its fitted value highly sensitive to experimental noise and producing a strongly asymmetric distribution with a pronounced upper tail.

We conclude that profile likelihood-based $95\,\%$ confidence intervals ($\mathrm{CI}_{P,95}$) offer a more consistent and inter-convertible method for representing uncertainty across all thermodynamic quantities. These asymmetric intervals are calculated using the Fisher–Snedecor F-distribution by systematically stepping a selected parameter through fixed values while minimizing the residual sum of squares (RSS) over the remaining free parameters. Unlike standard errors, this approach ensures a perfect correspondence between the upper and lower uncertainty limits when transforming between K_b and ΔG, preserving all information regarding experimental variability. For example, for a simulated titration with a true $K_\mathrm{b} = 2 \times 10^6, \mathrm{M}^{-1}$ and $\Delta H = 41.8, \mathrm{kJ\,mol}^{-1}$, the profile likelihood method ($CI_{P,95}$) produces identical corresponding intervals ($[1.44, 3.30] \times 10^6, \mathrm{M}^{-1}$ for K_b and $[-37.2, -35.1], \mathrm{kJ\,mol}^{-1}$ for ΔG) regardless of which parameter is directly fitted. In contrast, standard asymptotic-symmetric intervals ($CI_{S,95}$) fail to maintain mathematical correspondence after parameter transformation. Ultimately, the results establish that asymmetric confidence intervals are essential for the accurate interpretation and reusability of biophysical data and should replace standard symmetric errors in protein–ligand thermodynamic studies.

Discussion

The ultimate goal of structure-based drug design is to predict how chemical modifications influence affinity and selectivity and to use this knowledge to design compounds that bind strongly to a desired target while avoiding interactions with other proteins. Despite major advances in structural biology, computational chemistry, and biophysics, this objective remains difficult to achieve. The results presented in this dissertation highlight several factors that complicate the interpretation and prediction of protein–ligand recognition.

The results presented in Section 3.1.1 Enthalpy-Entropy Compensation provide additional insight into the molecular origins of enthalpy–entropy compensation. Previous studies by Whitesides and co-workers [9, 139] demonstrated that relatively small ligand modifications may produce large changes in enthalpic and entropic contributions while having only modest effects on overall affinity for CA II, highlighting the importance of hydration and solvent reorganization in molecular recognition. The present results show that substantial differences in thermodynamic partitioning can also arise between closely related carbonic anhydrase isozymes despite highly conserved active-site architectures and similar ligand binding modes. This observation suggests that enthalpy–entropy compensation cannot be attributed solely to ligand-dependent effects but is strongly influenced by the local protein environment. Even subtle differences in active-site residues, hydration networks, or protein dynamics are sufficient to alter the balance between enthalpic and entropic contributions. Consequently, the thermodynamic signature of binding should be regarded as an emergent property of the entire protein–ligand system rather than a direct consequence of individual molecular interactions.

From a practical perspective, these observations also illustrate both the strengths and limitations of thermodynamic analysis. While decomposition of binding energy into enthalpic and entropic contributions

can reveal differences between protein–ligand complexes that appear equivalent when evaluated solely by affinity, interpretation of these contributions remains challenging because enthalpy and entropy reflect the combined effects of numerous coupled processes. As discussed by Klebe and others [140], assignment of individual thermodynamic contributions to specific molecular interactions is often not straightforward because changes in intermolecular contacts, hydration, conformational flexibility, and dynamics occur simultaneously. Nevertheless, the ability of thermodynamic signatures to distinguish between systems with similar structures and affinities demonstrates their value as sensitive probes of molecular recognition and highlights the complementary information they provide beyond conventional affinity measurements.

The findings described in Section 3.1.2 Affinity and Selectivity further emphasize the importance of conformational effects in protein–ligand recognition [141]. Numerous studies have demonstrated that relatively small structural modifications may alter ligand flexibility, conformational preferences, and protein dynamics, thereby producing unexpectedly large effects on binding. Gilson and co-workers [3, 10] have highlighted the importance of conformational entropy in molecular recognition and the challenges associated with accurately quantifying its contribution to binding, while Wand [142] and Akke [6, 70] and their colleagues have demonstrated through NMR studies that changes in protein or ligand dynamics can contribute substantially to binding thermodynamics. More recently, Wankowicz and co-workers [66] showed that conformational heterogeneity inferred also from X-ray crystallographic data can provide valuable insight into the entropic consequences of ligand binding. However, despite these advances, experimental characterization of conformational entropy remains considerably more demanding than determination of overall binding thermodynamics. In routine ITC experiments, only the total entropy change is obtained indirectly from measured Gibbs energies and enthalpies, whereas the individual contributions arising from protein conformational changes, ligand flexibility, solvent reorganization, and other processes generally cannot be separated. Consequently, the present observations illustrate both the importance of conformational effects and the current limitations in their characterization. The pronounced affinity losses observed upon oxidation of sulfur-containing substituents in the present study illustrate how subtle changes in ligand conformation may outweigh the expected increase in affinity associated with the introduction of electron-withdrawing substituents.

The results presented in Section 3.1.3 Structure-Thermodynamics Re-

lationships highlight the importance of distinguishing between observed and intrinsic thermodynamic parameters when interpreting protein–ligand interactions. The influence of linked protonation equilibria on binding thermodynamics has been recognized for decades, and several studies by Baker and Murphy [11], Whitesides and co-workers [143], Klebe and co-workers [140], as well as researchers in our laboratory [134] have emphasized that observed thermodynamic parameters may not directly reflect the energetics of molecular recognition. Nevertheless, intrinsic thermodynamic analysis remains relatively uncommon in contemporary protein–ligand studies because determination of the required protonation parameters is experimentally demanding and such information is unavailable for many protein–ligand systems [140, 144]. As a result, observed thermodynamic parameters are frequently interpreted as though they directly describe protein–ligand interactions. The present results demonstrate that protonation-linked contributions can substantially alter both the magnitude and interpretation of binding thermodynamics, suggesting that meaningful comparisons between ligands, proteins, and binding mechanisms often require consideration of intrinsic rather than observed parameters. More broadly, these findings illustrate that accurate structure–thermodynamics relationships depend not only on high-resolution structural information but also on rigorous separation of the underlying processes contributing to the measured thermodynamic signal.

The methodological studies described in Sections 3.2.1 FTSA Standardization and 3.2.2 Uncertainty Quantification emphasize the importance of experimental design and uncertainty quantification for reliable interpretation of protein–ligand binding data. Analysis of inhibition values reported in the literature [145] revealed substantial variability between independent studies, highlighting the challenges associated with comparing data generated using different experimental protocols and conditions. Such variability is particularly important for computational approaches, which frequently rely on published affinity data for model development, validation, and benchmarking. Inaccurate or inconsistent experimental measurements may therefore limit not only experimental interpretation but also predictive modeling efforts. Models trained on noisy experimental data cannot be expected to achieve predictive accuracy exceeding the quality of the underlying measurements. Similar concerns have been raised in the carbonic anhydrase field, where Liljas and co-workers [146] questioned the suitability of some widely cited inhibition datasets and argued that the precision and reliability of the reported measurements may have been overestimated. These observations demonstrate that meaningful structure–activity and

structure–thermodynamics relationships require not only high-quality experimental measurements but also realistic assessment of their uncertainty. While experimental uncertainty cannot be eliminated entirely [147–152], its rigorous quantification [153] is essential for distinguishing genuine biological effects from methodological variability and for enabling meaningful comparisons between studies.

Although the studies presented in this dissertation addressed different aspects of protein–ligand interactions, they collectively support the same central conclusion: binding affinity is a composite observable arising from multiple interconnected processes. Hydration, conformational changes, protonation equilibria, and experimental uncertainty can each substantially influence the interpretation of molecular recognition. Consequently, establishing meaningful structure–thermodynamics relationships requires more than structural information and affinity measurements alone; it also requires consideration of the processes that contribute to the observed experimental parameters. The results presented in this dissertation highlight both the potential and the limitations of structure-based drug design and demonstrate that accurate understanding of protein–ligand interactions depends on the ability to deconvolute observed thermodynamic parameters into their underlying physical contributions and relate them to structural information. Further progress in this field will depend on the ability to deconvolute observed thermodynamic parameters into the individual processes that govern binding, to understand their interplay, and to relate them to structural information.

Conclusions

1. Comparisons of closely related CAs revealed that minor differences in the active-site, including hydration and the presence of either a hydroxyl-bearing Thr or a methyl-bearing Val residue, were associated with the pronounced differences in ΔH and $T\Delta S$ contributions to binding ($\approx$40 kJ mol^{-1} despite similar binding geometries and ΔG). *These findings highlight the sensitivity of binding thermodynamics to local protein environments and illustrate the limitations of interpreting molecular recognition from affinity or structure alone.* (Publication 1)
2. Small chemical modifications produced marked changes in affinity and selectivity across CAs. Structural and thermodynamic analyses indicated that oxidation of sulfur-containing substituents promoted intramolecular hydrogen-bond formation with the sulfonamide group, altering ligand conformation and reducing productive interactions. *These findings demonstrate the highly cooperative nature of protein–ligand recognition.* (Publication 2)
3. Correction for linked protonation equilibria produced intrinsic thermodynamic parameters that were affected considerably from the observed values, demonstrating that meaningful comparisons of binding energetics require separation of binding and protonation contributions. (Publication 3)
4. Systematic evaluation of FTSA conditions demonstrated the importance of protocol standardization for obtaining comparable protein–ligand binding data. Asymmetric profile-likelihood confidence intervals provided a statistically appropriate representation of uncertainty, whereas symmetric standard errors are misleading for quantities transformed between affinity and thermodynamic scales. (Publication 4 and Publication 5)

Bibliography

[1] Gerhard Klebe. *Drug Design: From Structure and Mode-of-Action to Rational Design Concepts*. Springer Berlin Heidelberg, 2024. ISBN 978-3-662-68997-4 978-3-662-68998-1. doi: 10.1007/978-3-662-68998-1.

[2] William L. Jorgensen. The many roles of computation in drug discovery. *Science*, 303(5665):1813–1818, 2004. ISSN 1095-9203. doi: 10.1126/science.1096361.

[3] Huan-Xiang Zhou and Michael K. Gilson. Theory of free energy and entropy in noncovalent binding. *Chemical Reviews*, 109(9):4092–4107, 2009. ISSN 0009-2665, 1520-6890. doi: 10.1021/cr800551w.

[4] David L. Mobley and Michael K. Gilson. Predicting binding free energies: Frontiers and benchmarks. *Annual Review of Biophysics*, 46:531–558, 2017. ISSN 1936-1238. doi: 10.1146/annurev-biophys-070816-033654.

[5] Jack D. Dunitz. Win some, lose some: enthalpy-entropy compensation in weak intermolecular interactions. *Chemistry & Biology*, 2(11):709–712, 1995. ISSN 1074-5521. doi: 10.1016/1074-5521(95)90097-7.

[6] Johan Wallerstein, Vilhelm Ekberg, Majda Misini Ignjatović, Rohit Kumar, Octav Caldararu, Kristoffer Peterson, Sven Wernersson, Ulrika Brath, Hakon Leffler, Esko Oksanen, Derek T. Logan, Ulf J. Nilsson, Ulf Ryde, and Mikael Akke. Entropy–entropy compensation between the protein, ligand, and solvent degrees of freedom fine-tunes affinity in ligand binding to galectin-3c. *JACS Au*, 1(4):484–500, 2021. doi: 10.1021/jacsau.0c00094.

[7] J. E. Ladbury. Just add water! the effect of water on the specificity of protein-ligand binding sites and its potential application to drug design. *Chemistry & Biology*, 3(12):973–980, 1996. ISSN 1074-5521.

[8] Gerhard Klebe. Applying thermodynamic profiling in lead finding and optimization. *Nature Reviews Drug Discovery*, 14(2):95–110, 2015. ISSN 1474-1776. doi: 10.1038/nrd4486.

[9] Benjamin Breiten, Matthew R. Lockett, Woody Sherman, Shuji

Fujita, Mohammad Al-Sayah, Heiko Lange, Carleen M. Bowers, Annie Heroux, Goran Krilov, and George M. Whitesides. Water networks contribute to enthalpy/entropy compensation in protein-ligand binding. *Journal of the American Chemical Society*, 135 (41):15579–15584, 2013. ISSN 1520-5126. doi: 10.1021/ja4075776.

[10] Chia-en A. Chang, Wei Chen, and Michael K. Gilson. Ligand configurational entropy and protein binding. *Proceedings of the National Academy of Sciences*, 104(5):1534–1539, 2007. doi: 10.1073/pnas.0610494104.

[11] B M Baker and K P Murphy. Evaluation of linked protonation effects in protein binding reactions using isothermal titration calorimetry. *Biophysical Journal*, 71(4):2049–2055, 1996. ISSN 0006-3495.

[12] Asta Zubrienė and Daumantas Matulis. Observed versus intrinsic thermodynamics of inhibitor binding to carbonic anhydrases. In Daumantas Matulis, editor, *Carbonic Anhydrase as Drug Target: Thermodynamics and Structure of Inhibitor Binding*, pages 107–123. Springer International Publishing, 2019. ISBN 978-3-030-12780-0. doi: 10.1007/978-3-030-12780-0_8.

[13] Vijay M. Krishnamurthy, George K. Kaufman, Adam R. Urbach, Irina Gitlin, Katherine L. Gudiksen, Douglas B. Weibel, and George M. Whitesides. Carbonic anhydrase as a model for biophysical and physical-organic studies of proteins and protein-ligand binding. *Chem. Rev.*, 108(3):946–1051, 2008. ISSN 0009-2665. doi: 10.1021/cr050262p.

[14] Olivier J. Wouters, Martin McKee, and Jeroen Luyten. Estimated research and development investment needed to bring a new medicine to market, 2009-2018. 323(9):844–853, 2020. ISSN 0098-7484. doi: 10.1001/jama.2020.1166.

[15] Colin G. Rousseaux, William M. Bracken, and Silvia Guionaud. Chapter 1 - overview of drug development. In Wanda M. Haschek, Colin G. Rousseaux, Matthew A. Wallig, and Brad Bolon, editors, *Haschek and Rousseaux' s Handbook of Toxicologic Pathology (Fourth Edition)*, pages 3–48. Academic Press, 2023. ISBN 978-0-12-821047-5. doi: 10.1016/B978-0-12-821047-5.00016-6.

[16] Approval success rates of drug candidates based on target, action, modality, application, and their combinations. 14(3):1113–1122, 2021. ISSN 1752-8054. doi: 10.1111/cts.12980.

[17] A year in pharmacology: new drugs approved by the US food and drug administration in 2025. 399:11157–11179, 2026. ISSN 0028-1298. doi: 10.1007/s00210-026-05193-0.

[18] How were new medicines discovered? 10:507–519, 2011. ISSN 1474-1784. doi: 10.1038/nrd3480.

[19] The discovery of first-in-class drugs: origins and evolution. 13(8): 577–587, 2014. ISSN 1474-1784. doi: 10.1038/nrd4336.

[20] Visvaldas Kairys, Lina Baranauskiene, Migle Kazlauskiene, Asta Zubrienė, Vytautas Petrauskas, Daumantas Matulis, and Egidijus Kazlauskas. Recent advances in computational and experimental protein-ligand affinity determination techniques. *Expert Opinion on Drug Discovery*, 19(6):649–670, 2024. ISSN 1746-0441. doi: 10.1080/17460441.2024.2349169.

[21] Stephen K. Burley, Amy Wu-Wu, Shuchismita Dutta, Shridar Ganesan, and Steven X. F. Zheng. Impact of structural biology and the protein data bank on us fda new drug approvals of low molecular weight antineoplastic agents 2019–2023. 43(29):2229–2243, 2024. ISSN 1476-5594. doi: 10.1038/s41388-024-03077-2.

[22] Caught between a ROCK and a hard place: current challenges in structure-based drug design. 29(9):104106, 2024. ISSN 1359-6446. doi: 10.1016/j.drudis.2024.104106.

[23] A critical assessment of docking programs and scoring functions. 49:5912–5931, 2005. ISSN 0022-2623. doi: 10.1021/jm050362n.

[24] Comparative assessment of scoring functions: The CASF-2016 update. 59(2):895–913, 2018. ISSN 1549-9596. doi: 10.1021/acs.jcim.8b00545.

[25] The last mile problem: A critical assessment of physics-based and AI tools for small molecule binding prediction in virtual screening. 66(2026):5964–5977. ISSN 1549-960X. doi: 10.1021/acs.jcim.6c00942.

[26] Jean-Paul Renaud, Chun-wa Chung, U. Helena Danielson, Ursula Egner, Michael Hennig, Roderick E. Hubbard, and Herbert Nar. Biophysics in drug discovery: Impact, challenges and opportunities. *Nature Reviews Drug Discovery*, 15(10):679–698, 2016. ISSN 1474-1776. doi: 10.1038/nrd.2016.123.

[27] Remo Perozzo, Gerd Folkers, and Leonardo Scapozza. Thermodynamics of protein-ligand interactions: History, presence, and future aspects. *Journal of Receptor and Signal Transduction Research*, 24(1):1–52, 2004. ISSN 1079-9893.

[28] Bert L. Vallee and David S. Auld. Zinc coordination, function, and structure of zinc enzymes and other proteins. *Biochemistry*, 29(24): 5647–5659, 1990. ISSN 0006-2960. doi: 10.1021/bi00476a001.

[29] Protein-ligand interactions: Hydrodynamics and calorimetry, 2001.

[30] Caterina Bissantz, Bernd Kuhn, and Martin Stahl. A medicinal chemist's guide to molecular interactions. *Journal of Medicinal Chemistry*, 53(14):5061–5084, 2010. ISSN 0022-2623, 1520-4804. doi: 10.1021/jm100112j.

[31] S. Lindskog. Structure and mechanism of carbonic anhydrase. *Pharmacology & Therapeutics*, 74(1):1–20, 1997. ISSN 0163-7258. doi: 10.1016/s0163-7258(96)00198-2.

[32] A. Liljas, K. K. Kannan, P. C. Bergsten, I. Waara, K. Fridborg, B. Strandberg, U. Carlbom, L. Jarup, S. Lovgren, and M. Petef. Crystal structure of human carbonic anhydrase c. *Nat. New. Biol.*, 235(57):131–137, 1972. doi: 10/gjv9sf.

[33] Claudiu T. Supuran. Carbonic anhydrases–an overview. *Current Pharmaceutical Design*, 14(7):603–614, 2008. ISSN 1873-4286. doi: 10.2174/138161208783877884.

[34] Vincenzo Alterio, Anna Di Fiore, Katia D'Ambrosio, Claudiu T. Supuran, and Giuseppina De Simone. Multiple binding modes of inhibitors to carbonic anhydrases: How to design specific drugs targeting 15 different isoforms? *Chemical Reviews*, 112(8):4421–4468, 2012. ISSN 0009-2665, 1520-6890. doi: 10.1021/cr200176r.

[35] Denis Baronas, Birutė Knašienė, Aurelija Mickevičiūtė, Jelena Jachno, Evaldas Naujalis, Asta Zubrienė, and Daumantas Matulis. Inhibitor binding to metal-substituted metalloenzyme: Sulfonamide affinity for carbonic anhydrase IX. *Journal of Inorganic Biochemistry*, 256:112547, 2024. ISSN 0162-0134. doi: 10.1016/j.jinorgbio.2024.112547.

[36] Tjelvar S. G. Olsson, Mark A. Williams, William R. Pitt, and John E. Ladbury. The thermodynamics of protein-ligand interaction and solvation: insights for ligand design. *J. Mol. Biol.*, 384(4):1002–1017, 2008. ISSN 1089-8638. doi: 10.1016/j.jmb.2008.09.073.

[37] George M. Whitesides and Vijay M. Krishnamurthy. Designing ligands to bind proteins. *Quarterly Reviews of Biophysics*, 38(4):385–395, 2005. ISSN 0033-5835. doi: 10.1017/S0033583506004240.

[38] Gerhard Klebe. The use of thermodynamic and kinetic data in drug discovery: decisive insight or increasing the puzzlement? *ChemMedChem*, 10(2):229–231, 2015. ISSN 1860-7187. doi: 10.1002/cmdc.201402521.

[39] Steve W. Homans. Water, water everywhere — except where it matters? *Drug Discovery Today*, 12(13):534–539, 2007. ISSN 1359-6446. doi: 10.1016/j.drudis.2007.05.004.

[40] Tom Young, Robert Abel, Byungchan Kim, Bruce J. Berne, and Richard A. Friesner. Motifs for molecular recognition exploiting hydrophobic enclosure in protein–ligand binding. *Proceedings of the National Academy of Sciences*, 104(3):808–813, 2007. doi: 10.1073/pnas.0610202104.

[41] Robert Abel, Tom Young, Ramy Farid, Bruce J. Berne, and Richard A. Friesner. Role of the active-site solvent in the thermodynamics of factor xa ligand binding. *Journal of the American*

Chemical Society, 130(9):2817–2831, 2008. ISSN 0002-7863. doi: 10.1021/ja0771033.

[42] D. N. Silverman and S. Lindskog. The catalytic mechanism of carbonic anhydrase: implications of a rate-limiting proteolysis of water. *Accounts of Chemical Research*, 21:30–36, 1988. doi: doi.org/10.1021/ar00145a005.

[43] Balendu Sankara Avvaru, Chae Un Kim, Katherine H Sippel, Sol M Gruner, Mavis Agbandje-McKenna, David N Silverman, and Robert McKenna. A short, strong hydrogen bond in the active site of human carbonic anhydrase II. *Biochemistry*, 49(2):249–251, 2010. doi: 10.1021/bi902007b.

[44] Melissa A. Pinard, Brian Mahon, and Robert McKenna. Probing the surface of human carbonic anhydrase for clues towards the design of isoform specific inhibitors. *BioMed Research International*, 2015:e453543, 2015. ISSN 2314-6133. doi: 10.1155/2015/453543.

[45] Zoë Fisher, Andrey Y. Kovalevsky, Marat Mustyakimov, David N. Silverman, Robert McKenna, and Paul Langan. Neutron structure of human carbonic anhydrase II: a hydrogen-bonded water network "switch" is observed between pH 7.8 and 10.0. *Biochemistry*, 50(44):9421–9423, 2011. doi: 10.1021/bi201487b.

[46] Ryszard Michalczyk, Clifford J Unkefer, John-Paul Bacik, Tobias E Schrader, Andreas Ostermann, Andrey Y Kovalevsky, Robert McKenna, and Suzanne Zoë Fisher. Joint neutron crystallographic and NMR solution studies of tyr residue ionization and hydrogen bonding: Implications for enzyme-mediated proton transfer. *Proc. Natl. Acad. Sci. U.S.A.*, 112(18):5673–5678, 2015. doi: 10.1073/pnas.1502255112.

[47] Chae Un Kim, HyoJin Song, Balendu Sankara Avvaru, Sol M. Gruner, SangYoun Park, and Robert McKenna. Tracking solvent and protein movement during CO2 release in carbonic anhydrase II crystals. *Proceedings of the National academy of Sciences of the United States of America*, 113(19):5257–5262, 2016. doi: 10.1073/pnas.1520786113.

[48] J. K. Kim, C. L. Lomelino, B. S. Avvaru, B. P. Mahon, R. McKenna, S. Park, and C. U. Kim. Active-site solvent replenishment observed during human carbonic anhydrase II catalysis. *IUCrJ*, 5(1):93–102, 2018. ISSN 2052-2525. doi: 10.1107/S2052252517017626.

[49] Rose Mikulski, Dayne West, Katherine H. Sippel, Balendu Sankara Avvaru, Mayank Aggarwal, Chingkuang Tu, Robert McKenna, and David N. Silverman. Water networks in fast proton transfer during catalysis by human carbonic anhydrase II. *Biochemistry*, 52(1):125–131, 2013. ISSN 0006-2960, 1520-4995. doi: 10.1021/bi301099k.

[50] David N. Silverman and Robert McKenna. Solvent-mediated proton transfer in catalysis by carbonic anhydrase. *Accounts of Chemical Research*, 40(8):669–675, 2007. ISSN 0001-4842. doi: 10.1021/ar7000588.

[51] Jin Kyun Kim, Seon Woo Lim, Hannah Jeong, Cheol Lee, Seoyoon Kim, Dong Woo Son, Rajeev Kumar, Jacob T. Andring, Carrie Lomelino, Jennifer L. Wierman, Aina E. Cohen, Tae Joo Shin, Cheol-Min Ghim, Robert McKenna, Byung Hoon Jo, Duyoung Min, Jeong-Mo Choi, and Chae Un Kim. Fast product release requires active-site water dynamics in carbonic anhydrase. *Nature Communications*, 16(1):4404, 2025. ISSN 2041-1723. doi: 10.1038/s41467-025-59645-x.

[52] M. T. Record, C. F. Anderson, and T. M. Lohman. Thermodynamic analysis of ion effects on the binding and conformational equilibria of proteins and nucleic acids: the roles of ion association or release, screening, and ion effects on water activity. *Quarterly Reviews of Biophysics*, 11(2):103–178, 1978. ISSN 0033-5835. doi: 10.1017/s003358350000202x.

[53] Kim A. Sharp. Polyelectrolyte electrostatics: Salt dependence, entropic, and enthalpic contributions to free energy in the nonlinear poisson–boltzmann model. *Biopolymers*, 36(2):227–243, 1995. ISSN 1097-0282. doi: 10.1002/bip.360360210.

[54] Ken A. Dill. Dominant forces in protein folding. *Biochemistry*, 29 (31):7133–7155, 1990. ISSN 0006-2960. doi: 10.1021/bi00483a001.

[55] Adam Biela, Nader N. Nasief, Michael Betz, Andreas Heine, David Hangauer, and Gerhard Klebe. Dissecting the hydrophobic effect on the molecular level: the role of water, enthalpy, and entropy in ligand binding to thermolysin. *Angewandte Chemie (International Ed. in English)*, 52(6):1822–1828, 2013. ISSN 1521-3773. doi: 10.1002/anie.201208561.

[56] Phillip W. Snyder, Jasmin Mecinović, Demetri T. Moustakas, Samuel W. Thomas, Michael Harder, Eric T. Mack, Matthew R. Lockett, Annie Héroux, Woody Sherman, and George M. Whitesides. Mechanism of the hydrophobic effect in the biomolecular recognition of arylsulfonamides by carbonic anhydrase. *Proceedings of the National Academy of Sciences of the United States of America*, 108(44):17889–17894, 2011. ISSN 0027-8424. doi: 10.1073/pnas.1114107108.

[57] David Chandler. Interfaces and the driving force of hydrophobic assembly. *Nature*, 437(7059):640–647, 2005. ISSN 1476-4687. doi: 10.1038/nature04162.

[58] Steffen Glöckner, Khang Ngo, Björn Wagner, Andreas Heine, and Gerhard Klebe. The influence of varying fluorination patterns on

the thermodynamics and kinetics of benzenesulfonamide binding to human carbonic anhydrase II. *Biomolecules*, 10(4):509, 2020. doi: 10.3390/biom10040509.

[59] Sophie Purser, Peter R. Moore, Steve Swallow, and Véronique Gouverneur. Fluorine in medicinal chemistry. *Chemical Society Reviews*, 37(2):320–330, 2008. ISSN 0306-0012. doi: 10.1039/b610213c.

[60] Miguel Bernús, Gonzalo D. Núñez, Will C. Hartley, Marc Guasch, Jordi Mestre, Maria Besora, Jorge J. Carbó, and Omar Boutureira. Impact of fluorine pattern on lipophilicity and acid–base properties of 2-(thiofluoroalkyl)pyridines: Insights from experiments and statistical modeling. *Journal of Medicinal Chemistry*, 68(4):4787–4800, 2025. ISSN 0022-2623. doi: 10.1021/acs.jmedchem.4c03045.

[61] Xing Du, Yi Li, Yuan-Ling Xia, Shi-Meng Ai, Jing Liang, Peng Sang, Xing-Lai Ji, and Shu-Qun Liu. Insights into Protein–Ligand Interactions: Mechanisms, Models, and Methods. *International Journal of Molecular Sciences*, 17(2), 2016. ISSN 1422-0067. doi: 10.3390/ijms17020144.

[62] Sven Lindskog and David N. Silverman. The catalytic mechanism of mammalian carbonic anhydrases. In Prof Dr W. Richard Chegwidden, Nicholas D. Carter, and Yvonne H. Edwards, editors, *The Carbonic Anhydrases*, number 90 in EXS 90, pages 175–195. Birkhäuser Basel, 2000. ISBN 978-3-0348-9570-5 978-3-0348-8446-4.

[63] Virginija Dudutienė, Asta Zubrienė, Visvaldas Kairys, Alexey Smirnov, Joana Smirnovienė, Janis Leitans, Andris Kazaks, Kaspars Tars, Lena Manakova, Saulius Gražulis, and Daumantas Matulis. Isoform-selective enzyme inhibitors by exploring pocket size according to the lock-and-key principle. *Biophysical Journal*, 119: 1513–1524, 2020. ISSN 1542-0086. doi: 10.1016/j.bpj.2020.08.037.

[64] Kendra King Frederick, Michael S. Marlow, Kathleen G. Valentine, and A. Joshua Wand. Conformational entropy in molecular recognition by proteins. *Nature*, 448(7151):325–329, 2007. ISSN 1476-4687. doi: 10.1038/nature05959.

[65] A Joshua Wand. The dark energy of proteins comes to light: conformational entropy and its role in protein function revealed by NMR relaxation. *Current Opinion in Structural Biology*, 23(1): 75–81, 2013. ISSN 0959-440X. doi: 10.1016/j.sbi.2012.11.005.

[66] Charlotte A Miller and Stephanie A Wankowicz. Binding entropy can be predicted by crystallographic ensembles.

[67] Stefan Senger, Chuen Chan, Máire A. Convery, Julia A. Hubbard, Gita P. Shah, Nigel S. Watson, and Robert J. Young. Sulfonamide-related conformational effects and their importance in structure-based design. *Bioorganic & Medicinal Chemistry Letters*, 17(10): 2931–2934, 2007. ISSN 0960-894X. doi: 10.1016/j.bmcl.2007.02.034.

[68] David D Boehr, Ruth Nussinov, and Peter E Wright. The role of dynamic conformational ensembles in biomolecular recognition. *Nature Chemical Biology*, 5(11):789–796, 2009. ISSN 1552-4450, 1552-4469. doi: 10.1038/nchembio.232.

[69] Ruth Nussinov, Buyong Ma, and Chung-Jung Tsai. Multiple conformational selection and induced fit events take place in allosteric propagation. *Biophysical chemistry*, 186:22–30, 2014. ISSN 0301-4622. doi: 10.1016/j.bpc.2013.10.002.

[70] Maria Luisa Verteramo, Olof Stenström, Majda Misini Ignjatovic, Octav Caldararu, Martin A. Olsson, Francesco Manzoni, Hakon Leffler, Esko Oksanen, Derek T. Logan, Ulf J. Nilsson, Ulf Ryde, and Mikael Akke. Interplay between conformational entropy and solvation entropy in protein–ligand binding. *Journal of the American Chemical Society*, 2019. ISSN 0002-7863. doi: 10.1021/jacs.8b11099.

[71] D. E. Koshland. Application of a theory of enzyme specificity to protein synthesis. *Proceedings of the National Academy of Sciences of the United States of America*, 44(2):98–104, 1958. ISSN 0027-8424. doi: 10.1073/pnas.44.2.98.

[72] Ernesto Freire. Do enthalpy and entropy distinguish first in class from best in class? *Drug Discovery Today*, 13(19):869–874, 2008. ISSN 1359-6446. doi: 10.1016/j.drudis.2008.07.005.

[73] Craig A. Behnke, Isolde Le Trong, Jeff W. Godden, Ethan A. Merritt, David C. Teller, Jürgen Bajorath, and Ronald E. Stenkamp. Atomic resolution studies of carbonic anhydrase II. *Acta Crystallogr. D*, 66(5):616–627, 2010. doi: 10.1107/S0907444910006554.

[74] Himanshu Singh, Chandan K. Das, Suresh K. Vasa, Kristof Grohe, Lars V. Schäfer, and Rasmus Linser. The active site of a prototypical "rigid" drug target is marked by extensive conformational dynamics. *Angewandte Chemie International Edition*, 2020. ISSN 1433-7851, 1521-3773. doi: 10.1002/anie.202009348.

[75] Himanshu Singh, Suresh K. Vasa, Harish Jangra, Petra Rovó, Christopher Päslack, Chandan K. Das, Hendrik Zipse, Lars V. Schäfer, and Rasmus Linser. Fast microsecond dynamics of the protein–water network in the active site of human carbonic anhydrase II studied by solid-state NMR spectroscopy. *Journal of the American Chemical Society*, 141(49):19276–19288, 2019. ISSN 0002-7863. doi: 10.1021/jacs.9b05311.

[76] Suresh K. Vasa, Himanshu Singh, Kristof Grohe, and Rasmus Linser. Assessment of a large enzyme–drug complex by proton-detected solid-state NMR spectroscopy without deuteration. *Angewandte Chemie International Edition*, 58(17):5758–5762, 2019. ISSN 1521-3773. doi: 10.1002/anie.201811714.

[77] Divya Rai, Satyajit Khatua, and Srabani Taraphder. Structure and dynamics of the isozymes II and IX of human carbonic anhydrase. *ACS Omega*, 7(35):31149–31166, 2022. doi: 10.1021/acsomega.2c03356.

[78] Joshua A. Hull, Cheol Lee, Jin Kyun Kim, Seon Woo Lim, Jaehyun Park, Sehan Park, Sang Jae Lee, Gisu Park, Intae Eom, Minseok Kim, HyoJung Hyun, Jacob E. Combs, Jacob T. Andring, Carrie Lomelino, Chae Un Kim, and Robert McKenna. XFEL structure of carbonic anhydrase II: a comparative study of XFEL, NMR, x-ray and neutron structures. *Acta Crystallographica. Section D, Structural Biology*, 80:194–202, 2024. ISSN 2059-7983. doi: 10.1107/S2059798324000482.

[79] Vytautas Petrauskas, Lina Baranauskienė, Asta Zubrienė, and Daumantas Matulis. Isothermal Titration Calorimetry and Fluorescent Thermal and Pressure Shift Assays in Protein-Ligand Interactions. In *Biocalorimetry*, pages 261–280. CRC Press, 2016. doi: 10.1201/b20161-18.

[80] Gediminas Skvarnavičius, Daumantas Matulis, and Vytautas Petrauskas. Change in Volume Upon Inhibitor Binding to Carbonic Anhydrases by Fluorescent Pressure Shift Assay. In Daumantas Matulis, editor, *Carbonic Anhydrase as Drug Target: Thermodynamics and Structure of Inhibitor Binding*, pages 97–106. Springer International Publishing, Cham, 2019. ISBN 978-3-030-12780-0.

[81] Lehninger, Albert L, David L. Nelson, and Michael M. Cox. *Lehninger Principles of Biochemistry*. Worth Publishers, New York, 5th edition, 2000.

[82] John E. Ladbury. Calorimetry as a tool for understanding biomolecular interactions and an aid to drug design. *Biochemical Society Transactions*, 38(4):888–893, 2010. ISSN 1470-8752. doi: 10.1042/BST0380888.

[83] Jerome M Fox, Mengxia Zhao, Michael J Fink, Kyungtae Kang, and George M Whitesides. The Molecular Origin of Enthalpy/Entropy Compensation in Biomolecular Recognition. page 31, 2018.

[84] N. U. Meldrum and F. J. W. Roughton. Carbonic anhydrase. Its preparation and properties. *The Journal of Physiology*, 80(2):113–142, 1933. ISSN 1469-7793. doi: 10.1113/jphysiol.1933.sp003077.

[85] Carbonic anhydrase: Mechanism, regulation, links to disease, and industrial applications, 2014.

[86] The carbonic anhydrases: Current and emerging therapeutic targets, 2021.

[87] Ashok Aspatwar and Seppo Parkkila. Carbonic anhydrase-related proteins VIII, x, and XI: Evolutionary divergence and emerging biological roles. In *The Enzymes*, volume 59, pages 177–194. Elsevier,

2026. ISBN 978-0-443-47086-8. doi: 10.1016/bs.enz.2026.05.004.

[88] Carrie L. Lomelino, Jacob T. Andring, and Robert McKenna. Crystallography and Its Impact on Carbonic Anhydrase Research. *International Journal of Medicinal Chemistry*, 2018:9419521, 2018. ISSN 2090-2069. doi: 10.1155/2018/9419521.

[89] K. K. Kannan, B. Notstrand, K. Fridborg, S. Lovgren, A. Ohlsson, and M. Petef. Crystal structure of human erythrocyte carbonic anhydrase b. three-dimensional structure at a nominal 2.2-Å resolution. *Proc. Natl. Acad. Sci. U. S. A.*, 72(1):51–55, 1975.

[90] A. E. Eriksson, T. A. Jones, and A. Liljas. Refined structure of human carbonic anhydrase II at 2.0 a resolution. *Proteins*, 4(4): 274–282, 1988. doi: 10.1002/prot.340040406.

[91] J. F. Krebs, J. A. Ippolito, D. W. Christianson, and C. A. Fierke. Structural and functional importance of a conserved hydrogen bond network in human carbonic anhydrase II. *J. Biol. Chem.*, 268 (36):27458–27466, 1993.

[92] Chingkuang Tu, Minzhang Qian, Haiqian An, Nina R. Wadhwa, David Duda, Craig Yoshioka, Yashash Pathak, Robert McKenna, Philip J. Laipis, and David N. Silverman. Kinetic Analysis of Multiple Proton Shuttles in the Active Site of Human Carbonic Anhydrase. *J. Biol. Chem.*, 277(41):38870–38876, 2002. ISSN 0021-9258, 1083-351X. doi: 10.1074/jbc.M20E5791200.

[93] R. S. Alexander, L. L. Kiefer, C. A. Fierke, and D. W. Christianson. Engineering the zinc binding site of human carbonic anhydrase II: structure of the his-94–>cys apoenzyme in a new crystalline form. *Biochemistry*, 32(6):1510–1518, 1993.

[94] Zoë Fisher, Jose A. Hernandez Prada, Chingkuang Tu, David Duda, Craig Yoshioka, Haiqian An, Lakshmanan Govindasamy, David N. Silverman, and Robert McKenna. Structural and kinetic characterization of active-site histidine as a proton shuttle in catalysis by human carbonic anhydrase II. *Biochemistry*, 44(4): 1097–1105, 2005. doi: 10.1021/bi0480279.

[95] John F. Domsic, Balendu Sankara Avvaru, Chae Un Kim, Sol M. Gruner, Mavis Agbandje-McKenna, David N. Silverman, and Robert McKenna. Entrapment of carbon dioxide in the active site of carbonic anhydrase II. *J. Biol. Chem.*, 283(45):30766–30771, 2008. doi: 10.1074/jbc.M805353200.

[96] A. E. Eriksson and A. Liljas. Refined structure of bovine carbonic anhydrase III at 2.0 a resolution. *Proteins*, 16(1):29–42, 1993. doi: 10.1002/prot.340160104.

[97] T. Stams, S. K. Nair, T. Okuyama, A. Waheed, W. S. Sly, and D. W. Christianson. Crystal structure of the secretory form of membrane-associated human carbonic anhydrase IV at 2.8-a resolution. *Proc.*

Natl. Acad. Sci. U. S. A., 93(24):13589–13594, 1996.

[98] Mayank Aggarwal, Christopher D. Boone, Bhargav Kondeti, and Robert McKenna. Structural annotation of human carbonic anhydrases. *J. Enzyme Inhib. Med. Chem.*, 28(2):267–277, 2013. ISSN 1475-6366, 1475-6374. doi: 10.3109/14756366.2012.737323.

[99] Ewa S Pilka, Grazyna Kochan, Udo Oppermann, and Wyatt W Yue. Crystal structure of the secretory isozyme of mammalian carbonic anhydrases CA VI: implications for biological assembly and inhibitor development. *Biochem. Biophys. Res. Commun.*, 419 (3):485–489, 2012. doi: 10.1016/j.bbrc.2012.02.038.

[100] Vincenzo Alterio, Mika Hilvo, Anna Di Fiore, Claudiu T. Supuran, Peiwen Pan, Seppo Parkkila, Andrea Scaloni, Jaromir Pastorek, Silvia Pastorekova, Carlo Pedone, and others. Crystal structure of the catalytic domain of the tumor-associated human carbonic anhydrase IX. *Proc. Natl. Acad. Sci. U. S. A.*, 106(38):16233–16238, 2009.

[101] Katarina Koruza, A. Briana Murray, Brian P. Mahon, Jesse B. Hopkins, Wolfgang Knecht, Robert McKenna, and S. Zoë Fisher. Biophysical characterization of cancer-related carbonic anhydrase IX. *International Journal of Molecular Sciences*, 21(15):5277, 2020. ISSN 1422-0067. doi: 10.3390/ijms21155277.

[102] D. A. Whittington, A. Waheed, B. Ulmasov, G. N. Shah, J. H. Grubb, W. S. Sly, and D. W. Christianson. Crystal structure of the dimeric extracellular domain of human carbonic anhydrase XII, a bitopic membrane protein overexpressed in certain cancer tumor cells. *Proc. Natl. Acad. Sci. U.S.A.*, 98(17):9545–9550, 2001. doi: 10.1073/pnas.161301298.

[103] Anna Di Fiore, Simona Maria Monti, Mika Hilvo, Seppo Parkkila, Vincenza Romano, Andrea Scaloni, Carlo Pedone, Andrea Scozzafava, Claudiu T. Supuran, and Giuseppina De Simone. Crystal structure of human carbonic anhydrase XIII and its complex with the inhibitor acetazolamide. *Proteins*, 74(1):164–175, 2009. doi: 10.1002/prot.22144.

[104] Vincenzo Alterio, Peiwen Pan, Seppo Parkkila, Martina Buonanno, Claudiu T. Supuran, Simona M. Monti, and Giuseppina De Simone. The structural comparison between membrane-associated human carbonic anhydrases provides insights into drug design of selective inhibitors. *Biopolymers*, 101(7):769–778, 2014. ISSN 1097-0282. doi: 10.1002/bip.22456.

[105] S. Lindskog and J. E. Coleman. The catalytic mechanism of carbonic anhydrase. *Proc Natl Acad Sci U S A*, 70(9):2505–8, 1973.

[106] S. Zoë Fisher, Andrey Y. Kovalevsky, John F. Domsic, Marat Mustyakimov, Robert McKenna, David N. Silverman, and Paul A.

Langan. Neutron Structure of Human Carbonic Anhydrase II: Implications for Proton Transfer. *Biochemistry*, 49(3):415–421, 2010. ISSN 0006-2960. doi: 10.1021/bi901995n.

[107] S. Zoë Fisher, Mayank Aggarwal, Andrey Y. Kovalevsky, David N. Silverman, and Robert McKenna. Neutron diffraction of acetazolamide-bound human carbonic anhydrase II reveals atomic details of drug binding. *Journal of the American Chemical Society*, 134 (36):14726–14729, 2012. ISSN 1520-5126. doi: 10.1021/ja3068098.

[108] T. Mann and D. Keilin. Sulphanilamide as a Specific Inhibitor of Carbonic Anhydrase. *Nature*, 146(3692):164, 1940. ISSN 1476-4687. doi: 10.1038/146164a0.

[109] Nicholas A. Meanwell. Fluorine and fluorinated motifs in the design and application of bioisosteres for drug design. *Journal of Medicinal Chemistry*, 61(14):5822–5880, 2018. ISSN 1520-4804. doi: 10.1021/acs.jmedchem.7b01788.

[110] Fabrizio Carta, Andrea Scozzafava, and Claudiu T. Supuran. Sulfonamides: A patent review (2008 – 2012). *Expert Opinion on Therapeutic Patents*, 22(7):747–758, 2012. ISSN 1354-3776. doi: 10.1517/13543776.2012.698264.

[111] Claudiu T. Supuran. How many carbonic anhydrase inhibition mechanisms exist? *Journal of Enzyme Inhibition and Medicinal Chemistry*, 31(3):345–360, 2016. ISSN 1475-6366, 1475-6374. doi: 10.3109/14756366.2015.1122001.

[112] Katia D'Ambrosio, Anna Di Fiore, Vincenzo Alterio, Emma Langella, Simona Maria Monti, Claudiu T. Supuran, and Giuseppina De Simone. Multiple binding modes of inhibitors to human carbonic anhydrases: An update on the design of isoform-specific modulators of activity. *Chemical Reviews*, 125(1):150–222, 2025. ISSN 0009-2665. doi: 10.1021/acs.chemrev.4c00278.

[113] Sarfraz Ahmad, Muhammad Usman Mirza, Mamoona Nazir, Lee Yean Kee, Noorsaadah Binti Abdrahman, Iskandar Abdullah, and John F. Trant. A comprehensive review of the structural basis for the selectivity of sulfonamide-based inhibitors for carbonic anhydrase isoforms IX and XII over carbonic anhydrase II based on the available high quality crystallographic data. *Archives of Biochemistry and Biophysics*, 777:110682, 2026. ISSN 0003-9861. doi: 10.1016/j.abb.2025.110682.

[114] Tautvydas Kojis, Helgi B. Schiöth, Lina Baranauskiene, and Daumantas Matulis. Trends in drug discovery for carbonic anhydrases: FDA approvals, clinical trials, molecular functions, and therapeutic potential. *Pharmacological Research*, 228:108210, 2026. ISSN 10436618. doi: 10.1016/j.phrs.2026.108210.

[115] Aurelija Mickevičiūtė, Vaida Juozapaitienė, Vilma Michailovienė,

Jelena Jachno, Jurgita Matulienė, and Daumantas Matulis. Recombinant production of 12 catalytically active human CA isoforms. In Daumantas Matulis, editor, *Carbonic Anhydrase as Drug Target: Thermodynamics and Structure of Inhibitor Binding*, pages 15–37. Springer International Publishing, 2019. ISBN 978-3-030-12780-0. doi: 10.1007/978-3-030-12780-0_2.

[116] Egidijus Kazlauskas, Vytautas Petrauskas, Vaida Paketurytė, and Daumantas Matulis. Standard operating procedure for fluorescent thermal shift assay (FTSA) for determination of protein–ligand binding and protein stability. *European Biophysics Journal*, 50(3):373–379, 2021. ISSN 0175-7571, 1432-1017. doi: 10.1007/s00249-021-01537-1.

[117] Vytautas Petrauskas, Egidijus Kazlauskas, Marius Gedgaudas, Lina Baranauskienė, Asta Zubrienė, and Daumantas Matulis. Thermal shift assay for protein–ligand dissociation constant determination. *TrAC Trends in Analytical Chemistry*, 170:117417, 2024. ISSN 0165-9936. doi: 10.1016/j.trac.2023.117417.

[118] Asta Zubrienė, Egidijus Kazlauskas, Lina Baranauskienė, Vytautas Petrauskas, and Daumantas Matulis. Isothermal titration calorimetry and thermal shift assay in drug design. *European Pharmaceutical Review*, 16:56–59, 2011.

[119] Andrea Ilari and Carmelinda Savino. Protein structure determination by x-ray crystallography. *Methods in Molecular Biology (Clifton, N.J.)*, 452:63–87, 2008. ISSN 1064-3745. doi: 10.1007/978-1-60327-159-2_3.

[120] Alexey Smirnov, Elena Manakova, Saulius Gražulis, Robert McKenna, and Daumantas Matulis. Structures of human carbonic anhydrases and their complexes with inhibitors. In Daumantas Matulis, editor, *Carbonic Anhydrase as Drug Target: Thermodynamics and Structure of Inhibitor Binding*, pages 179–202. Springer International Publishing, 2019. ISBN 978-3-030-12780-0. doi: 10.1007/978-3-030-12780-0_13.

[121] Kaspars Tars and Daumantas Matulis. X-ray crystallographic structures of high-affinity and high-selectivity inhibitor complexes with CA IX that plays a special role in cancer. In Daumantas Matulis, editor, *Carbonic Anhydrase as Drug Target: Thermodynamics and Structure of Inhibitor Binding*, pages 203–213. Springer International Publishing, 2019. ISBN 978-3-030-12780-0. doi: 10.1007/978-3-030-12780-0_14.

[122] Joana Smirnovienė, Lina Baranauskienė, Asta Zubrienė, and Daumantas Matulis. A standard operating procedure for an enzymatic activity inhibition assay. *European Biophysics Journal*, 50(3):345–352, 2021. ISSN 1432-1017. doi: 10.1007/s00249-021-01530-8.

[123] Visvaldas Kairys, Lina Baranauskiene, Migle Kazlauskiene, Daumantas Matulis, and Egidijus Kazlauskas. Binding affinity in drug design: experimental and computational techniques. *Expert Opinion on Drug Discovery*, pages 1–14, 2019. ISSN 1746-0441, 1746-045X. doi: 10.1080/17460441.2019.1623202.

[124] Joana Smirnovienė, Vytautas Smirnovas, and Daumantas Matulis. Picomolar inhibitors of carbonic anhydrase: Importance of inhibition and binding assays. *Anal. Biochem.*, 522:61–72, 2017. ISSN 0003-2697. doi: 10.1016/j.ab.2017.01.022.

[125] Darius Lingė, Marius Gedgaudas, Andrius Merkys, Vytautas Petrauskas, Antanas Vaitkus, Algirdas Grybauskas, Vaida Paketurytė, Asta Zubrienė, Audrius Zakšauskas, Aurelija Mickevičiūtė, Joana Smirnovienė, Lina Baranauskienė, Edita Čapkauskaitė, Virginija Dudutienė, Ernestas Urniežius, Aleksandras Konovalovas, Egidijus Kazlauskas, Kirill Shubin, Helgi B Schiöth, Wen-Yih Chen, John E Ladbury, Saulius Gražulis, and Daumantas Matulis. PLBD: protein–ligand binding database of thermodynamic and kinetic intrinsic parameters. *Database*, 2023:baad040, 2023. ISSN 1758-0463. doi: 10.1093/database/baad040.

[126] Daumantas Matulis and Rex Lovrien. 1-Anilino-8-Naphthalene Sulfonate Anion-Protein Binding Depends Primarily on Ion Pair Formation. *Biophys. J.*, 74(1):422–429, 1998. ISSN 0006-3495. doi: 10.1016/S0006-3495(98)77799-9.

[127] Piotras Cimmperman, Lina Baranauskienė, Simona Jachimovičiūtė, Jelena Jachno, Jolanta Torresan, Vilma Michailovienė, Jurgita Matulienė, Jolanta Sereikaitė, Vladas Bumelis, and Daumantas Matulis. A Quantitative Model of Thermal Stabilization and Destabilization of Proteins by Ligands. *Biophysical Journal*, 95 (7):3222–3231, 2008. ISSN 00063495. doi: 10.1529/biophysj.108.134973.

[128] Marius Gedgaudas, Denis Baronas, Egidijus Kazlauskas, Vytautas Petrauskas, and Daumantas Matulis. Thermott: A comprehensive online tool for protein–ligand binding constant determination. *Drug Discovery Today*, 27(8):2076–2079, 2022. ISSN 1359-6446. doi: 10.1016/j.drudis.2022.05.008.

[129] T. Wiseman, S. Williston, J. F. Brandts, and L. N. Lin. Rapid measurement of binding constants and heats of binding using a new titration calorimeter. *Analytical Biochemistry*, 179(1):131–137, 1989. ISSN 0003-2697.

[130] Thomas H. Scheuermann and Chad A. Brautigam. High-precision, automated integration of multiple isothermal titration calorimetric thermograms: new features of NITPIC. *Methods (San Diego, Calif.)*, 76:87–98, 2015. ISSN 1095-9130. doi: 10.1016/j.ymeth.2014.11.024.

[131] Peter Schuck, Huaying Zhao, and Chad A. Brautigam. Chapter 7 - unbiased baseline determination, global analysis, and multimethod analysis of titration isotherms in SEDPHAT and NITPIC. In Munishwar Nath Gupta, Anthony Mittermaier, and Justin Di Trani, editors, *Isothermal Titration Calorimetry in Enzymology*, Foundations and Frontiers in Enzymology, pages 119–140. Academic Press, 2026. ISBN 978-0-443-21848-4. doi: 10.1016/B978-0-443-21848-4.00009-1.

[132] Huaying Zhao, Grzegorz Piszczek, and Peter Schuck. SEDPHAT – a platform for global ITC analysis and global multi-method analysis of molecular interactions. *Methods*, 76:137–148, 2015. ISSN 10462023. doi: 10.1016/j.ymeth.2014.11.012.

[133] Chad A. Brautigam. Calculations and publication-quality illustrations for analytical ultracentrifugation data. *Methods in Enzymology*, 562:109–133, 2015. ISSN 1557-7988. doi: 10.1016/bs.mie.2015.05.001.

[134] Vaida Linkuvienė, Asta Zubrienė, Elena Manakova, Vytautas Petrauskas, Lina Baranauskienė, Audrius Zakšauskas, Alexey Smirnov, Saulius Gražulis, John E. Ladbury, and Daumantas Matulis. Thermodynamic, kinetic, and structural parameterization of human carbonic anhydrase interactions toward enhanced inhibitor design. *Quarterly Reviews of Biophysics*, 51, 2018. ISSN 0033-5835, 1469-8994. doi: 10.1017/S0033583518000082.

[135] Robert N. Goldberg, Nand Kishore, and Rebecca M. Lennen. Thermodynamic quantities for the ionization reactions of buffers. *J. Phys. Chem. Ref. Data*, 31(2):231–370, 2002. ISSN 0047-2689. doi: 10.1063/1.1416902.

[136] Audrius Zakšauskas, Vaida Paketurytė-Latvė, Alberta Jankūnaitė, Edita Čapkauskaitė, Yann Becart, Alexey Smirnov, Klára Pospíšilová, Janis Leitans, Jiří Brynda, Andris Kazaks, Lina Baranauskienė, Elena Manakova, Saulius Gražulis, Visvaldas Kairys, Kaspars Tars, Pavlína Řezáčová, and Daumantas Matulis. Affinity and selectivity of protein–ligand recognition: A minor chemical modification changes carbonic anhydrase binding profile. *Journal of Medicinal Chemistry*, 2025. ISSN 0022-2623. doi: 10.1021/acs.jmedchem.5c01421.

[137] V. Paketurytė-Latvė, A. Smirnov, E. Manakova, L. Baranauskiene, V. Petrauskas, A. Zubrienė, J. Matulienė, V. Dudutienė, E. Čapkauskaitė, A. Zakšauskas, J. Leitans, S. Gražulis, K. Tars, and D. Matulis. From x-ray crystallographic structure to intrinsic thermodynamics of protein–ligand binding using carbonic anhydrase isozymes as a model system. *IUCrJ*, 11(4):556–569, 2024. ISSN 2052-2525. doi: 10.1107/S2052252524004627.

[138] Vaida Paketurytė, Vytautas Petrauskas, Asta Zubrienė, Olga Abian, Margarida Bastos, Wen-Yih Chen, Maria João Moreno, Georg Krainer, Vaida Linkuvienė, Arthur Sedivy, Adrian Velazquez-Campoy, Mark A. Williams, and Daumantas Matulis. Uncertainty in protein-ligand binding constants: asymmetric confidence intervals versus standard errors. *European biophysics journal: EBJ*, 2021. ISSN 1432-1017. doi: 10/gjr8hp.

[139] Jerome M. Fox, Kyungtae Kang, Madhavi Sastry, Woody Sherman, Banumathi Sankaran, Peter H. Zwart, and George M. Whitesides. Water-Restructuring Mutations Can Reverse the Thermodynamic Signature of Ligand Binding to Human Carbonic Anhydrase. *Angewandte Chemie (International Ed. in English)*, 2017. ISSN 1521-3773. doi: 10.1002/anie.201609409.

[140] Gerhard Klebe. Thermodynamic data remain a hot tip for decoding binding affinity and water impact on protein–ligand complex formation to assist lead optimization. *Journal of Medicinal Chemistry*, 69(4):3719–3730, 2026. ISSN 0022-2623. doi: 10.1021/acs.jmedchem.5c03100.

[141] J. Boström, P. O. Norrby, and T. Liljefors. Conformational energy penalties of protein-bound ligands. *Journal of Computer-Aided Molecular Design*, 12(4):383–396, 1998. ISSN 0920-654X. doi: 10.1023/a:1008007507641.

[142] A. Joshua Wand and Kim A. Sharp. Measuring Entropy in Molecular Recognition by Proteins. *Annual Review of Biophysics*, 47(1):41–61, 2018. doi: 10.1146/annurev-biophys-060414-034042.

[143] Vijay M. Krishnamurthy, Brooks R. Bohall, Chu-Young Kim, Demetri T. Moustakas, David W. Christianson, and George M. Whitesides. Thermodynamic parameters for the association of fluorinated benzenesulfonamides with bovine carbonic anhydrase II. *Chemistry, an Asian Journal*, 2(1):94–105, 2007. ISSN 1861-471X. doi: 10.1002/asia.200600360.

[144] Helge Vatheuer, Oscar Palomino-Hernández, Janis Müller, Phillip Galonska, Serghei Glinca, and Paul Czodrowski. Protonation effects in protein-ligand complexes – a case study of endothiapepsin and pepstatin a with computational and experimental methods. *ChemMedChem*, 20(8):e202400953, 2025. ISSN 1860-7187. doi: 10.1002/cmdc.202400953.

[145] Gregory A. Landrum and Sereina Riniker. Combining IC50 or ki values from different sources is a source of significant noise. *Journal of Chemical Information and Modeling*, 64(5):1560–1567, 2024. ISSN 1549-9596. doi: 10.1021/acs.jcim.4c00049.

[146] Bengt-Harald Jonsson and Anders Liljas. Perspectives on the classical enzyme carbonic anhydrase and the search for inhibitors.

Biophysical Journal, 119(7):1275–1280, 2020. ISSN 0006-3495. doi: 10.1016/j.bpj.2020.08.020.

[147] Joel Tellinghuisen and John D. Chodera. Systematic errors in isothermal titration calorimetry: Concentrations and baselines. *Analytical Biochemistry*, 414(2):297–299, 2011. ISSN 00032697. doi: 10.1016/j.ab.2011.03.024.

[148] Joel Tellinghuisen. Isothermal titration calorimetry at very low c. *Analytical Biochemistry*, 373(2):395–397, 2008. ISSN 00032697. doi: 10.1016/j.ab.2007.08.039.

[149] Joel Tellinghuisen. Optimizing experimental parameters in isothermal titration calorimetry. *The Journal of Physical Chemistry B*, 109 (42):20027–20035, 2005. ISSN 1520-6106. doi: 10.1021/jp053550y.

[150] Joel Tellinghuisen. Optimizing experimental parameters in isothermal titration calorimetry: Variable volume procedures. *The Journal of Physical Chemistry B*, 111(39):11531–11537, 2007. ISSN 1520-6106, 1520-5207. doi: 10.1021/jp074515p.

[151] Joel Tellinghuisen. Optimizing isothermal titration calorimetry protocols for the study of 1:1 binding: Keeping it simple. *Biochimica et Biophysica Acta (BBA) - General Subjects*, 1860(5):861–867, 2016. ISSN 03044165. doi: 10.1016/j.bbagen.2015.10.011.

[152] Žiga Medoš, Marija Bešter-Rogač, Epameinondas Leontidis, and Joel Tellinghuisen. Systematic errors in isothermal titration calorimetry: The role of feedback power and effects of mixing and diffusion on concentrations. *Analytical Biochemistry*, page 116010, 2025. ISSN 0003-2697. doi: 10.1016/j.ab.2025.116010.

[153] Joel Tellinghuisen. Can you trust the parametric standard errors in nonlinear least squares? yes, with provisos. *Biochimica et Biophysica Acta (BBA) - General Subjects*, 2017. ISSN 0304-4165. doi: 10.1016/j.bbagen.2017.12.016.

Santrauka
(Summary in Lithuanian)

Terminų žodynėlis

Kai kuriems disertacijoje vartojamiems terminams nėra nusistovėjusių lietuviškų atitikmenų, todėl šiame žodynėlyje pateikiami terminai ir jų apibrėžtys, kurie yra vartojami šiame darbe.

Jungimosi stiprumas (angl. *affinity*) – ligando ir baltymo sąveikos stiprumą apibūdinanti charakteristika (kiekybiškai išreiškiama parametrais K_b, K_d arba ΔG).

Profilinis tikėtinumas (angl. *profile likelihood*) – statistinis metodas pasikliautiniesiems intervalams nustatyti netiesiniuose modeliuose, geriau atspindintis parametrų (pvz., K_b) paklaidų asimetriją.

Slopiklis (angl. *inhibitor*) – cheminis junginys, kuris jungiasi prie fermento ir sumažina arba visiškai sustabdo jo katalizinį aktyvumą.

Stebimasis parametras (angl. *observed parameter*) – eksperimentiškai išmatuota vertė (žymima indeksu *obs*), kuri apima ne tik tiesioginę sąveiką, bet ir susietas protonizacijos reakcijas.

Tikrasis parametras (angl. *intrinsic parameter*) – termodinaminis dydis (žymimas indeksu *int*), apibūdinantis baltymo ir ligando sąveikos energiją, atsižvelgus į susietų protonacijos pusiausvyrų indėlį.

Pagrindinės santrumpos

Santraukoje vartojamos tos pačios santrumpos ir kintamieji kaip pagrindinėje disertacijos dalyje. Vartojamos šios pagrindinės santrumpos: CA – karboanhidrazė; AZM – acetazolamidas; FTSA – fluorescencinis terminio poslinkio metodas; ITC – izoterminė titravimo kalorimetrija; PDB – Baltymų duomenų bankas (angl. *Protein Data Bank*); PLBD – Baltymų–ligandų jungimosi duomenų bazė (angl. *Protein–Ligand Binding Database* (plbd.org)).

Įvadas

Vienas svarbiausių vaistų kūrimo uždavinių yra junginių, gebančių selektyviai ir stipriai jungtis prie biologinių taikinių, paieška ir optimizavimas. Struktūrinės biologijos, biofizikos ir kompiuterinės chemijos pažanga reikšmingai išplėtė galimybes tirti baltymų ir ligandų sąveikas, todėl šios disciplinos tapo neatsiejama šiuolaikinio racionalaus vaistų projektavimo dalimi [1, 2]. Aukštos skiriamosios gebos struktūros, molekulinės simuliacijos ir struktūra grįsto vaistų projektavimo metodai suteikia vertingos informacijos apie sąveikas bei padeda optimizuoti perspektyvius junginius [3]. Nepaisant to, tiksliai prognozuoti, kaip struktūriniai pokyčiai paveiks jungimosi stiprumą ir selektyvumą, išlieka didelis ir sunkus iššūkis [4].

Baltymų ir ligandų atpažinimą lemia sudėtinga tarpmolekulinių sąveikų, hidratacijos, protonacijos pusiausvyrų ir konformacinės dinamikos visuma. Nors šie veiksniai kartu nulemia jungimosi termodinamiką, jų individualų indėlį dažnai sudėtinga atskirti ir kiekybiškai įvertinti. Dėl šios priežasties struktūriškai panašūs junginiai gali pasižymėti netikėtai skirtingomis jungimosi savybėmis, o panašus jungimosi stiprumas gali būti pasiekiamas iš esmės skirtingais mechanizmais. Šių ryšių supratimas išlieka svarbus tiek eksperimentinių, tiek kompiuterinių molekulinio atpažinimo tyrimų tikslas.

Baltymų ir ligandų sąveikų interpretaciją bei prognozavimą ypač apsunkina keli veiksniai:

- **Entalpijos ir entropijos kompensacija bei hidratacijos tinklai.** Jungimosi stiprumą lemia entalpinių ir entropinių indėlių pusiausvyra, o šie indėliai dažnai vienas kitą kompensuoja [5]. Todėl panašus jungimosi stiprumas gali būti pasiekiamas skirtingais termodinaminiais mechanizmais. Tokie skirtumai dažnai siejami su hidratacijos tinklų persitvarkymu, kurį vis dar sudėtinga tiksliai apibūdinti ir prognozuoti [6–9].
- **Konformaciniai efektai.** Nedideli cheminės struktūros pokyčiai gali pakeisti ligando geometriją, lankstumą ir vidumolekulines sąveikas, taip paveikdami energijos sąnaudas, reikalingas jungimuisi palankiai konformacijai įgyti. Tokie pokyčiai gali reikšmingai paveikti jungimąsi, net jei tiesioginės baltymo ir ligando sąveikos išlieka beveik nepakitusios [6, 10].
- **Stebimoji ir tikroji termodinamika.** Eksperimentais nustatyti jungimosi parametrai dažnai apima su protonizacijos procesais ir

buferinio tirpalo savybėmis susijusius indėlius [11, 12]. Todėl stebimi termodinaminiai parametrai ne visuomet tiesiogiai atspindi tikrąją molekulinio atpažinimo energiją, o tai apsunkina mechanistinę rezultatų interpretaciją ir skirtingų sistemų palyginimą.

Šie veiksniai rodo, kad molekulinio atpažinimo negalima visapusiškai suprasti remiantis vien suminio jungimosi stiprumo matavimais ar statinėmis struktūromis. Todėl būtina pasirinkti tinkamą modelinę sistemą, leidžiančią sistemingai tirti struktūrinių, termodinaminių ir aplinkos veiksnių įtaką jungimuisi. Karboanhidrazės (CA) yra tinkama modelinė sistema šiems klausimams nagrinėti [13]. Nors jų katalizinio centro architektūra yra labai konservatyvi, nedideli aktyviojo centro aminorūgščių ir hidratacijos tinklų organizacijos skirtumai gali lemti reikšmingus ligandų atpažinimo skirtumus. Sulfonamidiniai slopikliai šiems tyrimams ypač tinkami, nes turi bendrą karboanhidrazės cinko joną koordinuojančią funkcinę grupę, tačiau leidžia sistemiškai modifikuoti pakaitus, sąveikaujančius su skirtingomis aktyviojo centro sritimis. Tai suteikia galimybę detaliai tirti, kaip struktūriniai pokyčiai veikia jungimosi termodinamiką, stiprumą ir selektyvumą.

Patikima struktūros ir termodinamikos ryšių interpretacija reikalauja ne tik mechanistinio supratimo, bet ir tinkamo eksperimentinio neapibrėžtumo įvertinimo, ypač lyginant parametrus, gaunamus taikant netiesinius jungimosi modelius. Pagrindinė šios disertacijos hipotezė yra ta, kad prasmingi ryšiai tarp baltymo-ligando struktūros ir termodinamikos gali būti nustatyti tik sistemingai įvertinus atskirų molekulinį atpažinimą lemiančių procesų indėlį ir eksperimentinį neapibrėžtumą.

Tikslas:

Tirti ir kiekybiškai įvertinti struktūrinius, termodinaminius ir molekulinės aplinkos veiksnius, lemiančius baltymų ir ligandų molekulinį atpažinimą, naudojant karboanhidrazes ir pirminius sulfonamidus kaip modelinę sistemą.

Uždaviniai:

1. Nustatyti, kaip nedideli baltymo aktyviojo centro aminorūgščių, ligando struktūros ir hidratacijos tinklų skirtumai veikia entalpinių ir entropinių indėlių pusiausvyrą baltymo ir ligando sąveikos metu. (Publikacija 1)

2. Tirti nedidelių ligando cheminių modifikacijų poveikį ligando konformacijai, įskaitant vidumolekulinių vandenilinių ryšių susidarymą ir konformacinę energiją, bei jų reikšmę sąveikos stiprumui ir selektyvumui. (Publikacija 2)

3. Atskirti su baltymo ir ligando jungimusi susietų protonizacijos procesų indėlius nuo stebimųjų eksperimentinių parametrų ir apskaičiuoti tikruosius termodinaminius parametrus, nepriklausančius nuo protonizacijos. (Publikacija 3)

4. Standartizuoti FTSA eksperimentinius protokolus patikimam sąveikos stiprumo nustatymui bei naudoti asimetrinius profilinio tikėtinumo (angl. *profile likelihood*) pasikliautinuosius intervalus, siekiant tiksliai įvertinti ir interpretuoti neapibrėžtį netiesiniuose sąveikos modeliuose. (Publikacija 4 ir Publikacija 5)

Mokslinis naujumas

Šios disertacijos mokslinis naujumas pagrįstas integruotu požiūriu į baltymo ir ligando atpažinimo tyrimus, derinant didelės skiriamosios gebos struktūrinę analizę, tikrąją jungimosi termodinamiką ir griežtą neapibrėžčių vertinimą. Šiame darbe neapsiribojama vien jungimosi stiprumo matavimais; parodoma, kaip ligando struktūra, baltymo aplinka, hidratacijos tinklai bei su protonacija susietos pusiausvyros kartu formuoja molekulinį atpažinimą.

Pagrindiniai nauji rezultatai:

- **Struktūrinių skirtumų vaidmuo formuojant skirtingus termodinaminius mechanizmus:** parodyta, kad izofermentai (CA II, CA XII ir CA XIII) pasiekia panašų jungimosi stiprumą per iš esmės priešingus entalpinius-entropinius mechanizmus. Šiuos termodinaminius skirtumus lemia subtilūs aktyviojo centro liekanų skirtumai ir konservatyvių hidratacijos tinklų organizacijos ypatumai. (Publikacija 1)
- **Įžvalgos apie ligando konformacijos energijos kainą:** nustatyta, kad sieros atomo oksidacijos laipsnio pakeitimas (iš sulfanilo į sulfinilą ir sulfonilą) pakeitė jungimosi stiprumą iki milijono kartų. Šis stiprumo sumažėjimas susijęs su nepalankių vidumolekulinių vandenilinių ryšių susidarymu, kurie lemia nepalankią ligando konformaciją ir sukuria sterines kliūtis sąveikai su karboanhidrazėmis. (Publikacija 2)
- **Tikrųjų termodinaminių parametrų atskyrimas nuo stebimųjų:** parodyta, kad su jungimusi susietos protonacijos pusiausvyros reikšmingai veikia eksperimentiškai nustatomus stebimuosius termodinaminius parametrus. Šių indėlių atskyrimas leido nustatyti prasmingas sąsajas tarp didelės skiriamosios gebos struktūrinių duomenų ir tikrųjų molekulinio atpažinimo energijų. (Publikacija 3)
- **Nuoseklus neapibrėžties pateikimas tarp termodinaminių dydžių:** pabrėžta, kad įprasti simetriniai paklaidų įverčiai veda prie klaidingų interpretacijų, kai jungimosi stiprumas perskaičiuojamas iš disociacijos konstantų į Gibso energijas. Priešingai, asimetriniai profilinio tikėtinumo pasikliautinieji intervalai (angl. *profile-likelihood confidence intervals*) išsaugojo tikrąją neapibrėžties struktūrą ir užtikrino nuoseklią interpretaciją skirtingose jungimosi stiprumo išraiškose (Publikacija 4 ir Publikacija 5)

Ginamieji teiginiai

- Nedideli baltymų ir ligandų struktūriniai skirtumai gali lemti neproporcingai didelius molekulinio atpažinimo ir selektyvumo pokyčius, nes jungimąsi lemia visa molekulinė aplinka, įskaitant protonacijos pusiausvyras, hidrataciją, konformacinius efektus ir tarpmolekulines sąveikas. (Publikacija 1, Publikacija 2 ir Publikacija 3)
- Molekulinis baltymų ir ligandų atpažinimas negali būti visapusiškai suprastas remiantis vien struktūrine informacija ir stebimaisiais termodinaminiais parametrais; patikimai interpretacijai būtina integruoti atominės raiškos struktūrinius duomenis ir tikruosius termodinaminius parametrus. (Publikacija 1, Publikacija 2 ir Publikacija 3)
- Neapibrėžties pateikimo būdas daro įtaką baltymo ir ligando jungimosi matavimų interpretacijai; asimetriniai profilinio tikėtinumo pasikliautinieji intervalai (angl. *profile-likelihood confidence intervals*) užtikrina nuoseklų neapibrėžties aprašymą, o įprastos simetrinės standartinės paklaidos yra tam netinkamos. (Publikacija 4 ir Publikacija 5)

Literatūros apžvalgos apibendrinimas

Struktūra grįstas vaistų kūrimas: galimybės ir iššūkiai

Naujų vaistinių preparatų kūrimas ir vystymas yra itin brangus ir rizikingas procesas, reikalaujantis didelių finansinių investicijų [14]. Šis procesas paprastai trunka apie 10-15 metų [15], o kandidatų atmetimo rizika išlieka milžiniška - net ir patekus į klinikinių tyrimų stadiją, bendra patvirtinimo tikimybė tėra apie $12{,}8\,\%$ [16]. Nepaisant to, struktūrinė informacija yra kritiškai svarbi: pavyzdžiui, 2019-2023 m. patvirtintų 34 priešvėžinių mažos molekulinės masės vaistų vystymui struktūrinė biologija turėjo įtakos visais atvejais, o daugiau nei $80\,\%$ atvejų vaistai sukurti taikant struktūra grįstą projektavimą [21].

Svarbiausias uždavinys ankstyvosiose vaistų paieškos stadijose (ieškant pirminių junginių-lyderių bei optimizuojant jų struktūrą) yra sukurti molekules, pasižyminčias dideliu sąveikos stiprumu ir selektyvumu tiksliniam baltymui. Struktūra grįstas vaistų kūrimas (angl.

Structure-Based Drug Design) naudoja trimačius taikinio struktūros duomenis tam, kad ligandų optimizavimas būtų kuo racionalesnis. Nors rentgeno kristalografija atskleidžia atskirų atomų sąveikas komplekse, ji tiesiogiai nenusako paties prisijungimo stiprumo. Racionalų vaistų kūrimą apsunkina tai, kad bet kokia cheminė ligando modifikacija vienu metu veikia desolvataciją, konformacinius efektus, protonizacijos pusiausvyrą bei entropiją. Todėl eksperimentinėse struktūrose stebima sąveika dažnai tiesiogiai nenurodo jos įnašo į bendrą sąveikos energiją.

Kompiuteriniai modeliavimo metodai [20], skirti kiekybiškai prognozuoti sąveikas, vis dar turi fizikinio detalumo bei tikslumo ribotumų.

- Molekulinis dokingas (angl. *molecular docking*) įverčio funkcijomis padeda nuspėti ir įvertinti jungimosi pozas (angl. *scoring functions*), tačiau sąveikos stiprumo prognozavimas išlieka labai netikslus ir stipriai priklauso nuo modelio pasirinkimo.
- Molekulinė dinamika (angl. *molecular dynamics*, MD) leidžia tirti molekulių struktūros pokyčius, tirpiklio ir jonų judėjimą. Tačiau įprasti MD skaičiavimai neleidžia tiesiogiai įvertinti skirtingų molekulės būsenų stabilumo. Taip pat dažnai yra reikalingi labai ilgi skaičiavimai, kad būtų gauti patikimi rezultatai.
- Kvantinė mechanika (angl. *quantum mechanics*, QM) leidžia įvertinti sąveikas naudojant elektroninės struktūros skaičiavimus, tačiau reikalauja didelių skaičiavimo išteklių.
- Mašininis mokymasis (angl. *machine learning*, ML) nuspėja pozas ir sąveikos stiprumą iš eksperimentinių bei struktūrinių duomenų, tačiau jo tikslumas visiškai priklauso nuo mokymo duomenų kokybės bei modelio validavimo.

Todėl išlieka svarbu integruoti atominės raiškos struktūrinius duomenis su išsamiais eksperimentiniais termodinaminiais tyrimais, siekiant aiškintis veiksnius, lemiančius baltymų ir ligandų sąveiką.

Baltymo ir ligando sąveikas lemiantys veiksniai

Baltymų ir ligandų sąveika lemia biologinių sistemų funkcionavimą ir vaistinių junginių veiksmingumą. Ligando prisijungimą prie

baltymo lemia įvairių tarpmolekulinių sąveikų visuma, įskaitant metalo koordinacinius ryšius, vandenilinius ryšius, elektrostatines sąveikas, hidrofobinį efektą, van der Waalso kontaktus bei kitas sąveikas. Šiame darbe kaip modelinė sistema yra naudojamos karboanhidrazės ir benzensulfonamidai. Biofiziniai tyrimai rodo, kad apie $60\,\%$–$65\,\%$ karboanhidrazių ir sulfonamidų komplekso stabilizavimo energijos kyla iš tiesioginės koordinacinės sąveikos su kataliziniu $\mathrm{Zn^{II}}$ [35], kuri veikia kaip pagrindinis inkaras, o kitos nekovalentinės sąveikos veikia papildomai jungimosi stiprumą bei selektyvumą. Šių sąveikų indėlis

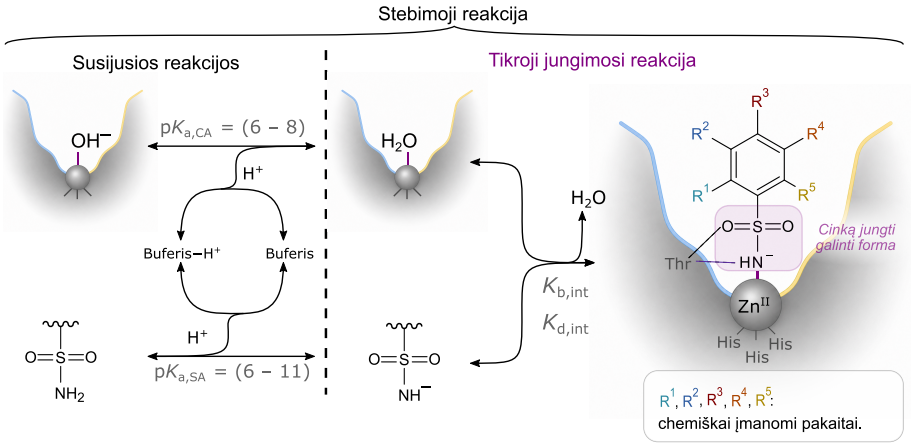

S.1 pav.: Bendra karboanhidrazių ir pirminių sulfonamidų atpažinimo schema. Schemoje apibendrinami pirminių sulfonamidų prisijungimo prie kataliziškai aktyvių žmogaus karboanhidrazių izofermentų ypatumai (ypatingą dėmesį skiriant benzensulfonamidams, kurie yra pagrindinis šio darbo objektas) ir pristatomos sąvokos, aptariamos vėlesniuose skyriuose. Prisijungimas yra susietas su abiejų partnerių (de)protonizacijos pusiausvyromis, nurodant apytiksles $\mathrm{p}K_\mathrm{a}$ vertes. Konservatyvų cinką rišantį motyvą sudaro sulfonamido azoto koordinacija su $\mathrm{Zn^{II}}$ jonu ir vandeniliniai ryšiai su Thr199. Šis motyvas, esantis sandūroje tarp hidrofobiškesnės ir hidrofiliškesnės aktyviojo centro pusių (atitinkamai geltonos ir mėlynos spalvos), sudaro bendrą struktūrinį inkarą. Be šio motyvo, sulfonamidų pakaitų įvairovė ir skirtinga individualių izofermentų aktyviojo centro aplinka lemia įvairius sąveikos ypatumus, turinčius įtakos sąveikos stiprumui, selektyvumui ir prisijungimo termodinamikai. Eksperimentiškai stebimas prisijungimas papildomai apima susijusias protonizacijos reakcijas; į jas atsižvelgus galima nustatyti tikruosius prisijungimo parametrus, kurie tiesiogiai atspindi baltymo ir ligando sąveiką.

priklauso ne tik nuo tiesioginių baltymo ir ligando kontaktų, bet ir nuo aplinkos savybių, ypač vandens molekulių tinklų organizacijos bei protonacijos pusiausvyrų (Pav. S.1).

Baltymo–ligando jungimąsi apibūdina pagrindiniai termodinaminiai parametrai: Gibso energijos pokytis (ΔG), entalpijos pokytis (ΔH) ir entropijos pokytis (ΔS). Nors jungimosi stiprumą nusako ΔG, jo vertę dažnai lemia skirtingas entalpinių ir entropinių veiksnių balansas. Dažnai stebimas entalpijos–entropijos kompensacijos reiškinys, kai palankesni entalpiniai pokyčiai kompensuojami mažiau palankiais entropiniais pokyčiais arba atvirkščiai, todėl panašų jungimosi stiprumą gali lemti skirtingi molekuliniai mechanizmai [8].

Svarbų vaidmenį taip pat atlieka vandens molekulių reorganizacija ir desolvatacija, nes ligandui jungiantis dalis aktyviojo centro vandens molekulių pašalinama arba persitvarko, reikšmingai paveikdama jungimosi termodinamiką [7, 9, 36–38]. Eksperimentiniai tyrimai rodo, kad vandens molekulių išlaisvinimas iš aktyviojo centro hidrofobinių sričių gali suteikti palankų entropinį įnašą, o stipriai struktūrizuotų vandens molekulių tinklo išlaikymas arba naujų vandenilinių ryšių suformavimas gali prisidėti prie palankaus entalpinio indėlio. Tyrimų, detaliai analizuojančių šiuos reiškinius, vis dar yra nedaug, o kiekvienas baltymo ir ligando sąveikos atvejis pasižymi unikaliomis savybėmis. Dėl šios priežasties nėra bendrų, visoms sistemoms tinkamų gairių, o tai apsunkina itin tikslių prognozavimo modelių sukūrimą.

Žmogaus karboanhidrazės ir pirminiai sulfonamidai kaip modelinė sistema

Karboanhidrazės [84] (CAs; EC 4.2.1.1) yra metalofermentų šeima, katalizuojanti grįžtamąją anglies dioksido hidratacijos reakciją. Žmogaus α klasės karboanhidrazių šeimą sudaro 15 izofermentų, iš kurių 12 yra kataliziškai aktyvūs [13]. Trys izofermentai - CA VIII, CA X ir CA XI - kataliziškai neaktyvūs (vadinami su karboanhidrazėmis susijusiais baltymais), kadangi juose nėra cinką koordinuojančių histidinų [87] ir šiame darbe jie nėra nagrinėjami. Nepaisant didelio struktūrinio panašumo, aktyvūs izofermentai pasižymi skirtinga lokalizacija, fiziologinėmis funkcijomis ir slopiklių atpažinimo savybėmis.

Visų kataliziškai aktyvių žmogaus karboanhidrazių aktyviajame centre yra Zn^{II} jonas, koordinuotas trijų histidino liekanų (His94, His96,

His119) ir vandens molekulės arba hidroksido jono [88]. Aktyvusis centras sudarytas iš:

- labiau hidrofobinės srities, kurią formuoja Val121, Val143, Leu198 ir Trp209 bei kitos aminorūgštys.
- labiau hidrofilinės srities, kurioje vandenilinių ryšių tinklas yra išsidėstęs aplink Thr199 ir Glu106 bei konservatyvias vandens molekules.
- kataliziškai svarbaus protonų pernešėjo His64, kuris keičia konformacijas tarp vidinės (angl. *inward*) ir išorinės (angl. *outward*), perduodamas protonus iš aktyviojo centro į tirpiklį per vandeniliniais ryšiais susietų vandens molekulių tinklą.

Nors katalizinė architektūra tarp izofermentų išlieka labai panaši, nedideli aminorūgščių skirtumai aktyviojo centro prieigoje keičia ertmės geometriją, paviršiaus elektrostatines savybes ir vandens tinklų organizaciją, todėl gali lemti reikšmingus jungimosi stiprumo ir selektyvumo skirtumus. Šie skirtumai puikiai iliustruojami tirtų izofermentų pavyzdžiais (aminorūgščių skirtumai lyginami su modeliniu baltymu vadinama CA II, naudojant jos aminorūgščių numeraciją):

- CA IV yra ekstraląstelinis, su membrana per GPI (angl. *glycosylphosphatidylinositol*) inkarą susietas izofermentas, stabilizuotas disulfidiniu ryšiu (Cys6 ir Cys11) ir glikozilinimu [97]. Jo aktyviojo centro ertmė yra siauresnė ir mažiau prieinama tirpikliui dėl tokių prieigos skirtumų kaip Leu60→Gln, Asn67→Met, Ile91→Lys, Phe131→Val, Leu141→Ile ir Ala135→Gln.
- CA IX yra tiesiogiai su navikų hipoksija susijęs transmembraninis izofermentas, kurio katalizinis domenas sudaro homodimerą, stabilizuotą disulfidine jungtimi (Cys119–Cys299) ir N-glikozilinimu ties Asn309 [100, 101]. Jo aktyviajame centre esantys skirtumai Leu60→Arg, Ile91→Leu, Phe131→Val (pašalinta reikšminga sterinė kliūtis) bei Ala135→Leu sukuria erdvesnę ir labiau hidrofobinę kišenę, puikiai pritaikytą didesniems ir selektyviems slopikliams nei CA II ir likusioms karboanhidrazėms.
- CA XIII būdingi tokie skirtumai kaip Leu60→Ser, Asn67→Ser ir Ile91→Arg, o 200-ojoje pozicijoje esantis Val200 (skirtingai nei Thr200 CA II) [103] keičia vandens molekulės W_1 padėtį ir stabilizavimą. CA II izofermente Thr200 stabilizuoja W_1 vandeniliniu

ryšiu, o CA XIII esantis Val200 tokio ryšio sudaryti negali. Šis skirtumas gali prisidėti prie izofermentams būdingų aktyviojo centro hidratacijos ir jungimosi termodinamikos skirtumų, kaip aptarta disertacijos rezultatų dalyje.

Plačiausiai ištirta karboanhidrazių slopiklių klasė yra sulfonamidai [110–113]. Jų deprotonuota sulfonamido grupė tiesiogiai koordinuojasi prie katalizinio cinko jono, išstumdama su juo susijusią vandens molekulę (Pav. S.1). Be šios pagrindinės sąveikos, slopiklių jungimosi stiprumą ir selektyvumą lemia papildomi vandeniliniai ryšiai, hidrofobiniai kontaktai bei sąveikos su aktyviojo centro vandens molekulių tinklais.

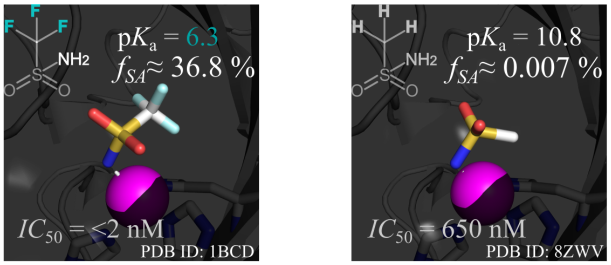

S.2 pav.: Sulfonamido $\mathrm{p}K_\mathrm{a}$ efektas stebimai sąveikai su karboanhidrazėmis. Trifluormetansulfonamido (TFMSA, kairėje) ir metansulfonamido (MSA, dešinėje), susijungusių su žmogaus CA II, palyginimas. Abu slopikliai pasižymi panašiu jungimusi - jie koordinuoja katalizinį $\mathrm{Zn^{II}}$ per deprotonuotą sulfonamido azoto atomą. Metilo grupę pakeitus stipriai elektronus traukiančia trifluormetilo grupe, sulfonamido $\mathrm{p}K_\mathrm{a}$ sumažėja nuo 10,8 iki 6,3 ir todėl, esant pH 7,0, su cinku besijungiančio sulfonamido anijono dalis (f_SA) padidėja nuo maždaug $0{,}007\,\%$ iki $36{,}8\,\%$. Dėl šios priežasties gerokai didesnį TFMSA slopinamąjį aktyvumą (IC_{50} < 2 nM), palyginti su MSA (IC_{50} = 650 nM), lemia didesnė aktyvios, deprotonuotos, su cinku besijungiančios formos dalis, o ne reikšmingi baltymo ir ligando sąveikų skirtumai. Struktūros pateiktos pagal PDB įrašus 1BCD (TFMSA) ir 8ZWV (MSA); $\mathrm{p}K_\mathrm{a}$ ir IC_{50} vertės paimtos iš literatūros [109].

Kadangi slopikliai jungiasi tik deprotonuotos anijoninės formos pavidalu, o pats fermentas turi būti $\mathrm{Zn^{II}}$-$\mathrm{H_2O}$ formos, šis procesas yra stipriai susietas su (de)protonizacijos pusiausvyromis tirpale [11, 12]. Tai reiškia, kad eksperimentiškai stebimas (angl. *observed*) jungimosi stiprumas yra visuomet mažesnis už tikrąjį (angl. *intrinsic*), o viena geriausių šios įtakos iliustracijų yra metansulfonamido (MSA) ir trifluormetansulfonamido (TFMSA) palyginimas (Figure S.2). Abu slopikliai

su CA II jungiasi beveik identiškai koordinuodami cinko joną, tačiau stipriai elektronus traukianti CF_3 grupė sumažina TFMSA $\mathrm{p}K_\mathrm{a}$ iki 6,3 (MSA $\mathrm{p}K_\mathrm{a}$ yra 10,8). Dėl šio rūgštingumo skirtumo, esant pH 7,0, TFMSA deprotonizuotos formos tirpale yra net $36{,}8\,\%$, o MSA - vos $0{,}007\,\%$, kas nulemia drastišką stebimo aktyvumo skirtumą tirpale ($IC_{50} < 2\,\mathrm{nM}$ prieš $650\,\mathrm{nM}$) [109], nors jų tikroji sąveikos energija su baltymu išlieka panaši. Todėl būtent tikrieji jungimosi parametrai turėtų būti naudojami modeliavimo etapuose.

Karboanhidrazės turi įvairių kliniškai naudojamų sulfonamidų ir jų darinių pagrindo slopiklių [114]. Acetazolamidas (AZM) išlieka klasikiniu ir plačiausiai ištirtu etaloniniu slopikliu, pasižyminčiu dideliu sąveikos stiprumu, tačiau kaip ir daugelis - ribotu selektyvumu tarp atskirų izofermentų. Būtent selektyvumo paieškos išlieka vienas svarbiausių uždavinių.

Nepaisant gausių struktūrinių ir termodinaminių duomenų apie karboanhidrazių ir sulfonamidų sąveikas, vis dar sudėtinga susieti nedidelius baltymo ir ligando struktūros skirtumus su jų poveikiu jungimosi termodinamikai ir selektyvumui. Karboanhidrazių ir sulfonamidų kompleksai yra tinkama modelinė sistema šiems ryšiams tirti, nes sulfonamidams būdingas konservatyvus jungimosi prie cinko jono būdas, o jų sąveikos su skirtingų izofermentų aktyviojo centro aplinka skiriasi [13]. Tai leidžia sistemiškai tirti, kaip baltymo ir ligando struktūra bei molekulinė aplinka lemia jungimosi termodinamiką ir selektyvumą [1].

Metodų apibendrinimas

Šioje disertacijoje taikytų pagrindinių metodų seka pateikta S.3 pav. Tyrimuose buvo naudojamos rekombinantinės žmogaus karboanhidrazės ir sulfonamidiniai slopikliai.

Baltymo ir ligando sąveikos buvo charakterizuojamos biofizikiniais metodais, daugiausia fluorescenciniu terminio poslinkio metodu ir izoterminio titravimo kalorimetrija, nustatant stebimąsias jungimosi konstantas ir termodinaminius parametrus. Lygiagrečiai eksperimentiškai buvo nustatyti ligandų protonizacijos parametrai, o atitinkami karboanhidrazės izofermentų protonizacijos parametrai buvo paimti iš ankstesnių tyrimų.

Vėliau stebimieji jungimosi parametrai buvo koreguojami atsižvelgiant į su jungimusi susietas protonizacijos reakcijas, siekiant nustatyti

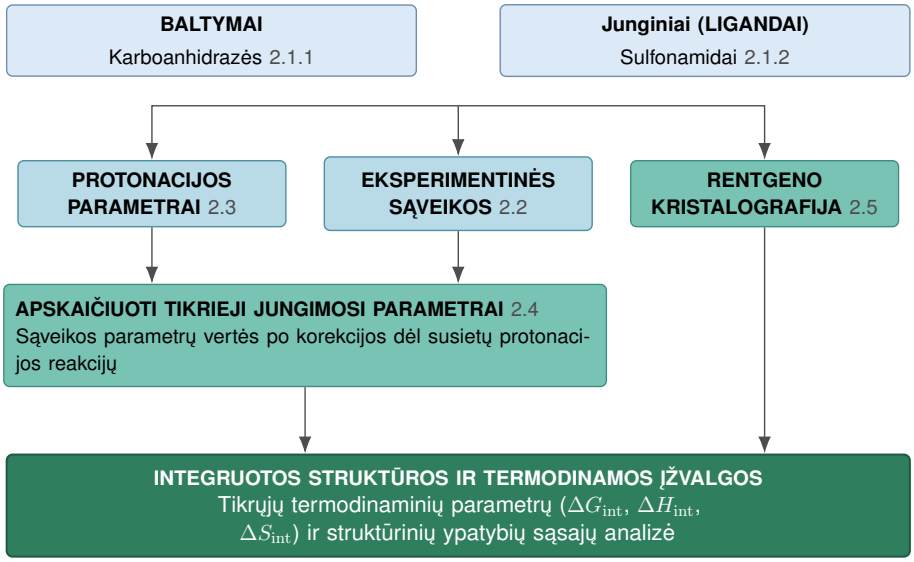

S.3 pav.: Disertacijoje taikytų eksperimentinių ir analizės metodų schema. Baltymų ir ligandų sąveikos duomenys, protonizacijos parametrai ir rentgeno spindulių kristalografijos struktūros buvo integruoti siekiant apskaičiuoti tikruosius termodinaminius parametrus ir ištirti struktūros bei termodinamikos sąsajas karboanhidrazių ir jų slopiklių sistemose.

tikruosius termodinaminius parametrus, nepriklausančius nuo eksperimentinių sąlygų (pH bei buferinio tirpalo) ir todėl tinkamus skirtingoms sistemoms palyginti. Struktūrinė informacija apie baltymo ir ligando kompleksus buvo gauta rentgeno spindulių kristalografijos metodu. Galiausiai tikrieji termodinaminiai parametrai buvo susieti su struktūriniais duomenimis. Šių metodų visuma leido išanalizuoti ryšius tarp baltymo ir ligando jungimosi termodinamikos bei karboanhidrazės ir slopiklių kompleksų struktūrinių ypatybių, siekiant gauti slopiklių kūrimui svarbių įžvalgų.

Išsamūs eksperimentinių procedūrų ir duomenų analizės metodų aprašymai pateikti publikacijose, sudarančiose šios disertacijos pagrindą.

Medžiagos

Karboanhidrazių izofermentai

Šiame darbe naudota CA raiškos ir gryninimo platforma buvo sukurta ir daugelį metų plėtojama daugelio laboratorijos narių bei bendradarbių

pastangomis. Autorė nuoširdžiai dėkoja už jų indėlį ir šiam tyrimui suteiktus baltymų išteklius.

Dvylika CA izofermentų buvo gauti rekombinantiniu būdu kaip viso ilgio baltymai arba sutrumpintos jų konstrukcijos, išlaikančios katalizinį domeną. Daugumos izofermentų raiška buvo vykdoma *Escherichia coli* ląstelėse, naudojant pagal konkrečių baltymų poreikius parinktas padermes, pvz., BL21(DE3), Rosetta 2(DE3) ir Origami B(DE3) [115]. Kadangi bakterijų ląstelėse nepavyko gauti stabilios rekombinantinės CA IX, jos katalizinis domenas buvo gautas naudojant žinduolių ląstelių raiškos sistemas (FreeStyle 293-F arba Expi293F) [115]. Baltymai buvo gryninami taikant kiekvienam izofermentui pritaikytus Ni^{2+} chelatinimo, jonų mainų ir sulfonamidų ligandais pagrįstos chromatografijos metodų derinius. Baltymų grynumas, molekulinė masė ir katalizinis aktyvumas buvo vertinami atitinkamai SDS-PAGE, didelės skiriamosios gebos masių spektrometrijos (HR-MS) ir sustabdytos srovės (angl. *stopped-flow*) CO_2 hidratacijos metodais. Išsamios baltymų konstrukcijų sekos, raiškos sąlygos ir gryninimo procedūros pateiktos [115].

Informacija apie rekombinantinius baltymus taip pat pateikiama PLBD duomenų bazėje: https://plbd.org/db/main/protein. Eksperimentinių duomenų rinkiniai ir atitinkamos eksperimentuose naudotos baltymų partijos yra susieti ir aprašyti šioje duomenų bazėje.

Baltymų mėginiai buvo laikomi $-80\,^{\circ}\mathrm{C}$ temperatūroje. Prieš eksperimentus, kuomet būtina, baltymų laikymo buferinis tirpalas buvo pakeičiamas į atitinkamam eksperimentui naudojamą buferinį tirpalą. Baltymų koncentracijos buvo nustatomos spektrofotometriškai, naudojant atitinkamus jų molinius ekstinkcijos koeficientus ties $280\,\mathrm{nm}$.

Sulfonamidiniai slopikliai

Šiame darbe tirti sulfonamidiniai junginiai buvo susintetinti laboratorijoje bendradarbių. Atsižvelgiant į junginių seriją, buvo taikomos skirtingos sintezės strategijos, įskaitant nukleofilinio pakeitimo, alkilinimo, amidinimo ir oksidacijos reakcijas. Junginių tapatumas ir grynumas buvo patvirtinti tinkamais analizės metodais, daugiausia branduolių magnetinio rezonanso spektroskopija ir masių spektrometrija. Išsamios sintezės, gryninimo ir charakterizavimo procedūros aprašytos atitinkamose publikacijose, kuriomis grindžiama ši disertacija. Informacija apie susintetintus junginius, įskaitant jų laboratorinius identifikatorius, pateikiama PLBD duomenų bazėje (https://plbd.org/db/main/compound).

Visų junginių pradiniai tirpalai buvo ruošiami DMSO, įprastos koncentracijos $10\,\mathrm{mM}$ to (numerical range) $50\,\mathrm{mM}$, o prieš naudojimą jie buvo skiedžiami atitinkamais eksperimentiniais buferiniais tirpalais.

Eksperimentinis baltymo ir ligando sąveikų nustatymas

Šioje disertacijoje naudotų biofizikinių ir biocheminių metodų išsamias apžvalgas galima rasti nurodytuose literatūros šaltiniuose: fluorescencinis terminio poslinkio metodas (FTSA) [116, 117], izoterminė titravimo kalorimetrija (ITC) [118], rentgeno spindulių kristalografija [119–121], sustabdyto srauto (angl. *stopped-flow*) CO_2 hidratacijos aktyvumo metodas [122] ir kitus papildomus metodus, nurodytus atitinkamose į disertaciją įtrauktose publikacijose.

Metodų skyriuje apibendrinami eksperimentiniai metodai ir procedūros, svarbūs šioje disertacijoje pateiktų rezultatų interpretacijai. Išsamūs eksperimentų protokolai, konkretiems tyrimams taikytos sąlygos, naudota įranga ir duomenų analizės procedūros pateiktos atitinkamose į disertaciją įtrauktose publikacijose.

Siekiant užtikrinti duomenų atsekamumą ir atkuriamumą, eksperimentinių duomenų rinkiniai ir su jais susiję metaduomenys buvo registruojami duomenų bazėje (PLBD; https://plbd.org) [125]. Rentgeno spindulių kristalografijos būdu gauti struktūriniai duomenys registruoti duomenų banke (angl. *Protein Data Bank*, PDB).

Fluorescencinis terminio poslinkio metodas

Fluorescencinis terminio poslinkio metodas (FTSA) buvo pagrindinis metodas, taikytas stebimosioms jungimosi konstantoms nustatyti daugeliui šioje disertacijoje tirtų sąveikų. Gautos konstantos vėliau buvo koreguojamos atsižvelgiant į su jungimusi susietas protonizacijos reakcijas ir taip apskaičiuojamos tikrosios jungimosi konstantos, kaip aprašyta skyriuje 3.2.2.

Tyrimo metu baltymo terminis išsivyniojimas stebimas naudojant aplinkai jautrius fluorescencinius dažus, kurie jungiasi prie atsivėrusių hidrofobinių sričių ir keičia fluorescencijos intensyvumą [126, 127]. Ligando jungimasis keičia baltymo terminį stabilumą ir jo lydymosi temperatūrą (T_m). Baltymo ir ligando jungimosi konstantos buvo nustatomos

iš ligando sukeltų terminio stabilizavimo kreivių, taikant termodinaminius modelius, įdiegtus Microsoft Excel, o vėliau mūsų laboratorijoje sukurtoje Thermott internetinėje platformoje (thermott.com) [128].

Izoterminė titravimo kalorimetrija

Izoterminė titravimo kalorimetrija (ITC) buvo naudojama tiesiogiai matuoti baltymo ir ligando jungimosi metu išsiskiriančią arba sugeriamą šilumą [129]. Šiuo metodu buvo nustatomos stebimosios jungimosi entalpijos, jungimosi konstantos ir stechiometrija, o iš jų apskaičiuojami Gibso energijos ir entropijos pokyčiai. Stebimieji termodinaminiai parametrai vėliau buvo koreguojami atsižvelgiant į susietas protonizacijos reakcijas (3.2.2 skyrius).

Siekiant įvertinti su jungimusi susietas protonizacijos reakcijas, dalis eksperimentų buvo atliekama skirtingos jonizacijos entalpijos buferiuose [11]. ITC duomenų analizė apėmė bazinės linijos nustatymą, smailių integravimą, modelio pritaikymą ir termodinaminių parametrų nustatymą. Duomenys buvo analizuojami naudojant gamintojo programinę įrangą ir specializuotas programas NITPIC [130, 131], SEDPHAT [131, 132] bei GUSSI [133].

Protonizacijos parametrų nustatymas

Sulfonamidų $\mathrm{p}K_\mathrm{a}$ nustatymas

Sulfonamidinių slopiklių $\mathrm{p}K_\mathrm{a}$ buvo nustatytos UV–Vis spektrofotometrinio titravimo metodu [56]. Metodas pagrįstas sulfonamido grupės protonizaciją ir deprotonizaciją lydinčiais sugerties spektro pokyčiais. Spektrai buvo registruojami esant skirtingoms pH vertėms, o iš absorbancijos priklausomybės nuo pH nustatytos $\mathrm{p}K_\mathrm{a}$ vertės. Jos buvo naudojamos jungimuisi tinkamos ligando formos daliai apskaičiuoti ir stebimiesiems termodinaminiams parametrams koreguoti.

Sulfonamidų protonizacijos entalpijos nustatymas

Sulfonamidinių slopiklių protonizacijos entalpijos buvo nustatytos izoterminės titravimo kalorimetrijos (ITC) metodu, matuojant šilumą,

išsiskiriančią arba sugeriamą deprotonuotą sulfonamido grupę titruojant stipria rūgštimi. Iš kalorimetrinių duomenų nustatyta kiekvieno junginio protonizacijos entalpija ($\Delta H_{\mathrm{pr,SA}}$), kuri buvo naudojama stebimosioms jungimosi entalpijoms koreguoti.

Tikrųjų termodinaminių parametrų apskaičiavimas

Tikrieji termodinaminiai parametrai apibūdina paties baltymo ir ligando sąveiką, todėl yra tinkami objektyviam skirtingų kompleksų palyginimui, priešingai nei eksperimentiškai nustatomi stebimieji parametrai.

Sulfonamidai jungiasi deprotonuota forma, koordinuodami aktyviojo centro $\mathrm{Zn^{II}}$ joną ir išstumdami su juo koordinuotą vandens molekulę [107]. Kadangi eksperimentinėmis sąlygomis tik dalis ligando ir fermento yra jungimuisi tinkamos formos, stebimosios jungimosi konstantos ir entalpijos priklauso nuo pH, buferio ir protonizacijos pusiausvyrų [11, 12].

Siekiant tiesiogiai palyginti termodinaminius ir struktūrinius duomenis, stebimieji jungimosi parametrai buvo koreguojami atsižvelgiant į susietas protonizacijos reakcijas ir perskaičiuojami į tikruosius termodinaminius parametrus. Paveikslas S.2 iliustruoja šios korekcijos svarbą vertinant karboanhidrazių ir sulfonamidų jungimąsi.

Jungimosi konstantų koregavimas

Tikroji jungimosi konstanta $K_{\mathrm{b,int}}$ buvo apskaičiuota iš stebimosios jungimosi konstantos $K_{\mathrm{b,obs}}$, atsižvelgiant į jungimuisi tinkamų baltymo (f_{CA}) ir ligando (f_{SA}) formų dalis:

$$K_{\mathrm{b,int}} = \frac{K_{\mathrm{b,obs}}}{f_{\mathrm{CA}} \cdot f_{\mathrm{SA}}} \tag{S.1}$$

Protonuotos fermento formos dalis apskaičiuota pagal lygtį

$$f_{\mathrm{CA}} = \frac{10^{\mathrm{p}K_{\mathrm{a,CA}} - \mathrm{pH}}}{1 + 10^{\mathrm{p}K_{\mathrm{a,CA}} - \mathrm{pH}}} \tag{S.2}$$

o deprotonuotos sulfonamido formos dalis:

$$f_{\mathrm{SA}} = \frac{10^{\mathrm{pH}-\mathrm{p}K_{\mathrm{a,SA}}}}{1 + 10^{\mathrm{pH}-\mathrm{p}K_{\mathrm{a,SA}}}}. \tag{S.3}$$

Čia $\mathrm{p}K_{\mathrm{a,CA}}$ yra fermento aktyviajame centre su cinko jonu koordinuotos vandens molekulės rūgšties disociacijos konstanta, o $\mathrm{p}K_{\mathrm{a,SA}}$– sulfonamido grupės rūgšties disociacijos konstanta.

Tikroji jungimosi Gibso energija ΔG_{int} apskaičiuota pagal standartinę termodinaminę lygtį:

$$\Delta G_{\mathrm{int}} = -RT \ln(K_{\mathrm{b,int}}). \tag{S.4}$$

Jungimosi entalpijos ir entropijos koregavimas

Tikroji jungimosi entalpija ΔH_{int} apskaičiuota koreguojant stebimąją jungimosi entalpiją ΔH_{obs} pagal protonų pernašos reakcijas, susijusias su sulfonamido ir su cinku koordinuotos vandens molekulės deprotonizacija bei buferio protonizacija:

$$\Delta H_{\mathrm{int}} = \Delta H_{\mathrm{obs}} - n_1 \Delta H_{\mathrm{pr,SA}} - n_2 \Delta H_{\mathrm{pr,CA}} + (n_1 + n_2) \Delta H_{\mathrm{pr,buf}} \tag{S.5}$$

kur

$$n_1 = f_{\mathrm{SA}} - 1 \tag{S.6}$$

$$n_2 = 1 - f_{\mathrm{CA}}. \tag{S.7}$$

Parametrai n_1 ir n_2 apibūdina jungimosi metu perduodamų protonų skaičių.

Atskirų karboanhidrazės izofermentų $\mathrm{p}K_{\mathrm{a,CA}}$ ir $\Delta H_{\mathrm{pr,CA}}$ vertės buvo anksčiau nustatytos mūsų laboratorijoje [134], o buferių protonizacijos entalpijos ($\Delta H_{\mathrm{pr,buf}}$) paimtos iš publikuotų termodinaminių duomenų [135]. $\mathrm{p}K_{\mathrm{a,SA}}$ ir $\Delta H_{\mathrm{pr,SA}}$ vertės buvo nustatytos eksperimentiškai, kaip aprašyta aukščiau.

Tikrasis jungimosi entropijos pokytis apskaičiuotas iš tikrosios Gibso energijos ir entalpijos:

$$\Delta S_{\text{int}} = \frac{\Delta H_{\text{int}} - \Delta G_{\text{int}}}{T}. \tag{S.8}$$

Struktūriniai tyrimai

Karboanhidrazių ir ligandų kompleksų struktūros buvo nustatytos rentgeno spindulių kristalografijos metodu. CA izofermentų kristalai buvo auginami įprastai kambario temperatūroje sėdinčio lašo garų difuzijos metodu. Rekombinantiniai baltymai ultrafiltracijos būdu buvo koncentruojami iki $15\,\text{mg}\,\text{mL}^{-1}$ to (numerical range) $50\,\text{mg}\,\text{mL}^{-1}$, o kristalizacijos lašai ($0{,}1\,\mu\text{L}$ to (numerical range) $5\,\mu\text{L}$) ruošiami sumaišant baltymo ir rezervuaro tirpalus.

Optimizuotos kristalizacijos sąlygos priklausė nuo CA izofermento. CA I kristalizacijai dažniausiai naudotas $0{,}1\,\text{M}$ Tris-HCl (pH 8,5), $0{,}2\,\text{M}$ NaCl arba amonio sulfatas ir $20\,\%$ to (numerical range) $28\,\%$ PEG; CA II – $0{,}1\,\text{M}$ natrio bicinas (pH 9,0) ir $2{,}0\,\text{M}$ natrio malonatas (pH 7,0); CA XII – $0{,}1\,\text{M}$ amonio citratas (pH 7,0–7,2) ir $26\,\%$ to (numerical range) $30\,\%$ PEG 4000; CA XIII – natrio citrato arba acetato buferiai (pH 4,5–5,5) su $26\,\%$ to (numerical range) $30\,\%$ PEG 4000.

Baltymo ir ligando kompleksai daugiausia buvo gaunami išaugintus kristalus iki vienos savaitės mirkant rezervuaro tirpale su $0{,}5\,\text{mM}$ to (numerical range) $1{,}0\,\text{mM}$ ligando. CA I kompleksams buvo taikoma kokristalizacija. CA I ir CA II kristalai buvo greitai užšaldomi tiesiogiai iš kristalizacijos tirpalo, o CA XII ir CA XIII kristalams naudotas $15\,\%$ to (numerical range) $20\,\%$ etilenglikolio krioprotektoriaus tirpalas.

Rentgeno spindulių difrakcijos duomenys buvo renkami DESY sinchrotrono P13 ir P14 makromolekulinės kristalografijos stotyse (Hamburgas, Vokietija) arba Vilniaus universiteto Gyvybės mokslų centre naudojant Rigaku MM007-HF difraktometrą. Struktūros buvo nustatomos molekulinio pakeitimo metodu, kaip paieškos modelius naudojant anksčiau nustatytas karboanhidrazių struktūras. Modeliai buvo iteratyviai konstruojami ir tikslinami pagal eksperimentinį elektronų tankį.

Daugumą šioje disertacijoje pateiktų kristalinių struktūrų nustatė disertacijos autorė. Dalį CA IX ir CA XII struktūrų nustatė bendradarbiai Dr. Jānis Leitāns ir Prof. Dr. Kaspars Tars (Latvijos biomedicininių

tyrimų ir studijų centras, Latvija). Visas į disertaciją įtrauktas struktūras autorė analizavo vertindama baltymo ir ligando sąveikas, jungimosi centro hidrataciją ir struktūrinius požymius, susijusius su termodinaminiais jungimosi parametrais.

Išsamios kristalizacijos sąlygos, difrakcijos duomenų rinkimo parametrai, struktūrų tikslinimo ir validavimo rodikliai bei naudota programinė įranga pateikti atitinkamose į šią disertaciją įtrauktose publikacijose.

Rezultatai

Baltymo ir ligando atpažinimą lemiantys veiksniai

Šiame skyriuje pristatomi tyrimai nagrinėja molekulinius veiksnius, lemiančius baltymo ir ligando atpažinimą, naudojant karboanhidrazių ir sulfonamidų sistemą. Išskirtinis dėmesys skiriamas tam, kaip termodinaminiai mechanizmai, ligando struktūra ir baltymo aplinka prisideda prie baltymų ir ligandų jungimosi stiprumo bei selektyvumo. Pirmiausia tiriamas entalpijos ir entropijos kompensacijos reiškinys, siekiant atskleisti, kaip panašus jungimosi stiprumas gali susidaryti dėl iš esmės skirtingų energetinių mechanizmų. Vėliau nagrinėjama nedidelių ligando modifikacijų įtaka jungimosi stiprumui ir selektyvumui. Galiausiai, struktūriniai ir termodinaminiai duomenys integruojami siekiant nustatyti sąsajas tarp baltymo ir ligando struktūros bei jungimosi energijos.

Entalpijos ir entropijos kompensavimas

Šioje dalyje apibendrinami publikacijos Paketurytė-Latvė ir kt. 2026 m. rezultatai:

Vaida Paketurytė-Latvė, Audrius Zakšauskas, Visvaldas Kairys, Edita Čapkauskaitė, Martynas Bagdonas, Alexey Smirnov, Elena Manakova, Saulius Gražulis, Daumantas Matulis

Enthalpy–Entropy Compensation in Inhibitor Binding to Carbonic Anhydrase Isozymes
Disertacijos pateikimo metu rankraštis buvo recenzuojamas. Išspausdi-

nus disertaciją, straipsnis buvo priimtas publikuoti moksliniame žurnale Biophysical Journal. Straipsnio DOI: 10.1016/j.bpj.2026.09.032.

Mano indėlį sudarė tyrimo koncepcijos kūrimas, eksperimentinis jungimosi termodinamikos nustatymas ITC metodu, tikrųjų termodinaminių parametrų skaičiavimas ir analizė, rentgeno kristalografinė analizė, entalpijos ir entropijos kompensacijos reiškinių interpretavimas bei rankraščio rengimas.

Siekant ištirti molekulines entalpijos ir entropijos kompensacijos priežastis, buvo tiriama sulfonamidinių slopiklių serija (konkrečiai - šešių *ortho*, *meta*-dipakeistų benzensulfonamidų serija, junginiai 4a–4d, 4h ir 7h) trijų žmogaus karboanhidrazių izofermentų – CA II, CA XII ir CA XIII – atžvilgiu. Nors šių fermentų bendrosios struktūros yra labai konservatyvios ir jie tos pačios klasės slopiklius jungia panašiu stiprumu, jų aktyvieji centrai skiriasi tik keliomis aminorūgščių pozicijomis. Ši sistema sudarė sąlygas nustatyti, kaip nedideli baltymo aplinkos skirtumai veikia termodinaminius mechanizmus, lemiančius ligando atpažinimą. Jungimosi stiprumai ir kiti termodinaminiai parametrai buvo nustatyti naudojant FTSA ir ITC (šis tyrimas papildomai leido nustatyti jungimosi entalpijas) metodus, o rentgenostruktūrinė analizė suteikė informaciją apie atitinkamų baltymo ir ligando kompleksų struktūras. Buvo nustatytos septynios kompleksų su CA II (PDB kodai: 3OEN, 3OEO, 3OIC), CA XII (PDB: 3OFA, 3OFB) ir CA XIII (PDB: 3OFP, 3OFN) kristalinės struktūros.

Eksperimentiškai nustatyti (stebimieji) termodinaminiai parametrai buvo pakoreguoti atsižvelgiant į visas su sulfonamidų jungimusi susietas protonacijos pusiausvyras, įskaitant ligando deprotonaciją, cinko jono koordinuotos hidroksido grupės protonaciją bei buferio jonizaciją. Šis skaičiavimas rėmėsi eksperimentiškai nustatytais sulfonamidų $\mathrm{p}K_\mathrm{a}$: junginiams 4a-4d ir 4h nustatyta $\mathrm{p}K_{\mathrm{a,SA}}$ = 9,8 bei protonacijos entalpija $\Delta H_{\mathrm{pr,SA}} = -35{,}2\,\mathrm{kJ\,mol^{-1}}$, o junginiui 7h - $\mathrm{p}K_{\mathrm{a,SA}}$ = 8,9 ir $\Delta H_{\mathrm{pr,SA}} = -30{,}4\,\mathrm{kJ\,mol^{-1}}$ (naudojant TRIS buferį, kurio $\Delta H_{\mathrm{pr,buf}} = -46{,}56\,\mathrm{kJ\,mol^{-1}}$). Atlikus šią analizę, buvo gauti tikrieji termodinaminiai parametrai (ΔG_{int}, ΔH_{int} ir $-T\Delta S_{\mathrm{int}}$), atspindintys tik pačią baltymo ir ligando sąveiką. Tikrosios Gibso energijos lyginant jungimąsi tarp izofermentų kito nedaug, tuo tarpu tikrosios entalpijos ir entropijos skyrėsi dešimtimis $\mathrm{kJ\,mol^{-1}}$. Pavyzdžiui, junginio 4a tikroji Gibso energija jungiantis prie CA II ir CA XIII skyrėsi vos $2{,}1\,\mathrm{kJ\,mol^{-1}}$ (atitinkamai $-59{,}3\,\mathrm{kJ\,mol^{-1}}$ ir $-61{,}4\,\mathrm{kJ\,mol^{-1}}$), tačiau atitinkamos tikrosios entalpijos skirtumas siekė net $37{,}2\,\mathrm{kJ\,mol^{-1}}$ (atitinkamai $-26{,}8\,\mathrm{kJ\,mol^{-1}}$ ir $-64{,}0\,\mathrm{kJ\,mol^{-1}}$). Šį skirtumą visiškai kompensavo

priešingas entropinio indėlio pokytis (čia $-T\Delta S_{\mathrm{int}}$ pakito nuo labai palankaus $-32{,}5\,\mathrm{kJ\,mol^{-1}}$ sistemoje su CA II iki nepalankaus $2{,}6\,\mathrm{kJ\,mol^{-1}}$ su CA XIII). Šie stebėjimai įrodo, kad panašus jungimosi stiprumas gali susidaryti dėl iš esmės skirtingų energetinių mechanizmų balansavimo.

Nustatytas ryškus, nuo izofermento priklausantis entalpijos ir entropijos kompensacijos pobūdis, stebimas visoje tirtoje junginių serijoje. Jungimąsi prie CA II lėmė palanki entropija, o jungimąsi prie CA XIII - entalpija, kol CA XII pasižymėjo tarpiniais termodinaminiais profiliais. Apibendrinant, vidutinis santykinis jungimosi Gibso energijos pasiskirstymas tarp tirtų junginių parodė, kad visų reakcijų suminis jungimasis prie CA II buvo $\sim$70 % nulemtas entropijos ($\sim$30 % entalpijos), CA XII buvo tarpinis ($\sim$70 % entalpijos, $\sim$30 % entropijos), o jungimasis prie CA XIII buvo beveik visiškai nulemtas entalpijos ($\sim$100 % entalpijos, 0 % entropijos). Svarbu tai, kad šie skirtumai tarp izofermentų buvo gerokai didesni už tuos, kuriuos sukėlė paties ligando struktūros modifikacijos; tai rodo, kad šiuo atveju pagrindinis termodinaminio skirtumo veiksnys yra baltymo aplinka, o ne ligandas. Rezultatai dar kartą pabrėžė, kad vien stebimaisiais termodinaminiais parametrais grįsta analizė gali būti klaidinanti, nes su protonacija susiję procesai gali reikšmingai iškraipyti tiek entalpijos, tiek entropijos indėlius, todėl šiam palyginimui buvo būtina atlikti su protonizacija susijusių pusiausvyrų korekciją.

Didelės raiškos kristalinės struktūros atskleidė, kad nepaisant ryškių termodinaminių skirtumų, visų slopiklių bendri jungimosi būdai yra labai panašūs: jie koordinuoja katalizinį cinko joną per deprotonuotą sulfonamidinę grupę ir visuose kompleksuose formuoja panašius vandenilinius ryšius su Thr199. Nepaisant to, nustatyti keli subtilūs aktyviojo centro architektūros skirtumai toliau nuo šios konservatyvios jungimosi srities, kurie yra pagrindiniai stebimos termodinaminės elgsenos veiksniai. Konkrečiai, ties 62 pozicija esantis Asn izofermentuose CA II ir CA XII gali suformuoti tiesioginį vandenilinį ryšį su ligandu, tuo tarpu trumpesnis Ser62 izofermente CA XIII lemia netiesioginį vandenilinį ryšį per vandens molekulę. Ties 131 pozicija CA II ir CA XIII turi Phe, o CA XII turi Ala aminorūgštį (be to, Phe131 pasižymėjo neįprastu ir retu konformaciniu paslankumu reaguodamas į skirtingus ligandus). Kitas pastebimas skirtumas nustatytas ties 200 pozicija, kurią užima Thr izofermentuose CA II ir CA XII, tačiau Val - izofermente CA XIII, o tai reikšmingai keičia vietinę hidratacijos aplinką šalia benzensulfonamido grupės. Šių struktūrinių variacijų pakako, kad būtų pakeista pusiausvyra tarp entalpinių ir entropinių varomųjų jėgų, kartu išlaikant bendrą jungimosi stiprumą.

Šie rezultatai rodo, kad panašūs jungimosi stiprumai gali atsirasti dėl

iš esmės skirtingų energetinių mechanizmų, o subtilūs aktyviojo centro architektūros pokyčiai gali reikšmingai pakeisti entalpinių ir entropinių indėlių balansą nedarydami įtakos bendram stiprumui. Didžiausi skirtumai buvo susiję su baltymo izofermentu, o ligando struktūros modifikacijomis turėjo gerokai mažesnį efektą šiuo atveju. Šie skirtumai dera su izofermentams būdinga aktyviojo centro hidratacija, kur vandens organizacijos skirtumai ir dehidratacijos energetiniai kaštai jungiantis ligandui lemia skirtingus termodinamius profilius. Konkrečiai, CA II izofermente Thr200 trumpu vandeniliniu ryšiu stabilizuoja tvarkingą vandens molekulę W1, kurios išstūmimas prisijungiant ligandui sukuria labai palankų tirpiklio entropijos indėlį. Priešingai, Val200 izofermente CA XIII negali suformuoti šio stabilizuojančio vandenilinio ryšio, todėl ten esantis aktyviojo centro vandens tinklas yra mažiau tvarkingas ir laisvesnis, o jo reorganizacija suteikia nežymų entropinį pokytį, taip nulemdama dominuojantį entalpinį jungimosi pobūdį. Integruojant tikrųjų termodinaminių parametrų analizę su didelės raiškos struktūriniu apibūdinimu, tyrime sukuriamas išsamus sulfonamidų atpažinimo struktūros ir termodinamikos modelis. Šie rezultatai suteikia svarbių įžvalgų apie molekulines entalpijos ir entropijos kompensacijos priežastis bei pabrėžia būtinybę atsižvelgti tiek į struktūrinius, tiek į termodinaminius veiksnius racionaliai projektuojant selektyvius ligandus.

Jungimosi stiprumas ir selektyvumas

Šioje dalyje apibendrinami publikacijos [136] rezultatai:

Audrius Zakšauskas, **Vaida Paketurytė-Latvė**, Alberta Jankūnaitė, Edita Čapkauskaitė, Yann Becart, Alexey Smirnov, Klára Pospíšilová, Janis Leitans, Jiří Brynda, Andris Kazaks, Lina Baranauskienė, Elena Manakova, Saulius Gražulis, Visvaldas Kairys, Kaspars Tars, Pavlína Řezáčová, Daumantas Matulis

Affinity and Selectivity of Protein-Ligand Recognition: A Minor Chemical Modification Changes Carbonic Anhydrase Binding Profile
J. Med. Chem., 2025, 68 (16), 17752–17773.
DOI: 10.1021/acs.jmedchem.5c01421

Mano indėlį sudarė eksperimentinis jungimosi stiprumo nustatymas

FTSA metodu, tikrosios jungimosi termodinamikos analizė, rentgeno struktūrinė kristalografinė analizė, selektyvumo tendencijų interpretavimas bei duomenų analizė ir rankraščio rengimas. Prie šios publikacijos svariai prisidėjo Dr. A. Zakšausko, Dr. A. Jankūnaitės, Dr. E. Čapkauskaitės bei Yann Becart atlikta tiriamų junginių organinė sintezė. Svarbu pažymėti, kad nepriklausomus fermentų slopinimo eksperimentus atliko K. Pospíšilová. Tai leido parodyti stiprią koreliaciją tarp nepriklausomai atliktų jungimosi (FTSA) ir slopinimo (SFA) duomenų.

Šiame tyrime sistemingai nagrinėta, kaip nedidelės *orto*-pakeistų benzensulfonamidų cheminės modifikacijos iš esmės keičia jungimosi stiprumą ir selektyvumą žmogaus karboanhidrazės (CA) izofermentų atžvilgiu. Buvo susintetinta apie 50 naujų junginių, atstovaujančių septynias chemines klases pagal sieros oksidacijos laipsnį ir jungiančiojo tilto heteroatomus (įskaitant 4-sulfanil-, 4-sulfinil- ir 4-sulfonil-esterius bei benzamidus, kartu su 4-amino-benzamidais). Jungimosi stiprumas visiems 12 kataliziškai aktyvių žmogaus CA izofermentų buvo nustatytas naudojant FTSA, kurią papildė „stopped-flow“ fermentinis slopinimas bei struktūrinė rentgenostruktūrinė analizė.

Maži struktūriniai pokyčiai lėmė jungimosi stiprumo skirtumus, siekiančius kelias eiles. Konkrečiai, 4-sulfanil-pakeisti benzensulfonamidai pasižymėjo išskirtinai stipriu ir selektyviu jungimusi prie CA IX, o jų tikrosios disociacijos konstantos pasiekė pikomolinį diapazoną. Pavyzdžiui, cikloheksilsulfanilesteris 4b pasižymėjo išskirtine $K_{\mathrm{d,int}}$, lygia $1\,\mathrm{pM}$ ($0{,}0010\,\mathrm{nM}$) taikinio CA IX atžvilgiu, o jungimasis su CA II šimtus kartų silpnesnis ($K_{\mathrm{d,int}} = 0{,}49\,\mathrm{nM}$). Be to, nors stambus adamantilsulfanilesteris 4g pasiekė panašų stiprumą CA IX ($K_{\mathrm{d,int}} = 3\,\mathrm{pM}$) su kelis šimtus kartų didesniu selektyvumu prieš CA II, mažesnis metilsulfanilo analogas 4h šį selektyvumą prarado. Priešingai, sulfanilo grupės oksidacija iki sulfinilo ar sulfonilo žymiai sumažino sąveiką ir beveik panaikino selektyvumą CA IX izofermentui, nepaisant minimalių viso molekulinio karkaso pokyčių. Pavyzdžiui, sulfinilo darinys 7b ir sulfonilo darinys 9b rodė stipriai sumažėjusį ar dingusi jungimąsi CA IX (atitinkamai $28\,\mathrm{nM}$ ir $320\,\mathrm{nM}$)

$K_{\mathrm{d,int}}$ buvo gautos iš stebimųjų disociacijos konstantų, įvertinus nuo pH priklausančias tiek sulfonamido grupės, tiek prie cinko koordinuotos vandens molekulės protonacijos pusiausvyras. Ši analizė parodė, kad jungimasis nebuvo susijęs vien tik su $\mathrm{p}K_{\mathrm{a}}$ poslinkiais, bet atspindėjo tikrąją baltymo ir ligando sąveiką. Ši korekcija yra kritinė, nes nors stiprus elektronus sutraukiantis sulfinilo ir sulfonilo grupių efektas sumažino sulfonamido $\mathrm{p}K_{\mathrm{a,SA}}$ beveik visu pH vienetu (nuo 9,8 sulfanilo

junginiams iki 8,9 sulfoksidams) ir padidino deprotonuoto ligando dalį, paruoštą koordinuoti cinko joną prie pH 7,0, jų tikrosios jungimosi konstantos iš tikrųjų buvo šimtus tūkstančių kartų silpnesnės. Tai pabrėžia ΔG_{int} ir kitų tikrųjų parametrų svarbą patikimai analizuojant CA slopiklių struktūros ir jungimosi stiprumo sąsajas.

Esterių ir benzamidų analogų palyginimas parodė, kad benzamidai prie CA izofermentų paprastai jungėsi silpniau, nors keli iš jų išlaikė pastebimą selektyvumą CA IX atžvilgiu. Pakaito dydis ir hidrofobiškumas buvo lemiami veiksniai: didelės hidrofobinės grupės optimizavo sąveikas didesniame (negu kituose izofermentuose) CA IX aktyviajame centre, tačiau sukėlė sterines kliūtis mažesnių aktyviųjų centrų izofermentuose, taip nulemdamos selektyvumą.

Konformacijų analizė suteikė struktūrinį jungimosi stiprumo tendencijų paaiškinimą. Didelio jungimosi stiprumo sulfanil-pakeisti ligandai jungėsi su karboanhidrazėmis tokiu būdu, kuris optimizavo hidrofobinį efektą ir vadenilinių ryšių tinklus bei svarbiausia sudarydami koordinacinį ryšį su cinko jonu. Tiksliau, devynios naujai nustatytos struktūros (įskaitant CA II-4c, CA IX-4d ir CA XIII-4d; PDB ID: 9FPQ, 9R8X, 9FPW atitinkamai) parodė, kad ligando esterio grupė sudaro tiesioginį vandenilinį ryšį su Asn62 izofermente CA II, tačiau pereina į vandens tarpininkaujamą vandenilinių ryšių tinklą su Gln70/Asn65 izofermente CA IX bei Ser64/Asn69 izofermente CA XIII. Be to, junginio 4h kristalografinė analizė komplekse su CA II (PDB ID: 9FPS) atskleidė netipinį jungimosi būdą su dviem ligando molekulėmis, kur antroji molekulė jungiasi neklasikiniu būdu aktyviojo centro periferijoje per hidrofobines ir vandens tarpininkaujamas sąveikas. Tuo tarpu sulfinilo ir sulfonilo dariniai pasižymėjo nepalankiais vidumolekuliniais vandeniliniais ryšiais, lemiančius jungimuisi su karboanhidrazėmis netinkamą konformaciją. Molekulinis dokinimas sėkmingai atkūrė eksperimentines sulfanil-pakeistų junginių tendencijas, tačiau negebėjo paaiškinti sulfonilo darinių elgsenos, kuri buvo nulemta vidumolekulinių ryšių energijos.

Apibendrinant, rezultatai rodo, kad vieno *orto* pakaito oksidacijos laipsnis ir konformacinis lankstumas gali nulemti jungimosi stiprumą CA izofermentams ir selektyvumą kelių eilių diapazone. Šis darbas nustato aiškų mechanistinį ryšį tarp subtilių cheminių modifikacijų, ligando konformacinės energetikos ir selektyvaus CA IX atpažinimo, suteikdamas vertingų gairių racionaliam karboanhidrazių slopiklių projektavimui. Ryškus nedidelių struktūrinių modifikacijų poveikis paskatino platesnį tyrimą, siekiant nustatyti, kaip struktūrinė informacija ir termodinaminiai parametrai gali būti integruoti aiškinant baltymo ir ligando atpažinimą.

Sąsajos tarp struktūros ir termodinamikos

Šioje dalyje apibendrinami publikacijos [137] rezultatai:

Vaida Paketurytė-Latvė, Alexey Smirnov, Elena Manakova, Lina Baranauskienė, Vytautas Petrauskas, Asta Zubrienė, Jurgita Matulienė, Virginija Dudutienė, Edita Čapkauskaitė, Audrius Zakšauskas, Janis Leitans, Saulius Gražulis, Kaspars Tars, Daumantas Matulis

From X-ray crystallographic structure to intrinsic thermodynamics of protein-ligand binding using carbonic anhydrase isozymes as a model system
IUCrJ, 2024, 11 (4), 556–569.
DOI: 10.1107/S2052252524004627

Mano indėlį sudarė publikacijos idėjos sukūrimas, baltymo ir ligando sąveikos termodinaminė analizė, struktūrinių ir termodinaminių duomenų integravimas bei rankraščio rengimas. Svarbu pabrėžti, kad daugumą jungimosi termodinaminių parametrų nustatymų atliko Dr. A. Zubrienė ir Dr. L. Baranauskienė, o dalį straipsnyje cituojamų kristalinių struktūrų nustatė Dr. A. Smirnov, Dr. E. Manakova ir Dr. J. Leitans. Ląstelių tyrimus atliko Dr. J. Matulienė.

Siekiant nustatyti koreliacijas tarp baltymo ir ligando struktūros bei jungimosi termodinamikos, rentgenostruktūrinės analizės duomenys buvo derinami su matavimais, gautais naudojant FTSA, ITC, fermentinio slopinimo bei metodus ląstelėse. Tyrime analizuota struktūriškai panašių sulfonamidinių slopiklių (daugiausiai fluorintų ir chlorintų benzensulfonamidų serijos) sąveika, pasižyminti itin skirtingu jungimosi stiprumu bei selektyvumu žmogaus karboanhidrazių izofermentams, didžiausią dėmesį skiriant su kietaisiais hipoksiniais navikais susijusiai CA IX. Siekiant įveikti su CA IX kristalizacija susijusius iššūkius, buvo naudota chimerinė CA IX (chCA IX) kaip itin tikslus atitikmuo, turintis šešias aktyviojo centro mutacijas (A65S, N67Q, I91L, F130V, V134L, L203A), įvestas į CA II.

Kristalinės struktūros atskleidė konservatyvų sulfonamidinių slopiklių jungimosi būdą: jie koordinuoja katalizinį Zn^{II} ir formuoja panašias sąveikas aktyviajame centre. Nepaisant to, ligandai, pasižymintys beveik identiškomis jungimosi pozomis, dažnai skyrėsi savo jungimosi su karboanhidrazėmis stiprumu keliomis eilėmis. Pavyzdžiui, struktūriškai itin panašūs slopikliai EA3-3 ir EA5-3 kompleksuose su

chCA IX ir CA II (abu kristalizuojasi $P2_1$ erdvinėje grupėje su beveik identiškais elementariosios narvelio parametrais) pasižymėjo panašiomis jungimosi konformacijomis, tačiau demonstravo visiškai skirtingą jungimosi stiprumą. Šie stebėjimai įrodė, kad vien struktūrinės informacijos nepakanka norint paaiškinti jungimosi stiprumą ar izofermentinį selektyvumą.

Skirtingų eksperimentinių metodų palyginimas išryškino individualių jungimosi analizių privalumus ir apribojimus. FTSA metodas pasižymėjo plačiausiu nustatymo diapazonu - nuo milimolinių iki pikomolinių K_d verčių, tuo tarpu fermentinio slopinimo analizės bei ITC metodas apsiribojo siauresniais matavimo intervalais. Kelių ortogonalinių metodų taikymas leido patikimiau apibūdinti baltymo ir ligando sąveikas.

Pagrindinis šio darbo rezultatas - tikrųjų termodinaminių parametrų nustatymas. Įvertinus su jungimusi susietas protonacijos pusiausvyras, stebimieji jungimosi duomenys buvo perskaičiuoti į ΔG_int, ΔH_int ir $-T\Delta S_\mathrm{int}$. Tam reikėjo įvertinti cinko koordinuotos hidroksido grupės protonaciją aktyviajame centre (fermento $\mathrm{p}K_\mathrm{a,CA}$ siekia 6–7, o CA I ir CA XIII atveju – iki 8) bei benzensulfonamido grupės deprotonaciją ($\mathrm{p}K_\mathrm{a,SA}$ paprastai yra tarp 8 ir 11). Šie tikrieji parametrai tiksliau atspindėjo baltymo ir ligando sąveikos pasekmes ir sudarė sąlygas nustatyti prasmingas struktūros ir termodinamikos sąsajas.

Kompleksinė analizė parodė, kad ligandų jungimosi stiprumą ir selektyvumą lemia sudėtinga struktūrinių, solvatacijos bei termodinaminių veiksnių sąveika. Nedidelės cheminės modifikacijos dažnai sukeldavo esminius tikrosios jungimosi energijos pokyčius, nepaisant tik subtilių skirtumų kristalografinėse struktūrose. Konkrečiai, uodegos metilo grupės (VD12-05) pakeitimas hidroksilo uodega (VD10-35) lėmė sistemingą $7,5$–$10,7\ \mathrm{kJ\,mol^{-1}}$ tikrosios Gibso energijos praradimą skirtinguose CA izofermentuose, nes polinė hidroksigrupė buvo linkusi formuoti vandenilinius ryšius su tirpikliu, o ne su baltymu. Priešingai, ciklooktilamino žiedo įvedimas *meta*-padėtyje (VD11-4-2) sukėlė sterinių trukdžių, kurie sumažino CA I jungimosi stiprumą $18{,}0\,\mathrm{kJ\,mol^{-1}}$ (1000 kartų), tačiau užtikrino $21{,}9\,\mathrm{kJ\,mol^{-1}}$ padidėjimą (4000 kartų) CA IX ir $14{,}9\,\mathrm{kJ\,mol^{-1}}$ CA XII izofermentui, taip nulemdamas net 100 000 kartų selektyvumą CA IX naudai prieš CA I. Be to, cikloheksano pakaitas junginyje EA2-3 optimizavo hidrofobines sąveikas padidintoje CA IX kišenėje, suteikdamas išskirtinai didelę tikrąją Gibso energiją, lygią $-75{,}0\,\mathrm{kJ\,mol^{-1}}$ (fentomoliniame diapazone). Šie rezultatai pabrėžia, kad patikimai baltymo ir ligando atpažinimo interpretacijai būtina integruoti struktūrinę informaciją su tikrųjų termodinaminių parametrų analize.

Apibendrinant, šiame darbe buvo sukurtas modelis, susiejantis rentgenostruktūrinės analizės duomenis su tikraisiais termodinaminiais parametrais, bei parodyta, kaip ši integracija gali pagerinti molekulinio atpažinimo supratimą ir padėti racionaliai projektuoti vaistus. Šį principą aiškiai iliustruoja priešingos varomi mechanizmai, lemiantys stiprių slopiklių jungimąsi: nors VD10-35 jungimasis su CA I yra dominuojančiai entalpinis ($\Delta H_{\mathrm{int}} = -76{,}8\,\mathrm{kJ\,mol^{-1}}$), selektyvus VD11-4-2 jungimasis su CA IX yra daugiausiai nulemtas entropijos ($-T\Delta S_{\mathrm{int}} = -47{,}5\,\mathrm{kJ\,mol^{-1}}$), nepaisant mažesnio entalpinio indėlio ($\Delta H_{\mathrm{int}} = -24{,}3\,\mathrm{kJ\,mol^{-1}}$), o abu kartu jie suformuoja itin stiprų kompleksą ($\Delta G_{\mathrm{int}} = -71{,}8\,\mathrm{kJ\,mol^{-1}}$).

Termodinaminių matavimų patikimumas

Patikima baltymo ir ligando atpažinimo interpretacija priklauso ne tik nuo struktūrinių ir termodinaminių duomenų kokybės, bet ir nuo šių duomenų gavimo bei analizės metodų. Eksperimentiniai apribojimai, parametrų tarpusavio priklausomybė (koreliacijos) ir statistinė neapibrėžtis gali daryti didelę įtaką jungimosi konstantų bei termodinaminių parametrų tikslumui ir interpretacijai. Šiame skyriuje pristatomi tyrimai nagrinėja du vienas kitą papildančius šios problemos aspektus: fluorescentinio terminio poslinkio metodo (FTSA) matavimų standartizavimą bei baltymo ir ligando jungimosi parametrų neapibrėžties vertinimą.

FTSA matavimų standartizavimas

Šioje dalyje apibendrinami publikacijos [116] rezultatai:

Egidijus Kazlauskas, Vytautas Petrauskas, **Vaida Paketurytė**, Daumantas Matulis

Standard Operating Procedure for Fluorescent Thermal Shift Assay (FTSA) for Determination of Protein-Ligand Binding and Protein Stability
Eur. Biophys. J., 2021, 50 (5), 707–714.
DOI: 10.1007/s00249-021-01537-1

Mano indėlį sudarė duomenų analizė ir interpretavimas, iliustracijų bei rankraščio teksto rengimas.

Tyrimas parodė, kad FTSA užtikrina atkuriamas, aukštos kokybės lydymosi kreives, tinkamas tiek baltymų stabilumui, tiek ligandų jungimosi stiprumui nustatyti plačiame diapazone (nuo 10^3 iki $10^{13}\mathrm{M}^{-1}$). Lydymosi temperatūra (T_m) nustatoma sigmoidinio denatūracijos virsmo vidurio taške, o eksperimentiniai temperatūriniai poslinkiai (ΔT_m) pritaikomi pusiausvyrinei jungimosi konstantai (K_b) skaičiuoti. Naudojant CA II (konkrečiai – acetazolamido iki $200\,\mu\mathrm{M}$ koncentracijos jungimąsi su $5\,\mu\mathrm{M}$ CA II, $2\,\%$ v/v DMSO ir $50\,\mu\mathrm{M}$ ANS) ir Hsp90α N-galinį domeną (ištirtą pH 5,0–10,5 diapazone daugiakomponentiniame acetato-borato-fosfato buferyje) kaip pavyzdžius qPCR aparate (naudojant išcentrinius rotorinius spektrofluorimetrus ir $10\,\mu\mathrm{L}$-$20\,\mu\mathrm{L}$ tūrius optimaliam temperatūros tolygumui), šis metodas patikimai nustatė ligandų sukeltus temperatūrinius poslinkius bei nuo pH priklausančius stabilumo pokyčius, patvirtindamas savo jautrumą tiek jungimosi, tiek tirpalo sąlygoms. Ligandų sukelti temperatūriniai poslinkiai leido nustatyti jungimosi konstantas plačiame sąveikų diapazone. Darbe taip pat atskleista, kad metodo veiksmingumas stipriai priklauso nuo dažų koncentracijos, baltymo grynumo, buferio sudėties bei DMSO koncentracijos, taip išryškinant pagrindinius veiksnius, lemiančius duomenų kokybę. Konkrečiai, sėkmingas matavimas priklauso nuo temperatūrai nejautraus buferio sudėties (naudojant fosfatinį arba HEPES vietoje TRIS, siekiant išvengti nuo temperatūros priklausomo pH poslinkio), DMSO koncentracijos (saugi ties $2\,\%$ v/v, tačiau destabilizuojanti esant ($\geq 4\,\%$)), baltymo struktūros (teikiant pirmenybę monomeriniams baltymams prieš sudėtingus oligomerinius darinius, kurie lemia persidengiančius efektų signalus), bei dažų parinkimo (rekomenduojant ANS su $\lambda_{EX/EM} \approx 350\,\mathrm{nm}/470\,\mathrm{nm}$ vietoje SYPRO Orange dėl silpnesnio pradinio fono, arba naudojant triptofano fluorescenciją). Apibendrinant, gauti rezultatai patvirtino, kad FTSA yra patikimas, mažas mėginių sąnaudas naudojantis ir našus metodas, tinkamas rutiniškam baltymų ir ligandų sąveikų apibūdinimui bei stabilumo atrankai.

Neapibrėžties vertinimas

Šioje dalyje apibendrinami publikacijos [138] rezultatai:

Vaida Paketurytė, Vytautas Petrauskas, Asta Zubrienė, Olga Abian, Margarida Bastos, Wen-Yih Chen, Maria João Moreno, Georg Krainer, Vaida Linkuvienė, Arthur Sedivy, Adrian Velazquez-Campoy, Mark A. Williams, Daumantas Matulis

Uncertainty in protein-ligand binding constants: asymmetric confidence intervals versus standard errors
Eur. Biophys. J., 2021, 50 (3–4), 661–670.
DOI: 10.1007/s00249-021-01518-4

Šis darbas buvo COST veiklos CA15126 (MOBIEU) užduotis, kilusi iš bendrų Europos biofizikų bendruomenės diskusijų, siekiant patobulinti molekulinių sąveikų neapibrėžties pateikimą. Mano indėlis į šį tyrimą apėmė dalyvavimą mokslinėse diskusijose, eksperimentų planavimą, duomenų analizę ir rankraščio rengimą.

Šis tyrimas parodo, kad simetrinės standartinės paklaidos, dažniausiai pateikiamos kaip $\pm x$, reikšmingai nuvertina tikrąjį baltymų–ligandų sąveikos konstantų neapibrėžtumą. Analizuojant tiek modeliuotus, tiek eksperimentinius duomenų rinkinius nustatyta, kad pusiausvyros jungimosi konstanta (K_b), disociacijos konstanta (K_d) ir Gibso energijos pokytis (ΔG) pasižymi iš esmės asimetriškais pasiskirstymais dėl juos siejančių logaritminių, eksponentinių ir atvirkštinių matematinių priklausomybių. Šių parametrų tarpusavio transformacijos dar labiau sustiprina pasiskirstymų asimetriją, todėl simetrinis paklaidų pateikimas yra statistiškai netinkamas ir gali lemti fiziškai neįmanomus rezultatus, pavyzdžiui, neigiamas jungimosi konstantų reikšmes. Pavyzdžiui, 1-uoju atveju (Case 1 publikacijoje), darant prielaidą, kad K_b pasiskirstymas yra normalusis, kurio vidurkis lygus $2{,}0 \cdot 10^7\,\mathrm{M}^{-1}$, o standartinis nuokrypis – $0{,}6 \cdot 10^7\,\mathrm{M}^{-1}$, transformavus į K_d gaunamas stipriai asimetriškas pasiskirstymas (asimetrijos koeficientas siekia 4,3), be to, normalusis pasiskirstymas priskiria teigiamą tikimybę fiziškai neįmanomoms neigiamoms K_b reikšmėms. Priešingai, jei normalumas taikomas ΔG su vidurkiu $-41{,}67\,\mathrm{kJ\,mol}^{-1}$ prie $25\,^\circ\mathrm{C}$ ir standartiniu nuokrypiu $0{,}77\,\mathrm{kJ\,mol}^{-1}$, gaunamas simetrinis $95\,\%$ pasikliautinasis intervalas $-43{,}18\,\mathrm{kJ\,mol}^{-1}$ to (numerical range) $-40{,}16\,\mathrm{kJ\,mol}^{-1}$, kurį tiesiogiai transformavus gaunamas prasmingas asimetrinis K_b $95\,\%$ pasikliautinasis intervalas $[1,09; 3,68] \times 10^7\mathrm{M}^{-1}$

Monte Karlo simuliacijos, atliktos 1:1 jungimosi titravimams, parodė, kad apskaičiuotos K_b reikšmės tampa vis labiau teigiamai asimetriškos didėjant jungimosi stiprumui, tuo tarpu ΔG išlieka artimesnis normaliam pasiskirstymui esant pakankamai optimalioms eksperimentinėms sąlygoms. Siekiant įvertinti eksperimentiškai realistišką situaciją, 2-uoju atveju (Case 2 publikacijoje) sumodeliuotas VP-ITC eksperimentas, kurį sudarė $20 \times 15\,\mu\mathrm{L}$ $200\,\mu\mathrm{M}$ ligando įšvirkštimai į $20\,\mu\mathrm{M}$ baltymo tirpalą, esant ($\Delta H = -10\,\mathrm{kJ\,mol}^{-1}$) ir pastoviam įšvirkštimo šilumos triu-

kšmui 3 µJ. Tokiomis sąlygomis, padidinus tikrąją K_b reikšmę nuo $2 \cdot 10^5\,\mathrm{M}^{-1}$ (Wiseman parametras $c = 4$) iki $2 \cdot 10^7\,\mathrm{M}^{-1}$ ($c = 400$), gautos K_b reikšmės pasiskirstymo asimetrijos koeficientas išaugo nuo 1,3 ((CI_{95}=[0,78;5,8]$\times 10^5\,\mathrm{M}^{-1}$)) iki net 23 (($CI_{95}$=[0,51;22]$\times 10^7\,\mathrm{M}^{-1}$)). Esant tokiai didelio jungimosi stiprumo c reikšmei, tik 3–4 duomenų taškai patenka į jungimosi izotermos pereinamąją sritį, todėl kreivės linkis, apribojantis K_b, yra prastai išreikštas, o gautos reikšmės tampa itin jautrios triukšmui ir suformuoja asimetrišką skirstinį su ilga viršutine uodega.

Su bendraautoriais priėjome išvadą, kad profilio tikėtinumo (angl. *profile likelihood*) metodu apskaičiuoti $95\,\%$ pasikliautinieji intervalai ($CI_{P,95}$) yra nuoseklesnis ir tarpusavyje transformuojamas neapibrėžtumo vaizdavimo būdas visiems termodinaminiams dydžiams. Asimetriniai intervalai yra apskaičiuojami naudojant Fisherio–Snedecoro F pasiskirstymą, sistemingai keičiant tiriamą parametrą fiksuotais žingsniais ir minimizuojant liekamųjų kvadratų sumą kitų laisvųjų parametrų atžvilgiu. Skirtingai nei standartinės paklaidos, šis metodas užtikrina visišką viršutinių ir apatinių neapibrėžtumo ribų atitikimą transformuojant tarp K_b ir ΔG, išsaugant visą informaciją apie eksperimentinį kintamumą. Pavyzdžiui, sumodeliuotam titravimui su tikrosiomis reikšmėmis (K_b = 2 $\times 10^6\,\mathrm{M}^{-1}$) ir ($\Delta H$ = 41,8 $\mathrm{kJ\,mol}^{-1}$), profilio tikėtinumo metodas ($CI_{P,95}$) duoda identiškus atitinkančius intervalus (([1,44;3,30] $\times 10^6$ M^{-1}) parametrui (K_b) ir ([-37,2;-35,1] $\mathrm{kJ\,mol}^{-1}$) parametrui (ΔG)), nepriklausomai nuo to, kuris iš jų buvo tiesiogiai optimizuojamas, tuo tarpu standartiniai asimptotiniai simetriniai intervalai ($CI_{S,95}$) šio sąryšio po transformacijos neišlaiko. Tad rezultatai rodo, kad asimetriniai pasikliautinieji intervalai yra būtini siekiant tiksliai interpretuoti ir pakartotinai naudoti biofizikinius duomenis, todėl baltymų–ligandų sąveikos tyrimuose jie turėtų pakeisti nusistovėjusias simetrines standartines paklaidas.

Diskusija

Pagrindinis struktūra paremto vaistų kūrimo tikslas yra numatyti, kaip cheminės modifikacijos veikia jungimosi stiprumą ir selektyvumą, bei panaudoti šias žinias kuriant junginius, kurie stipriai jungiasi prie norimo taikinio ir kartu nesąveikauja (arba silpnai sąveikauja) su kitais baltymais. Nepaisant didelės pažangos struktūrinės biologijos, kompiuterinės chemijos ir biofizikos srityse, šį tikslą pasiekti vis dar sudėtinga.

Šioje disertacijoje pateikti rezultatai išryškina keletą veiksnių, kurie apsunkina baltymų–ligandų atpažinimo interpretavimą ir prognozavimą.

Skyriuje Entalpijos–entropijos kompensavimas pateikti rezultatai suteikia papildomų įžvalgų apie molekulines entalpijos–entropijos kompensavimo priežastis. Ankstesni Whitesides ir bendradarbių darbai [9, 139] parodė, kad net ir nedidelės ligandų modifikacijos gali lemti didelius entalpijos ir entropijos pokyčius, nors bendras jungimosi stiprumas su CA II kinta tik nežymiai. Tai pabrėžia hidratacijos ir tirpiklio persitvarkymo svarbą molekuliniame atpažinime. Šiame darbe gauti rezultatai rodo, kad reikšmingi termodinaminių parametrų skirtumai gali atsirasti ir tarp karboanhidrazės izofermentų, nepaisant labai konservatyvios aktyviojo centro architektūros ir panašios ligandų jungimosi geometrijos. Tai rodo, kad entalpijos–entropijos kompensavimą lemia ne tik paties ligando savybės, bet ir aktyviojo centro aplinka bei kiti baltymo ypatumai. Net ir nedideli aktyviojo centro aminorūgščių liekanų, hidratacijos tinklų ar baltymo dinamikos skirtumai yra pakankami pakeisti entalpijos ir entropijos pusiausvyrą. Todėl jungimosi termodinaminės savybės turėtų būti vertinamos kaip visos baltymo–ligando sistemos savybė, o ne kaip tiesioginiai baltymo–ligando tarpmolekuliniai ryšiai.

Praktiniu požiūriu šie rezultatai atskleidžia tiek termodinaminės analizės galimybes, tiek jos ribotumus. Nors jungimosi energijos išskaidymas į entalpines ir entropines dedamąsias leidžia atskirti baltymo–ligando kompleksus, kurie, vertinant vien pagal jungimosi stiprumą, atrodo labai panašūs, šių dedamųjų interpretavimas išlieka sudėtingas, nes entalpija ir entropija atspindi daugelio tarpusavyje susijusių procesų bendrą poveikį. Kaip pažymėjo Klebe ir kiti autoriai [140], atskirų termodinaminių indėlių priskyrimas konkrečioms molekulinėms sąveikoms dažnai nėra tiesioginis, nes tarpmolekuliniai kontaktai, hidratacija, konformacinis lankstumas ir dinamika kinta vienu metu. Vis dėlto termodinaminių parametrų gebėjimas atskirti sistemas, pasižyminčias panašiomis struktūromis ir jungimosi stiprumais, rodo jų vertę tiriant molekulinio atpažinimo procesus ir pabrėžia papildomą informaciją, kurią jie suteikia greta įprastinių jungimosi stiprumo matavimų.

Skyriuje Jungimosi stiprumas ir selektyvumas aprašyti rezultatai dar kartą pabrėžia konformacinių veiksnių svarbą baltymų–ligandų atpažinimui. Daugybė tyrimų parodė, kad net ir nedidelės struktūrinės modifikacijos gali pakeisti ligando lankstumą, konformacines preferencijas ir baltymo dinamiką, taip sukeldamos netikėtai didelius jungimosi pokyčius. Gilson ir bendradarbiai [3, 10] pabrėžė konformacinės entropijos svarbą molekuliniame atpažinime bei sunkumus tiksliai įvertinant jos indėlį į jungimąsi, o Wand [142], Akke [6, 70] ir jų kolegos, rem-

damiesi NMR tyrimais, parodė, kad baltymo ar ligando dinamikos pokyčiai gali reikšmingai prisidėti prie jungimosi termodinamikos. Neseniai Wankowicz ir bendradarbiai [66] parodė, kad net iš rentgeno kristalografijos duomenų nustatytas konformacinis heterogeniškumas gali suteikti vertingų įžvalgų apie entropines ligando jungimosi pasekmes. Tačiau, nepaisant šios pažangos, eksperimentinis konformacinės entropijos charakterizavimas išlieka gerokai sudėtingesnis nei bendrų jungimosi termodinaminių parametrų nustatymas. Įprastiniuose ITC eksperimentuose bendras entropijos pokytis apskaičiuojamas netiesiogiai iš išmatuotų Gibso energijos ir entalpijos verčių. Tuo tarpu atskiri baltymo konformacinių pokyčių, ligando lankstumo, tirpiklio persitvarkymo ir kitų procesų indėliai dažniausiai negali būti išskirti. Todėl šiame darbe gauti rezultatai atskleidžia tiek konformacinių veiksnių svarbą, tiek dabartinius jų charakterizavimo ribotumus. Šiame tyrime stebėti ryškūs jungimosi stiprumo sumažėjimai oksiduojant sierą turinčius pakaitus rodo, kad ligando konformacijos pokyčiai gali nusverti tikėtiną jungimosi stiprėjimą, susijusį su elektronus ištraukiančių grupių įvedimu.

Skyriuje Sąsajos tarp struktūros ir termodinamikos pateikti rezultatai pabrėžia stebimų ir tikrųjų termodinaminių parametrų atskyrimo svarbą interpretuojant baltymų–ligandų sąveikas. Susietų protonacijos pusiausvyrų įtaka jungimosi termodinamikai žinoma jau kelis dešimtmečius, o Baker ir Murphy [11], Whitesides ir bendradarbių [143], Klebe ir bendradarbių [140] darbai bei mūsų laboratorijos tyrimai [134] pabrėžė, kad stebimi termodinaminiai parametrai nebūtinai tiesiogiai atspindi molekulinio atpažinimo energiją. Nepaisant to, tikrųjų termodinaminių parametrų analizė šiuolaikiniuose baltymų–ligandų tyrimuose vis dar naudojama palyginti retai, nes reikalingų protonacijos parametrų nustatymas yra eksperimentiškai sudėtingas, o daugeliui sistemų tokie duomenys apskritai nėra prieinami [140]. Dėl šios priežasties stebimi termodinaminiai parametrai dažnai interpretuojami taip, tarsi jie tiesiogiai apibūdintų baltymo–ligando sąveikas. Šiame darbe gauti rezultatai rodo, kad su protonacija susiję indėliai gali reikšmingai pakeisti tiek jungimosi termodinamikos dydį, tiek jos interpretaciją, todėl prasmingam ligandų, baltymų ir jungimosi mechanizmų palyginimui dažnai būtina remtis tikraisiais, o ne stebimais parametrais. Plačiau žvelgiant, šie rezultatai rodo, kad tikslios struktūros ir termodinamikos sąsajoms nustatyti reikalinga ne tik aukštos raiškos struktūrinė informacija, bet ir griežtas procesų, lemiančių išmatuotus termodinaminius parametrus, atskyrimas.

Skyriuose FTSA standartizavimas ir Neapibrėžties vertinimas aprašy-

ti metodologiniai tyrimai pabrėžia eksperimentų dizaino ir neapibrėžties vertinimo svarbą patikimai baltymų–ligandų jungimosi duomenų interpretacijai. Literatūroje publikuotų slopinimo verčių palyginimo analizė [145] atskleidė reikšmingą ir didelį rezultatų kintamumą tarp nepriklausomų tyrimų ir išryškino sunkumus, susijusius su skirtingomis eksperimentinėmis metodikomis bei sąlygomis gautų duomenų palyginimu. Toks kintamumas ypač svarbus skaičiavimo metodams, kurie modelių kūrimui, validavimui ir palyginimui dažnai remiasi publikuotais jungimosi duomenimis. Netikslūs ar tarpusavyje nesuderinami eksperimentiniai matavimai gali riboti ne tik eksperimentinių rezultatų interpretaciją, bet ir prognozuojančių modelių kūrimą. Negalima tikėtis, kad modeliai, apmokyti naudojant triukšmingus eksperimentinius duomenis, pasieks didesnį prognozavimo tikslumą nei leidžia pačių matavimų kokybė. Panašūs klausimai buvo keliami ir karboanhidrazių tyrimų srityje, kur Liljas ir bendradarbiai [146] suabejojo kai kurių plačiai cituojamų slopinimo duomenų rinkinių tinkamumu ir teigė, kad jų tikslumas bei patikimumas galėjo būti pervertinti. Šie pastebėjimai rodo, kad prasmingoms struktūros–aktyvumo ir struktūros–termodinamikos sąsajoms nustatyti reikalingi ne tik aukštos kokybės eksperimentiniai matavimai, bet ir realistiškas jų neapibrėžties įvertinimas. Nors eksperimentinės neapibrėžties visiškai pašalinti neįmanoma, jos griežtas įvertinimas yra būtinas norint atskirti tikrus biologinius efektus nuo metodologinio kintamumo ir užtikrinti prasmingą skirtingų tyrimų palyginimą.

Nors šiuose darbuose nagrinėti skirtingi baltymų–ligandų sąveikų aspektai, visi jie pagrindžia tą pačią pagrindinę išvadą – jungimosi stiprumas yra sudėtinis dydis, kurį lemia daugelis tarpusavyje susijusių procesų. Hidratacija, konformaciniai pokyčiai, protonacijos pusiausvyros ir eksperimentinė neapibrėžtis gali reikšmingai paveikti molekulinio atpažinimo supratimą. Todėl siekiant nustatyti prasmingas struktūros ir termodinamikos sąsajas nepakanka vien struktūrinės informacijos ar jungimosi stiprumo matavimų – būtina įvertinti ir procesus, kurie lemia stebimus eksperimentinius parametrus. Šioje disertacijoje pateikti rezultatai atskleidžia tiek struktūra paremto vaistų kūrimo galimybes, tiek jo ribotumus ir pabrėžia, kad tikslus baltymų–ligandų sąveikų supratimas priklauso nuo gebėjimo išskaidyti stebimus termodinaminius parametrus į atskirus juos formuojančius procesus bei susieti juos su struktūrine informacija. Tolesnė pažanga šioje srityje priklausys nuo vis detalesnio jungimąsi lemiančių procesų apibūdinimo, jų tarpusavio sąveikos supratimo ir jų indėlio į molekulinį atpažinimą įvertinimo.

Išvados

- Karboanhidrazių izofermentų palyginimas parodė, kad nedideli aktyviojo centro skirtumai, įskaitant hidrataciją bei Thr arba Val liekanos buvimą aktyviajame centre, buvo susiję su reikšmingais ΔH bei $T\Delta S$ skirtumais (siekusiais apie $40\,\mathrm{kJ\,mol^{-1}}$ nepaisant panašios prisijungimo geometrijos ir ΔG reikšmių). *Šie rezultatai pabrėžia tarpmolekulinės sąveikos termodinamikos jautrumą baltymo aktyviojo centro aplinkai ir atskleidžia molekulinio atpažinimo interpretavimo vien pagal sąveikos stiprumą ar struktūrą ribotumus.* (Publikacija 1)

- Nedidelės cheminės modifikacijos lėmė reikšmingus sąveikos stiprumo ir selektyvumo pokyčius įvairių CA izofermentų atžvilgiu. Analizė parodė, kad sieros turinčių pakaitų oksidacija skatino vidumolekulinių vandenilinių ryšių su sulfonamido grupe susidarymą, keitė ligando konformaciją ir silpnino baltymo ir ligando sąveiką. *Šie rezultatai atskleidžia, kad baltymo ir ligando atpažinimą lemia glaudžiai tarpusavyje susijusių veiksnių visuma.* (Publikacija 2)

- Atsižvelgus į su jungimusi susietas protonacijos pusiausvyras, buvo apskaičiuoti tikrieji termodinaminiai parametrai, kurie reikšmingai skyrėsi nuo stebimųjų reikšmių dėl protonacijos poveikio. Tai parodė, kad prasmingam sąveikos palyginimui būtina atskirti baltymo ir ligando jungimosi bei protonacijos indėlius į bendrą sąveikos termodinamiką. (Publikacija 3)

- Sisteminis FTSA eksperimentų sąlygų vertinimas parodė protokolų standartizavimo svarbą siekiant gauti tarpusavyje palyginamus baltymų ir ligandų jungimosi duomenis. Asimetriniai profilinio tikėtinumo (angl. *profile likelihood*) pasikliautinieji intervalai suteikė pagrįstą neapibrėžties įvertinimą, tuo tarpu simetrinės standartinės paklaidos yra klaidinančios dydžiams, transformuojamiems netiesiniuose modeliuose. (Publikacija 4 ir Publikacija 5)

Acknowledgements

I would like to express my gratitude to Prof. Daumantas Matulis for his guidance and continuous support throughout my studies. His scientific insight and dedication to understanding the fundamental principles of molecular recognition have profoundly influenced the way I approach scientific research.

I am sincerely grateful to Dr. Asta Zubrienė for introducing me to experimental research on protein–ligand interactions and for her support during the early stages of my scientific career; to Dr. Alexey Smirnov for sharing his expertise in X-ray crystallography and structural biology; and to Dr. Vytautas Petrauskas for shaping my approach to data analysis, scientific visualization, and problem-solving. I am also grateful to Dr. Visvaldas Kairys for valuable discussions on computational modeling and for his insights into the interpretation of ligand conformational rearrangements, including rotameric states and intermolecular hydrogen-bonding interactions. I also gratefully acknowledge Dr. Elena Manakova and her colleagues for their assistance with synchrotron diffraction data collection, as well as Dr. Saulius Gražulis for developing and maintaining the computational infrastructure and software tools used in crystallographic structure determination and analysis.

I am especially thankful to the organic synthesis experts Dr. Audrius Zakšauskas, Dr. Edita Čapkauskaitė, and Dr. Alberta Jankūnaitė for synthesizing and providing compounds that were essential for this research. I would also like to acknowledge the many colleagues whose work over the years established and maintained the protein and compound collections. I am especially grateful to Vilma Michailovienė (1968–2022), whose dedication to protein purification contributed substantially to the carbonic anhydrase platform used throughout this work. I also thank Aurelija Mickevičiūtė, Dr. Vaida Juozapaitienė, Dr. Jurgita Matulienė, Marius Gedgaudas, Jelena Jachno, Dr. Justina Kazokaitė-Adomaitienė, Dr. Virginija Dudutienė, Dr. Aivaras Vaškevičius, Dr. Benas Balandis, Dr. Irena Vaškevičienė, and many other colleagues and students whose

contributions are not individually acknowledged here but were nevertheless important to the work presented in this dissertation. I also thank Darius Lingė and Ernestas Urniežius for their assistance with the deposition of structural and binding data to the Protein–Ligand Binding Database (PLBD). I am thankful to Tomas Šimkūnas and Kristina Gluščiukaitė, whose collaboration provided me with valuable opportunities to develop my mentoring and scientific supervision skills.

I am grateful to all current and former members of the Department of Biothermodynamics and Drug Design for scientific discussions and for creating a supportive research environment. Over the years, the laboratory has been a place of scientific discovery and professional growth, where colleagues generously shared their knowledge, discussed ideas, helped solve experimental challenges, and provided encouragement throughout my doctoral journey. I would also like to thank Skaidrius Jukša and Jokūbas Preikša for their contributions to our ongoing computational modeling project and for many valuable discussions that helped shape future directions of my work. I am also thankful to all collaborators who contributed to the projects that shaped this dissertation. I am grateful to Dr. Joana Smirnovienė, Dr. Vytautas Petrauskas, and Prof. Daumantas Matulis for reviewing this dissertation and providing valuable comments and suggestions.

I gratefully acknowledge the financial support provided by the Research Council of Lithuania, Vilnius University, and other funding sources that supported my doctoral studies. Their support enabled the execution of the research presented in this dissertation and participation in scientific conferences, workshops, training schools, and collaborative activities in Lithuania and abroad. I would particularly like to acknowledge support from the Research Council of Lithuania through the project "Development and Application of a Protein–Ligand Interaction Database for Artificial Intelligence Solutions" (S-ITP-25-10).

Finally, I would like to thank my family. To my husband and son, thank you for your patience, understanding, and unwavering support. I also thank my father and sister for their support and belief in me. I am especially grateful to my mother, whose influence helped shape the person I am today. Although she is no longer here to see this achievement, her influence has accompanied me throughout this journey, and I know she would have been proud of this milestone.

Vaida Paketurytė-Latvė
Vilnius
November 5, 2026

PUBLICATIONS INCLUDED IN THE DISSERTATION

1. **Paketurytė-Latvė, V.**; Zakšauskas, A.; Kairys, V.; Čapkauskaitė, E.; Bagdonas, M.; Smirnov, A.; Manakova, E.; Gražulis, S.; Matulis, D. **Enthalpy–Entropy Compensation in Inhibitor Binding to Carbonic Anhydrase Isozymes**. 2026, 125 (21), 6148–6164. DOI: 10.1016/j.bpj.2026.09.032
2. Zakšauskas, A.; **Paketurytė-Latvė, V.**; Jankūnaitė, A.; Čapkauskaitė, E.; Becart, Y.; Smirnov, A.; Pospíšilová, K.; Leitans, J.; Brynda, J.; Kazaks, A.; Baranauskienė, L.; Manakova, E.; Gražulis, S.; Kairys, V.; Tars, K.; Řezáčová, P.; Matulis, D. **Affinity and Selectivity of Protein-Ligand Recognition: A Minor Chemical Modification Changes Carbonic Anhydrase Binding Profile**. *J. Med. Chem.* 2025, 68 (16), 17752–17773. DOI: 10.1021/acs.jmedchem.5c01421
3. **Paketurytė-Latvė, V.**; Smirnov, A.; Manakova, E.; Baranauskiene, L.; Petrauskas, V.; Zubrienė, A.; Matulienė, J.; Dudutienė, V.; Čapkauskaitė, E.; Zakšauskas, A.; Leitans, J.; Gražulis, S.; Tars, K.; Matulis, D. **From X-Ray Crystallographic Structure to Intrinsic Thermodynamics of Protein-Ligand Binding Using Carbonic Anhydrase Isozymes as a Model System**. *IUCrJ* 2024, 11 (4), 556–569. DOI: 10.1107/S2052252524004627
4. Kazlauskas, E.; Petrauskas, V.; **Paketurytė, V.**; Matulis, D. **Standard Operating Procedure for Fluorescent Thermal Shift Assay (FTSA) for Determination of Protein-Ligand Binding and Protein Stability**. *Eur. Biophys. J.* 2021, 50 (5), 707–714. DOI: 10.1007/s00249-021-01537-1
5. **Paketurytė, V.**; Petrauskas, V.; Zubrienė, A.; Abian, O.; Bastos, M.; Chen, W.-Y.; Moreno, M. J.; Krainer, G.; Linkuvienė, V.; Sedivy, A.; Velazquez-Campoy, A.; Williams, M. A.; Matulis, D. **Uncertainty in Protein–Ligand Binding Constants: Asymmetric Confidence Intervals versus Standard Errors**. *Eur. Biophys. J.* 2021, 50 (3-4), 661–670. DOI: 10.1007/s00249-021-01518-4

Publication 1

Enthalpy–Entropy Compensation in Inhibitor Binding to Carbonic Anhydrase Isozymes

Vaida Paketurytė-Latvė, Audrius Zakšauskas, Visvaldas Kairys, Edita Čapkauskaitė, Martynas Bagdonas, Alexey Smirnov, Elena Manakova, Saulius Gražulis, Daumantas Matulis

Biophys. J., 2026, 125 (21), 6148–6164

DOI: 10.1016/j.bpj.2026.09.032

Publication 2

Affinity and Selectivity of Protein-Ligand Recognition: A Minor Chemical Modification Changes Carbonic Anhydrase Binding Profile

Audrius Zakšauskas, **Vaida Paketurytė-Latvė**, Alberta Jankūnaitė, Edita Čapkauskaitė, Yann Becart, Alexey Smirnov, Klára Pospíšilová, Janis Leitans, Jiří Brynda, Andris Kazaks, Lina Baranauskienė, Elena Manakova, Saulius Gražulis, Visvaldas Kairys, Kaspars Tars, Pavlína Řezáčová, Daumantas Matulis

J. Med. Chem., 2025, 68 (16), 17752–17773

DOI: 10.1021/acs.jmedchem.5c01421

Publication 3

From X-ray crystallographic structure to intrinsic thermodynamics of protein-ligand binding using carbonic anhydrase isozymes as a model system

Vaida Paketurytė-Latvė, Alexey Smirnov, Elena Manakova, Lina Baranauskienė, Vytautas Petrauskas, Asta Zubrienė, Jurgita Matulienė, Virginija Dudutienė, Edita Čapkauskaitė, Audrius Zakšauskas, Janis Leitans, Saulius Gražulis, Kaspars Tars, Daumantas Matulis

IUCrJ., 2024, 11 (4), 556–569

DOI: 10.1107/S2052252524004627

Publication 4

Standard Operating Procedure for Fluorescent Thermal Shift Assay (FTSA) for Determination of Protein-Ligand Binding and Protein Stability

Egidijus Kazlauskas, Vytautas Petrauskas, **Vaida Paketurytė**, Daumantas Matulis

Eur. Biophys. J., 2021, 50 (5), 707–714.

DOI: 10.1007/s00249-021-01537-1

Publication 5

Uncertainty in protein–ligand binding constants: asymmetric confidence intervals versus standard errors

Vaida Paketurytė, Vytautas Petrauskas, Asta Zubrienė, Olga Abian, Margarida Bastos, Wen-Yih Chen, Maria João Moreno, Georg Krainer, Vaida Linkuvienė, Arthur Sedivy, Adrian Velazquez-Campoy, Mark A Williams, Daumantas Matulis

Eur. Biophys. J., 2021, 50, 3–4, 661–670

DOI: 10.1007/s00249-021-01518-4

PUBLICATIONS NOT INCLUDED IN THE DISSERTATION

During Doctoral Studies (2019–2026)

1. Žvirblis, M.; **Paketurytė-Latvė, V.**; Gedgaudas, M.; Lingė, D.; Urniežius, E.; Kojis, T.; Stančaitis, L.; Zakšauskas, A.; Mickevičiūtė, A.; Jachno, J.; Juozapaitienė, V.; Dudutienė, V.; Zubrienė, A.; Matulis, D. **Design of ortho/meta-substituted selective carbonic anhydrase IX inhibitors.** *Chemija* 2026, 37 (1), 29–42. DOI: 10.6001/chemija.2026.37.1.4
2. Zubrienė, A.; Kurtenoka, M.; **Paketurytė-Latvė, V.**; Leitans, J.; Manakova, E.; Žvirblis, M.; Kazaks, A.; Eimonta, V.; Tars, K.; Gražulis, S.; Petrauskas, V.; Matulienė, J.; Dudutienė, V.; Shubin, K.; Matulis, D. **Achieving femtomolar affinities in structure-based drug design**. *Eur. Biophys. J.* 2026, 55 (1), 55–62. DOI: 10.1007/s00249-025-01812-5
3. Vaškevičius, A.; Žvirblis, M.; Kurtenoka, M.; Leitans, J.; Manakova, E.; **Paketurytė-Latvė, V.**; Kvietkauskaitė, A.; Kazaks, A.; Eimonta, V.; Čerepenkaitė, K.; Kazokaitė-Adomaitienė, J.; Mickevičiūtė, A.; Juozapaitienė, V.; Tars, K.; Gražulis, S.; Matulienė, J.; Dudutienė, V.; Shubin, K.; Matulis, D.; Zubrienė, A. **Di-Meta-Substituted Fluorinated Benzenesulfonamides as Potent and Selective Anticancer Inhibitors of Carbonic Anhydrase IX and XII**. *J. Med. Chem.* 2025. DOI: 10.1021/acs.jmedchem.5c01142
4. Vaškevičius, A.; Trumpickaitė, G.; Parafjanovič, E.; Manakova, E.; Mickevičiūtė, A.; Gedgaudas, M.; Kojis, T.; **Paketurytė-Latvė, V.**; Smirnov, A.; Baranauskiene, L.; Gražulis, S.; Zubrienė, A.; Dudutienė, V.; Matulis, D. **Design of Rigid Compounds to Enhance Selectivity for Carbonic Anhydrase IX**. *Chem. Weinheim. Bergstr. Ger.* 2025, 31 (18), e202404409. DOI: 10.1002/chem.202404409

5. Lingė, D.; Gedgaudas, M.; Merkys, A.; Petrauskas, V.; Vaitkus, A.; Grybauskas, A.; **Paketurytė, V.**; Zubrienė, A.; Zakšauskas, A.; Mickevičiūtė, A.; Smirnovienė, J.; Baranauskienė, L.; Čapkauskaitė, E.; Dudutienė, V.; Urniežius, E.; Konovalovas, A.; Kazlauskas, E.; Shubin, K.; Schiöth, H. B.; Chen, W.-Y.; Ladbury, J. E.; Gražulis, S.; Matulis, D. **PLBD: Protein–Ligand Binding Database of Thermodynamic and Kinetic Intrinsic Parameters**. *Database* 2023, 2023, baad040. DOI: 10.1093/database/baad040

6. Zakšauskas, A.; Čapkauskaitė, E.; **Paketurytė-Latvė, V.**; Smirnov, A.; Leitans, J.; Kazaks, A.; Dvinskis, E.; Stančaitis, L.; Mickevičiūtė, A.; Jachno, J.; Jezepčikas, L.; Linkuvienė, V.; Sakalauskas, A.; Manakova, E.; Gražulis, S.; Matulienė, J.; Tars, K.; Matulis, D. **Methyl 2-Halo-4-Substituted-5-Sulfamoyl-Benzoates as High Affinity and Selective Inhibitors of Carbonic Anhydrase IX**. *Int. J. Mol. Sci.* 2022, 23 (1), 130. DOI: 10.3390/ijms23010130

7. Matulienė, J.; Žvinys, G.; Petrauskas, V.; Kvietkauskaitė, A.; Zakšauskas, A.; Shubin, K.; Zubrienė, A.; Baranauskienė, L.; Kačenauskaitė, L.; Kopanchuk, S.; Veiksina, S.; **Paketurytė-Latvė, V.**; Smirnovienė, J.; Juozapaitienė, V.; Mickevičiūtė, A.; Michailovienė, V.; Jachno, J.; Stravinskienė, D.; Sližienė, A.; Petrošiūtė, A.; Becker, H. M.; Kazokaitė-Adomaitienė, J.; Yaromina, A.; Čapkauskaitė, E.; Rinken, A.; Dudutienė, V.; Dubois, L. J.; Matulis, D. **Picomolar Fluorescent Probes for Compound Affinity Determination to Carbonic Anhydrase IX Expressed in Live Cancer Cells**. *Sci. Rep.* 2022, 12 (1), 17644. DOI: 10.1038/s41598-022-22436-1

8. Balandis, B.; Šimkūnas, T.; **Paketurytė-Latvė, V.**; Michailovienė, V.; Mickevičiūtė, A.; Manakova, E.; Gražulis, S.; Belyakov, S.; Kairys, V.; Mickevičius, V.; Zubrienė, A.; Matulis, D. **Beta and Gamma Amino Acid-Substituted Benzenesulfonamides as Inhibitors of Human Carbonic Anhydrases**. *Pharmaceuticals* 2022, 15 (4), 477. DOI: 10.3390/ph15040477

9. Baronas, D.; Dudutienė, V.; **Paketurytė, V.**; Kairys, V.; Smirnov, A.; Juozapaitienė, V.; Vaškevičius, A.; Manakova, E.; Gražulis, S.; Zubrienė, A.; Matulis, D. **Structure and Mechanism of Secondary Sulfonamide Binding to Carbonic Anhydrases**. *Eur. Biophys. J.* 2021, 50 (7), 993–1011. DOI: 10.1007/s00249-021-01561-1

10. Zakšauskas, A.; Čapkauskaitė, E.; Jezepčikas, L.; Linkuvienė, V.; **Paketurytė, V.**; Smirnov, A.; Leitans, J.; Kazaks, A.; Dvinskis, E.; Manakova, E.; Gražulis, S.; Tars, K.; Matulis, D. **Halogenated and Di-Substituted Benzenesulfonamides as Selective Inhibitors of Carbonic Anhydrase Isoforms**. *Eur. J. Med. Chem.* 2020, 185, 111825.

DOI: 10.1016/j.ejmech.2019.111825

Publications Prior to Doctoral Studies (2016–2019)

1. Vaškevičienė, I.; **Paketurytė, V.**; Pajanok, N.; Žukauskas, Š.; Sapijanskaitė, B.; Kantiminienė, K.; Mickevičius, V.; Zubrienė, A.; Matulis, D. **Pyrrolidinone-bearing methylated and halogenated benzenesulfonamides as inhibitors of carbonic anhydrases**. *Bioorg. Med. Chem.* 2019, 27, 322–337. DOI: 10.1016/j.bmc.2018.12.011

2. **Paketurytė, V.**; Linkuvienė, V.; Krainer, G.; Chen, W-Y.; Matulis, D. **Repeatability, precision, and accuracy of the enthalpies and Gibbs energies of a protein-ligand binding reaction measured by isothermal titration calorimetry**. *Eur. Biophys. J.* 2018, 48 (2), 139–152. DOI: 10.1007/s00249-018-1341-z

3. Čapkauskaitė, E.; Zubrienė, A.; **Paketurytė, V.**; Timm, D.; Tumkevičius, S.; Matulis, D. **Thiazole-substituted benzenesulfonamides as inhibitors of 12 human carbonic anhydrases**. *Bioorg. Chem.* 2018, 77, 534–541. DOI: 10.1016/j.bioorg.2018.02.004

4. Čapkauskaitė, E.; Zakšauskas, A.; Ruibys, V.; Linkuvienė, V.; **Paketurytė, V.**; Gedgaudas, M.; Kairys, V.; Matulis, D. **Benzimidazole design, synthesis, and docking to build selective carbonic anhydrase VA inhibitors**. *Biorg. Med. Chem.* 2018, 26 (3), 675–687. DOI: 10.1016/j.bmc.2017.12.035

5. Vaškevičienė, I.; **Paketurytė, V.**; Zubrienė, A.; Kantiminienė, K.; Mickevičius, V.; Matulis, D. **N-Sulfamoylphenyl- and N-Sulfamoylphenyl-N-thiazolyl-β-alanines and their derivatives as inhibitors of human carbonic anhydrases**. *Bioorg. Chem.* 2017, 75, 16–29. DOI: 10.1016/j.bioorg.2017.08.017

6. Paliulis, E.; **Paketurytė, V.**; Matulis, D. **Protease, Amylase and Lactase Enzyme Stability in Gastroval® Capsules after Incubation at Acidic pH and Elevated Temperature**. *Biochem. Physiol.: Open Access*. 2016. DOI: 10.4172/2168-9652.1000211

Book Chapters

1. **Paketurytė, V.**; Zubrienė, A.; Ladbury, J. E.; Matulis, D. **Intrinsic Thermodynamics of Protein-Ligand Binding by Isothermal Titration Calorimetry as Aid to Drug Design**. *Microcalorimetry of Biological Molecules*. New York: Springer. Methods Mol. Biol. 1964, 61–74. 2019. DOI: 10.1007/978-1-4939-9179-2_5
2. **Paketurytė, V.**; Zubrienė, A.; Chen, W.-Y.; Keller, S.; Bastos, M.; Todd, M. J.; Ladbury, J. E.; Matulis, D. **Inhibitor Binding to Carbonic Anhydrases by Isothermal Titration Calorimetry**. *Carbonic Anhydrase as Drug Target: Thermodynamics and Structure of Inhibitor Binding*. Cham: Springer International Publishing. 2019, 79–95. DOI: 10.1007/978-3-030-12780-0_6

Scientific Events and Courses Attended by the Author

This section includes only scientific events attended by the author and presentations personally delivered by the author; presentations given solely by co-authors are not listed.

During Doctoral Studies (2019–2026)

Scientific Conferences

1. **Paketurytė-Latvė, V.**; Smirnov, A.; Dudutienė, V.; Zubrienė, A.; Matulis, D. "Understanding Carbonic Anhydrase Inhibition: Structural and Thermodynamic Insights". *4th MOSBRI Scientific Conference*. Paris, France. 2025 06 10–13.

   –Oral presentation

2. **Paketurytė-Latvė, V.**; Petrauskas, V.; Zubrienė, A.; Matulis, D. "Constant Uncertainty in Protein-Ligand Binding: Asymmetric Confidence Intervals vs Standard Errors". *XXI Conference of the International Society for Biological Calorimetry ISBC 2022*. Vilnius, Lithuania. 2022 06 08–10.

   –Poster presentation

3. **Paketurytė, V.**; Smirnov, A.; Manakova, E.; Gražulis, S.; Matulis, D. "Crystallography of Human Carbonic Anhydrases with Inhibitors for Drug Design". *PDB50*. Online. 2021 05 04–05.

   –Poster and video presentation

4. **Paketurytė, V.**; Smirnov, A.; Jankūnaitė, A.; Zakšauskas, A.; Čapkauskaitė, E.; Matulis, D. "Correlations between Thermodynamics and Structure of Carbonic Anhydrase-Inhibitor Binding". *64th Annual*

Meeting of the Biophysical Society. San Diego, California, USA. 2020 02 15–19. (Funding: Research Council of Lithuania support for doctoral students' academic visits)

–Poster presentation

5. **Paketurytė, V.**; Smirnov, A.; Jankūnaitė, A.; Zakšauskas, A.; Čapkauskaitė, E.; Matulis, D. "Thermodynamics-Structure Correlations of Carbonic Anhydrase-Inhibitor Binding". *FEBS INSTRUCT MOBIEU Practical Course: HyThabio*. Grenoble, France. 2020 01 26–31.

   –Poster presentation

Courses

1. Training school (2026 02 22–03 29) "*HERCULES SCHOOL: Neutrons & Synchrotron Radiation for Science*"
2. Practical course, Grenoble, France (2020 03 26–31) FEBS INSTRUCT MOBIEU Practical course *"HyThabio": Hydrodynamic and thermodynamic analysis of biological macromolecules and their interactions*.
3. Practical course, Online (2021 02 01–03 10) "*Introduction to Molecular Modeling in Drug Discovery*". Organizer - Schrödinger, Inc.
4. Practical course, Online (2021 05 24–27) "*Instruct-ERIC course: Biophysics, structural mass spectrometry, and X-ray techniques*". Organizer - Institute of Biotechnology of the Czech Academy of Sciences.
5. Practical course, Online (2021 08 30–10 31) "*Pharmaceutical Bioinformatics*". Organizer - Uppsala University.

Prior to Doctoral Studies (2016–2019)

Scientific Conferences

1. **Paketurytė, V.**; Matulis, D. "Precision of ITC Measurements For Target-Based Drug Design". *The 6th NovAliX Conference – Biophysics in Drug Discovery*. Cannes, France. 2019 03 20–22.

   –Poster presentation

2. **Paketurytė, V.**; Matulis, D. "Intrinsic Affinity of N-Substituted Benzenesulfonamides to Carbonic Anhydrases". *Molecular Biophysics – ABC of the puzzle of Life (The third COST-sponsored ARBRE-MOBIEU plenary meeting)*. Zagreb, Croatia. 2019 03 18–20.

   –Poster presentation

3. **Paketurytė, V.**; Matulis, D. "Intrinsic Affinity of N-Substituted Benzenesulfonamides to Carbonic Anhydrases". *The COINS*. Vilnius, Lithuania. 2019 02 26–28.

   –Poster presentation

4. **Paketurytė, V.**; Jankūnaitė, A.; Smirnov, A.; Zakšauskas, A.; Zubrienė, A.; Matulis, D. "Intrinsic Thermodynamics of o-S-Substituted Benzenesulfonamide Binding to Carbonic Anhydrases". *XVth Conference of the Lithuanian Biochemical Society*. Dubingiai, Lithuania. 2018 06 26.

   –Oral presentation

5. **Paketurytė, V.**; Čapkauskaitė, E.; Zubrienė, A.; Matulis, D. "Binding and inhibition of catalytically active human carbonic anhydrases by thiazole-substituted benzenesulfonamides". *Open Readings*. Vilnius, Lithuania. 2018 03 23.

   –Poster presentation

6. **Paketurytė, V.**; Vaškevičienė, I.; Zubrienė, A.; Mickevičius, V.; Matulis, D. "Thermodynamic Analysis of Benzenesulfonamides Bearing Oxopyrrolidine Moiety Binding to Human Carbonic Anhydrases". *The COINS*. Vilnius, Lithuania. 2018 03 02.

   –Poster presentation

7. **Paketurytė, V.**; Linkuvienė, V.; Matulis, D. "Repeatability of enthalpies and Gibbs energies of a protein–ligand binding reaction measured by ITC". *62nd Annual Meeting of the Biophysical Society*. San Francisco, California, USA. 2018 02 18.

   –Oral presentation

8. **Paketurytė, V.**; Vaškevičienė, I.; Zubrienė, A.; Mickevičius, V.; Matulis, D. "Selective inhibitors of human carbonic anhydrase isoform VB". *VitaScientia*. Vilnius, Lithuania. 2018 01 03.

   –Poster presentation

9. **Paketurytė, V.**; Paliulis, E.; Matulis, D. "Enzyme survivability at acidic pH and high temperature". *European Biotechnology Congress*. Riga, Latvia. 2016 05 04–07.

   –Poster presentation

Internship

1. Internship. Malvern Instruments, Sweden (2017 04) - ITC precision measurements on PEAQ-ITC. *Advisor*: Dr. Natalia Markova

Curriculum Vitae (June 2026)

Vaida PAKETURYTĖ-LATVĖ

BIOCHEMIST | PROTEIN–LIGAND INTERACTIONS & DRUG DESIGN

vaida.paketuryte@gmc.vu.lt

ORCID: 0000-0003-0919-7826 | **Web of Science:** NDS-0906-2025 | **ResearchGate:** Vaida Paketuryte-Latve

SCIENTIFIC PROFILE

Biochemist specializing in protein–ligand interactions, binding thermodynamics, and structural studies of carbonic anhydrases. Research focuses on understanding molecular recognition through the integration of structural and thermodynamic approaches and their application to drug design.

RESEARCH AREAS

- Protein–ligand interactions
- Binding thermodynamics
- Molecular recognition
- Carbonic anhydrases (CA)
- Structure-based drug design

PATENTS

Co-inventor of carbonic anhydrase inhibitors synthesized on interconnecting linker chains:

- US2024000946A1
- EP4255886A1

HONORS & AWARDS

- President Kazys Grinius Memorial Scholarship for Academic Achievement (2018)
- Lithuanian Academy of Sciences Award for University Students' Research (2020)
- Vilnius University Academic Excellence Scholarship (2018, 2019, 2020)
- FEBS Youth Travel Fund Award (2020)
- COST MOBIEU Conference Award (2018) and STSM Fellowship (2017)

EDUCATION

2019–2026 (Leave: 2022–2024) — **Doctoral studies in Biochemistry** at Vilnius University, Life Sciences Center; Supervisor: Prof. Daumantas Matulis

2017–2019 — **M.Sc. in Biochemistry** *(Magna Cum Laude)* at Vilnius University, Life Sciences Center

2013–2017 — **B.Sc. in Biochemistry** at Vilnius University, Faculty of Chemistry

RESEARCH EXPERIENCE

2019–present — **Junior Scientist** at Department of Biothermodynamics and Drug Design, Institute of Biotechnology, Vilnius University

2017–2022 — **Researcher** at ThermoPharma Baltic

2016–2019 — **Laboratory Assistant** at Department of Biothermodynamics and Drug Design, Vilnius University

SUPERVISION

2022 — Scientific supervisor of BSc thesis (T. Šimkūnas)

2020 — Scientific consultant of BSc thesis (K. Gluščiukaitė)

RESEARCH PROJECTS

2017–2029 — Participation in 7 research projects, from student research initiatives to national and EU-funded programs.

PROFESSIONAL MEMBERSHIPS

Biophysical Society; ARBRE-MOBIEU; Lithuanian Biochemical Society (co-organizer of a national conference in 2018);

SCIENTIFIC OUTCOMES

2	20	14	40+	1500+
Book chapters	**Publications**	**Presentations**	**PDB structures**	**PLBD entries**
in scientific volumes	in international journals	oral and poster	of CA–ligand complexes	protein–ligand binding data

Vaida Paketurytė-Latvė

Structural Recognition in Carbonic Anhydrase–Sulfonamide Complexes: Isozyme and Ligand Effects on Binding Thermodynamics

Doctoral Dissertation
Natural Sciences
Biochemitry (N 004)

Struktūrinis atpažinimas karboanhidrazių–sulfonamidų kompleksuose: izofermentų ir ligandų efektai jungimosi termodinamikoje

Daktaro disertacija
Gamtos mokslai
Biochemija (N 004)

Vilnius University Press
9 Saulėtekio Ave., Building III, LT-10222 Vilnius
Email: info@leidykla.vu.lt, www.leidykla.vu.lt
bookshop.vu.lt, journals.vu.lt
Print run of 15 copies